Investigation of FAT10

Biochemical and Immunological Functions

Doctoral thesis for obtaining the

academic degree Doctor of Natural Sciences

(Dr. rer. nat)

submitted by

Cao, Jinjing

at the

Faculty of Sciences

Department of Biology

Konstanz, 2025

Date of the oral examination: **2025. 08. 06**

1. Reviewer: **PD Dr. Gunter Schmidtke**

2. Reviewer: **Prof. Dr. Alexander Bürkle**

Content

Abstract

HLA-F adjacent transcript 10 (FAT10) is a member of the ubiquitin-like modifier family. Similar to ubiquitin, FAT10 utilizes a distinct enzymatic cascade consisting of E1 activating, E2 conjugating, and E3 ligating enzymes to covalently link to substrate proteins, thereby targeting them directly for proteasomal degradation. To date, Parkin is the only identified E3 ligase for FAT10. However, the existence of additional E3 ligases remains an open question, which led us to develop a FAT10-based probe for screening potential E3 ligases. This is discussed in Chapter 3.

FAT10 is predominantly expressed in dendritic cells (DCs) and is upregulated during inflammation and in certain cancers. Interleukin-12 (IL-12), primarily secreted by DCs, B cells, monocytes, and macrophages, plays a critical role in $CD4^+$ T cell differentiation and IFN-γ production. We became interested in investigating the potential regulatory relationship between FAT10 and IL-12, as described in Chapter 2.

Additionally, previous reports showed that FAT10 is phosphorylated by IκB kinase β (IKKβ) in response to pro-inflammatory cytokine tumor necrosis factor (TNF) and during influenza A virus infection. This observation raised questions regarding the role of FAT10 phosphorylation in modulating its degradation dynamics, leading to the investigations presented in Chapter 1.

In chapter 1, we generated phospho-mimetic FAT10 mutant (FAT10 D) constructs and compared the differences in FAT10 degradation and conjugation between wild-type (FAT10 WT) and FAT10 D in the context of the E3 ligase TRIM25, the UBL-UBA protein NUB1L, and the proteasomal ubiquitin receptor RPN10. Our results showed that phospho-mimetic FAT10 exhibited enhanced conjugation efficiency relative to FAT10 WT. However, the phosphorylation of FAT10 did not impact the proteasomal degradation rate. Thus, phosphorylation appears to modulate FAT10's interactions with specific binding partners, such as NUB1L, without altering its primary degradation pathway.

In chapter 2, we explored whether FAT10 influences IL-12 secretion and signaling both in *vitro* and in *vivo*. Our findings demonstrated that FAT10 overexpression did not affect IL-12 production in dendritic cells, nor did FAT10 deficiency alter IL-12 signaling in T cells derived from $FAT10^{-/-}$ mice compared to C57BL/6 controls. Despite its abundant expression in dendritic cells, FAT10 does not appear to regulate IL-12 expression or downstream

signaling pathways under the conditions tested.

In chapter 3, we aimed to develop a biochemical probe to facilitate the identification of FAT10-specific E3 ligases. FAT10 was purified using Strep-Tactin affinity chromatography and chitin resin, while the E2 enzyme USE1 was isolated using Ni-affinity chromatography. Subsequently, using thiol–yne coupling chemistry, we generated FAT10-USE1 conjugates with a reactive C-terminus at the branching point. These conjugates will serve as molecular probes capable of screening potential FAT10 E3 ligases, thus providing a valuable tool for the study of FAT10ylation.

Collectively, these studies address critical gaps in the current understanding of FAT10 biology and provide novel experimental tools to facilitate future research.

Key Words: *FAT10, phospho-mimetic FAT10; FAT10ylation; degradation; TRIM25; NUB1L; RPN10, IL-12, STAT signaling, Th1 differentiation, USE1, Ni-affinity chromatography, Strep-Tactin, thiol–yne coupling reaction, E3 ligase*

Zusammenfassung

HLA-F adjacent transcript 10 (FAT10) ist ein Mitglied der Familie der Ubiquitin-ähnlichen Modifikatoren. Ähnlich wie Ubiquitin verwendet FAT10 eine Enzymkaskade, bestehend aus einem E1-Aktivierungs-, einem E2-Übetragungs - und E3-Ligase-Enzymen, um kovalent an Substratproteine gebunden zu werden, und diese gezielt dem proteasomalen Abbau zuzuführen. Bisher wurde Parkin als einzige E3-Ligase für FAT10 identifiziert. Die Existenz weiterer E3-Ligasen bleibt jedoch eine offene Frage, was uns dazu veranlasste, eine FAT10-basierte Sonde zur Identifizierung potenzieller E3-Ligasen zu entwickeln. Dies wird in Kapitel 3 erläutert.

FAT10 wird vorwiegend in dendritischen Zellen (DCs) exprimiert und während Entzündungen sowie in bestimmten Krebsarten hochreguliert. Interleukin-12 (IL-12), hauptsächlich sezerniert von DCs, B-Zellen, Monozyten und Makrophagen, spielt eine entscheidende Rolle bei der Differenzierung von $CD4^+$-T-Zellen und der Produktion von IFN-γ. Dies weckte unser Interesse, die potenzielle regulatorische Beziehung zwischen FAT10 und IL-12 zu untersuchen, wie in Kapitel 2 beschrieben.

Darüber hinaus zeigen frühere Studien, dass FAT10 durch die IκB-Kinase β (IKKβ) in Reaktion auf das pro-inflammatorischen Zytokin Tumornekrosefaktor (TNF), sowie während einer Infektion mit dem Influenzavirus A phosphoryliert wird. Diese Beobachtung warf Fragen über die Rolle der FAT10-Phosphorylierung bei der Modulation seiner Degradationsdynamik auf, die wir in Kapitel 1 untersucht haben.

In Kapitel 1 generierten wir phosphomimetische FAT10-Mutantenkonstrukte (FAT10D) und verglichen die Unterschiede in der Degradation und Konjugation zwischen Wildtyp-FAT10 (FAT10 WT) und FAT10D im Kontext der E3-Ligase TRIM25, des UBL-UBA-Proteins NUB1L und des proteasomalen Ubiquitinrezeptors RPN10. Unsere Ergebnisse zeigten, dass phosphomimetisches FAT10 eine erhöhte Konjugationseffizienz im Vergleich zu FAT10 WT aufwies. Allerdings hatte die Phosphorylierung von FAT10 keinen Einfluss auf die proteasomale Abbaurate. Demnach scheint die Phosphorylierung die Interaktion von FAT10 mit spezifischen Bindungspartnern wie NUB1L zu modulieren, ohne den primären Degradationsweg zu verändern.

In Kapitel 2 untersuchten wir, ob FAT10 die IL-12-Sekretion und -Signalübertragung sowohl in vitro als auch in vivo beeinflusst. Unsere

Ergebnisse zeigten, dass eine Überexpression von FAT10 die IL-12-Produktion in dendritischen Zellen nicht veränderte und dass ein FAT10-Defizit die IL-12-Signalübertragung in T-Zellen von FAT10$^{-/-}$ Mäusen im Vergleich zu C57BL/6-Kontrollmäusen nicht beeinträchtigte. Trotz seiner hohen Expression in DCs scheint FAT10 unter den getesteten Bedingungen weder die IL-12-Produktion noch die nachgeschalteten Signalwege wesentlich zu regulieren.

In Kapitel 3 verfolgten wir das Ziel, eine biochemische Sonde zu entwickeln, um FAT10-spezifische E3-Ligasen identifizieren zu können. Dazu reinigten wir FAT10 mittels Strep-Tactin-Affinitätschromatographie und Chitinagarose und isolierten das E2-Enzym USE1 durch Ni-affinity chromatography. Anschließend erzeugten wir, mit Hilfe der Thiol–Yne-Kupplungsreaktion, FAT10-USE1-Konjugate mit einem reaktiven C-Terminus an der Verzweigungsstelle. Diese Konjugate dienten als molekulare Sonden für das Screening potenzieller FAT10-E3-Ligasen und stellen somit ein wertvolles Werkzeug für die Untersuchung der FAT10ylierung dar.

Zusammenfassend schließen diese Arbeiten wichtige Lücken im aktuellen Verständnis der FAT10-Biologie und bieten neuartige experimentelle Werkzeuge, die zukünftige Forschungen erleichtern könnten.

***Schlagwörter**: FAT10, phosphomimetisches FAT10, FAT10ylierung, abbau, TRIM25, NUB1L, RPN10, IL-12, STAT-signalweg, Th1-differenzierung, USE1, Ni-affinity chromatography, Strep-Tactin, thiol–yne-kupplungsreaktion, E3 Ligase*

General introduction

Ubiquitin was discovered in 1975 [1] and was found to mediate protein degradation via the proteasome. It is a protein of 8.6 kDa consisting of 76 amino acid residues [2]. Protein ubiquitination is a post-translational modification involved in most biological processes in eukaryotic cells. In addition, it plays important roles in DNA repair, cell signaling, membrane protein trafficking, and endocytosis [3, 4].

FAT10 belongs to the family of ubiquitin-like modifiers (UBLs), which also includes several other members. As shown in the table below, examples include ATG8, ATG12, ISG15, NEDD8, and SUMO, among others [5-7].

ABBREVIATION	FULL NAME	FUNCTION
ATG8 [8-11]	Autophagy-related protein 8	Autophagy, nutrient recycling in plants
ATG12 [11-14]	Autophagy-related protein 12	Autophagy, nutrient recycling in plants
FAT10	HLA-F adjacent transcript 10	Ubiquitin-independent substrate degradation; induced by IFN-γ and TNF
ISG15 [15-18]	Interferon-stimulated gene 15	Transcription and pre-mRNA splicing during IFN response; induced by IFN-α/β
MNSFβ [19-21]	Monoclonal nonspecific suppressor factor β	May play a role in T cell activation
MUB [22-24]	Membrane-anchored ubiquitin-fold protein	Membrane protein regulation, signal transduction
NEDD8 [25-29]	Neural precursor cell expressed developmentally down-regulated protein 8	SCF complex activation, p53 transcriptional regulation
SUMO1-4 [30-33]	Small ubiquitin-like modifier 1–4	Substrate localization, protein interactions, nuclear transport, stress response
UBL5 [34-37]	Ubiquitin-like protein 5	Pre-mRNA splicing , stress-responsive regulator
UFM1 [38-40]	Ubiquitin-fold modifier 1	Function unknown; Uba5 induced during unfolded protein response
URM1 [41, 42]	Ubiquitin-related modifier 1	Budding, nutrient sensing, oxidative stress response

Table 0.1. The known ubiquitin-like modifiers. Adapted from [5-7].

Since the focus of this study is on FAT10, other ubiquitin-like modifiers will not be discussed in detail here. For further reading, please refer to their relevant literature.

Returning to the main topic, we will now introduce FAT10's structure, characteristics, functions, and the aims of the studies.

The structure and characteristics of FAT10

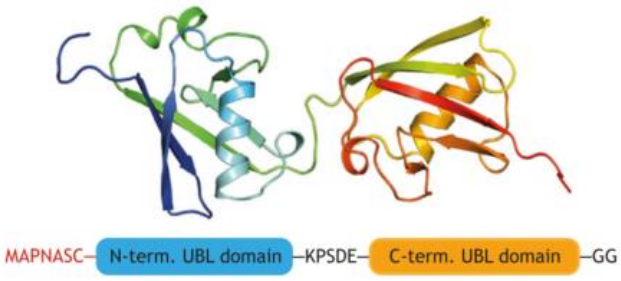

Figure 0.1. Ribbon representation of the 3D structure of human FAT10. Cited from [43].

FAT10, also known as ubiquitin D, is a protein of approximately 18 kDa composed of 165 amino acids, primarily involved in targeting proteins for proteasomal degradation. In 2018, Aichem and colleagues resolved the high-resolution structure of FAT10 using nuclear magnetic resonance (NMR). Their findings revealed that FAT10 consists of two domains—an N-terminal domain (N-domain) and a C-terminal domain (C-domain)—connected by a short, flexible linker sequence, KPSDE (Figure 0.1). A critical diglycine motif at the C-terminus of the C-domain is essential for FAT10-mediated protein degradation. Sequence analysis indicates that the N- and C-domains of FAT10 share 29% and 36% homology with those of ubiquitin, respectively. Despite their shared function in proteasomal targeting, FAT10 and ubiquitin differ significantly in structure and mechanism. In 2013, Schmidtke et al. compared FAT10 and ubiquitin and highlighted both their similarities and distinctions (Figure 0.2) [44].

Differences between ubiquitin and FAT10 as degradation signals

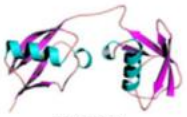

	Ubiquitin	FAT10
Degradation rate	slow (t1/2 ~ 9h)	fast (t1/2 ~ 1h)
Recycling	yes	no
Proteasome receptors	RPN10, RPN13	RPN10
Proteasome binding	polymer (>4)	monomer
RPN10 binding site	UIM1, UIM2	VWA
E1 enzyme(s)	UBE1, UBA6	UBA6
E2 enzyme(s)	~ 50	USE1
Tissue expression profile	ubiquitous	immune system
Inducibility	heat shock	IFN-γ/TNF-α

Figure 0.2. Differences between ubiquitin and FAT10 as degradation signals. Cited from [44].

FAT10 is characterized by a notably short half-life (~1 hour), in contrast to ubiquitin (~9 hours), possibly due to increased atomic fluctuations and looser domain folding in FAT10 [45]. Unlike ubiquitin, which typically forms polyubiquitin chains on target proteins and is recycled via deubiquitinases, FAT10 can function as a monomer, conjugating directly to substrate proteins and being degraded along with them.

The process of FAT10-mediated protein degradation, termed FAT10ylation, resembles ubiquitination and targets substrates for degradation via the 26S proteasome [7]. This pathway involves the E1-activating enzyme UBA6, the E2-conjugating enzyme USE1, and the E3 ligase (Figure 0.3). Notably, UBA6 and USE1 participate in both FAT10ylation and ubiquitination. Parkin, encoded by the *PARK2* gene, remains the only E3 ligase identified to date that facilitates FAT10 conjugation [43].

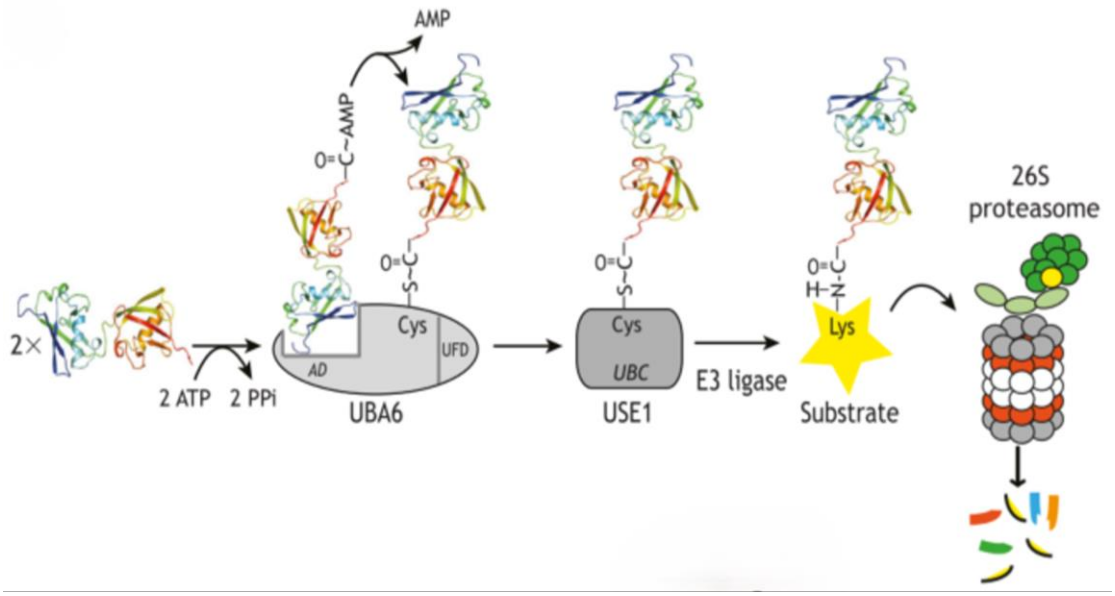

Figure 0.3. FAT10ylation is an ATP-consuming process. Cited from [43].

FAT10 is activated by UBA6 in an ATP-dependent manner, where a thioester bond forms between the C-terminal glycine of FAT10 and the active-site cysteine of UBA6, releasing AMP. FAT10 is subsequently transferred to USE1 through a similar thioester linkage. E3 ligase then facilitates the formation of an isopeptide bond between the ε-amino group of a lysine residue on the substrate and the C-terminal glycine of FAT10. Despite UBA6's bi-specificity, it exhibits higher affinity for FAT10 than for ubiquitin. USE1 also demonstrates UBA6-dependent FAT10 conjugation, albeit with slower kinetics compared to ubiquitination [46]. Interestingly, Aichem et al. showed that USE1 could auto-Fat10ylate itself in *cis*, and this self-modification does not hinder FAT10's ability to bind substrates [47].

To date, no specific de-FAT10ylating enzyme has been identified. FAT10 conjugation is generally considered irreversible and leads to simultaneous degradation of both FAT10 and its substrate. In studies involving OTUB1, FAT10 was shown to modulate OTUB1, although the reverse was not observed [48].

Schmidtke et al. demonstrated that FAT10 interacts with the proteasome both directly and indirectly (Figure 0.4) [44].

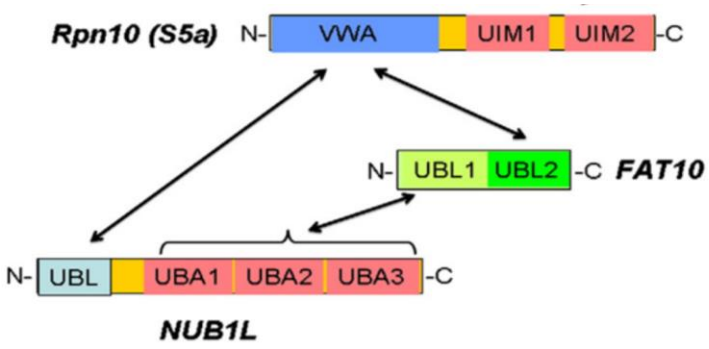

Figure 0.4. The 26S proteasome subunit RPN10 (S5a) as a docking site for FAT10, NUB1L, and ploy-ubiquitin. Cited from [44].

In 1994, Deveraux et al. identified RPN10, a 26S proteasomal subunit that binds ubiquitin conjugates [49]. RPN10, also known as S5a in mammals, contains an N-terminal von Willebrand factor A (VWA) domain and one or two ubiquitin-interacting motifs (UIMs) at the C-terminus [50]. Human RPN10 can bind both K48- and K63-linked ubiquitin chains [51]，whereas its yeast counterpart binds primarily to K48-linked chains [52]. In 2012, Rani et al. found that FAT10 interacts with the VWA domain of RPN10 [53], allowing direct recruitment of FAT10-tagged substrates for degradation.

NUB1L, a splicing variant of NEDD8 ultimate buster 1 (NUB1), contains an N-terminal ubiquitin-like (UBL) domain and three ubiquitin-associated (UBA) domains. Its UBA domains bind FAT10, but not ubiquitin [54, 55]. FAT10 binding to NUB1L facilitates activation of the 26S proteasome [56]. NUB1L accelerates FAT10-mediated degradation in a manner dependent on RPN10. Knockdown of RPN10 leads to FAT10 accumulation, underscoring the requirement for the RPN10-VWA interaction in proteasome-mediated degradation [53]. Furthermore, FAT10 competes with NUB1L for binding to hRPN10-VWA [53]. When NUB1L's UBA domains bind to FAT10's N-domain and its UBL domain binds to RPN10's VWA domain, FAT10 mediates protein degradation indirectly.

In 2012, Aichem et al. reported 571 endogenous FAT10-interacting proteins, predicting that 176 might be FAT10 substrates, while 395 participate in interactions [57]. Several of these interacting proteins are tightly associated with FAT10's functional roles, which are discussed in other sections.

PROTEIN	INTERACTION TYPE	FUNCTION
p62/SQSTM1 [57]	Covalent	Promotes protein degradation
UBE1 (Ubiquitin-activating enzyme E1) [58]	Covalent	Targets for proteasomal degradation

JunB [59]	Covalent	Proteasomal degradation
PCNA (Proliferating cell nuclear antigen) [60]	Covalent	Involved in DNA replication and DNA damage response
p53 [61, 62]	Covalent	Involved in Cell apoptosis, cell cycle arrest, and DNA repair
HUWE1 (HECT, UBA and WWE domain containing E3 ubiquitin protein ligase 1) [63]	Covalent	Involved in Cell proliferation and differentiation, DNA replication, DNA damage response and repair
β-catenin [64]	Non-covalent	Targeted to proteasome–mediated degradation
RIG-I (Retinoic acid-inducible gene I) [65, 66]	Non-covalent	Against RNA virus infection
MAD2 (Mitotic arrest deficient 2) [67, 68]	Non-covalent	The spindle assembly checkpoint protein
HDAC6 (Histone deacetylase 6) [69]	Non-covalent	Involved in aggresome formation, microtubule stability
AMBRA1 (Activating molecule in Beclin1-regulated autophagy) [63]	Non-covalent	Involved in canonical PINK1/Parkin-dependent and -independent mitophagy

Table 0.2. The interaction proteins with FAT10.

As a ubiquitin-like modifier (ULM), FAT10 participates in post-translational modifications (PTMs). According to the UniProt database, more than 450 PTMs have been identified, with notable modifications in FAT10 including phosphorylation, ubiquitination, and lysine acetylation [33, 70]. Like ubiquitin, which forms polyubiquitin chains via isopeptide bonds at lysine residues (Lys6, Lys11, Lys27, Lys29, Lys33, Lys48, Lys63) [2]. FAT10 uses its C-terminal diglycine motif for conjugation, typically modifying substrates as a monomer. Among FAT10's 17 lysines, several align with conserved ubiquitin residues, especially those corresponding to Lys27, Lys33, Lys48, and Lys63 (Figure 0.5). Raasi et al. proposed that only the lysine corresponding to ubiquitin's Lys48 is functionally conserved in murine FAT10 [71].

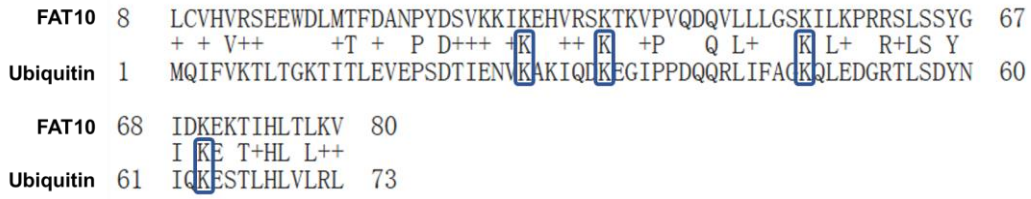

Figure 0.5. Conserved lysine residues in FAT10: corresponding sites to ubiquitin. Cited from NCBI-BLASTP.

FAT10 itself is subject to regulation via PTMs. Buchsbaum et al. reported that FAT10 undergoes increased ubiquitination prior to its degradation during apoptosis induction [72]. However, Hipp et al. showed that FAT10 degradation can proceed independently of ubiquitination using an E1 temperature-sensitive mutant [73], indicating ongoing debate regarding its dependence on ubiquitin pathways.

FAT10 can also undergo acetylation and phosphorylation. Kalveram et al. found that while a part of FAT10 is acetylated during interaction with HDAC6, acetylation is not essential for this interaction [69]. Phosphorylation predominantly occurs on serine, threonine, and tyrosine, with a relative frequency of 11.2:2.5:1 [74, 75]. Saxena et al. identified serines 62, 64, 95, 109 and threonine 77 as phosphorylated residues in FAT10 [76]. During TNF stimulation and Influenza A virus infection, FAT10 is phosphorylated by IKKβ, leading to downregulation of type I IFN expression.

Given the unique characteristics of FAT10, we will next explore its biological functions in greater detail.

The related functions of FAT10

FAT10 is predominantly expressed in immune cells such as DCs and B cells, as well as in immune-related organs including lymph nodes, liver, spleen, thymus, and the gastrointestinal tract [77-79]. Previous studies have shown that FAT10 expression is upregulated upon stimulation by pro-inflammatory cytokines, particularly TNF and interferon-γ (IFN-γ) [80]. In addition, FAT10 expression in DCs can also be induced by other immune stimuli such as lipopolysaccharide (LPS), poly inosinic-poly cytidylic acid (poly I:C), and CD40 ligand [81, 82]. These findings underscore the immunological relevance of FAT10.

Antigen presentation

FAT10 plays an important role in antigen processing and presentation. When fused to the N-terminus of the pp65 antigen derived from HCMV, FAT10 or ubiquitin facilitates its degradation via the proteasomal subunit RPN10 (S5a) and presentation as epitope. Notably, FAT10-mediated processing of pp65 is independent of the immunoproteasome and the proteasome activator PA28. Moreover, overexpression of NUB1L significantly enhances the presentation of the FAT10-tagged $pp65^{495–503}$ epitope. FAT10-pp65 enhances both direct and cross-presentation of HLA-A2-restricted epitopes by DCs [83].

Additionally, research by Pach et al. demonstrated that FAT10-fusion at the N-terminus of the LCMV nucleoprotein (NP) enhances MHC-I presentation of defective ribosomal products (DRiPs) derived from viral proteins [84]. FAT10 is also involved in MHC class II presentation. Mono-FAT10ylation of the autophagy adaptor protein p62 at several lysine residues leads to lysosomal degradation and subsequent peptide loading onto MHC class II molecules, which are then presented to $CD4^+$ T cells [57, 85, 86].

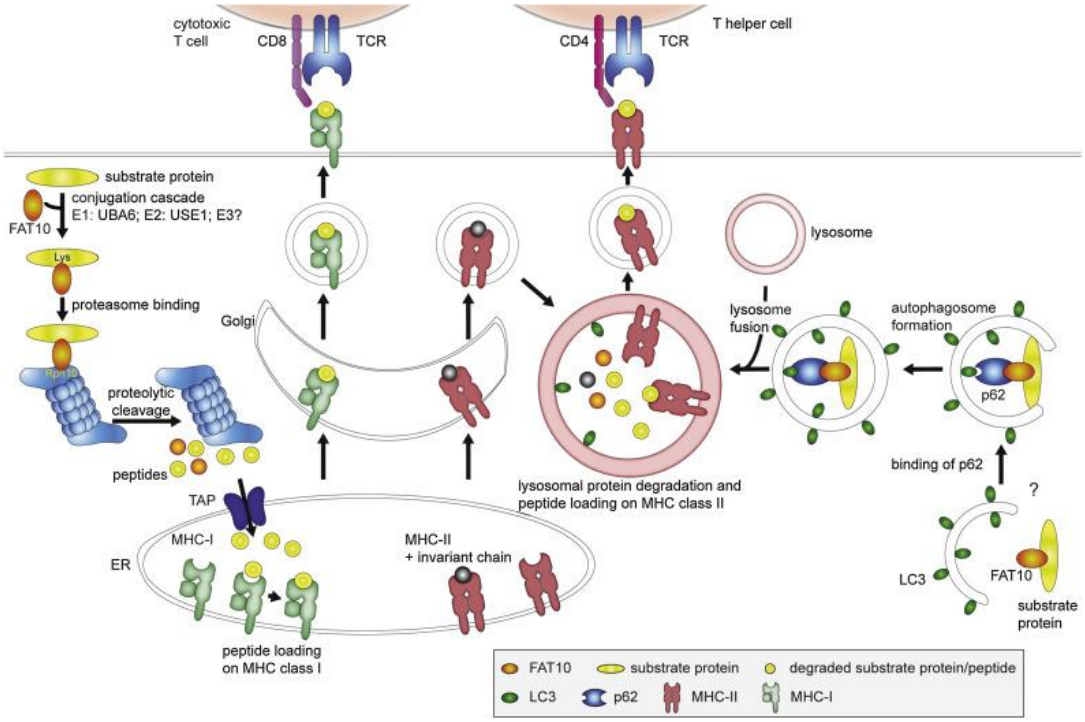

Figure 0.6. FAT10 in MHC class I and MHC class II antigen. Cited from [86].

Autophagy

During MHC class II antigen presentation, FAT10 is implicated in autophagy-related processes. Mono-FAT10ylated p62 interacts with LC3 on autophagosomes, leading to the formation of autophagosomes that eventually fuse with lysosomes. This process results in the degradation of the protein by lysosomes, with the resulting peptides being loaded onto MHC class II molecules [57, 85, 86].

FAT10 also modulates autophagy by promoting the degradation of SIRT1. It competes with SUMO1 for modification at the K734 site of SIRT1, thereby reducing LC3 deacetylation. This results in enhanced SIRT1 degradation through FAT10's C-terminal di-glycine motif, ultimately suppressing

autophagy and protecting cardiac tissue from ischemic injury [87].

In hepatocellular carcinoma (HCC), FAT10 stabilizes the E3 ubiquitin ligase NEDD4, leading to PTEN downregulation and activation of the AKT signaling pathway. This promotes autophagy and contributes to sorafenib resistance in HCC cells [88].

Mueller et al. found that the presence of autophagy regulator AMBRA1 decreases the formation of HUWE1-FAT10 conjugates. Conversely, FAT10 enhances the interaction between HUWE1 and AMBRA1, suggesting that FAT10ylation of HUWE1 facilitates its association with AMBRA1 [63].

Antibacterial role

FAT10 has been shown to cooperate with the autophagy adaptor p62 in labeling intracellular *Salmonella Typhimurium*, thereby promoting bacterial clearance. FAT10-deficient NRAMP1-transgenic mice exhibit higher susceptibility to oral *Salmonella* infection compared to wild-type counterparts, indicating FAT10's role in bacterial defense. Colocalization of FAT10 with autophagy proteins such as p62, NDP52, and LC3B further supports its involvement in antibacterial autophagy [89].

Antiviral role

Retinoic acid-induced protein-I (RIG-I), a cytosolic RNA sensor, plays a key role in innate immunity. However, aberrant RIG-I activity is associated with autoimmune and inflammatory diseases. Nguyen et al. demonstrated that that FAT10 binds non-covalently to the 2CARD domain of RIG-I, thereby modulating RIG-I's solubility and inhibiting the activation of IRF3 and NF-κB [65]. FAT10 is recruited into a RIG-I-TRIM25 repressor complex, preventing the formation of antiviral stress granules and sequestering active RIG-I from mitochondria. These findings suggest FAT10 acts as a novel negative regulator of RIG-I-mediated inflammation [65].

Upon H5N1 infection in BALB/c mice and human respiratory epithelial cell lines (A549 and BEAS-2B), FAT10 expression is induced via the RIG-I-NF-κB pathway. Elevated FAT10 suppresses type I interferon production, enhances viral replication, and reduces host cell viability [90].

Following LCMV infection, FAT10-deficient mice exhibit reduced IFN-γ secretion and IL-12 p40 mRNA expression, along with increased type I interferon production, suggesting that FAT10 fine-tunes the balance between type I and type II interferons during viral infection [91].

Tumorigenesis

FAT10 is overexpressed in a variety of cancers, including hepatocellular, gastric, colorectal, breast, bladder, pancreatic, and gliomas [61, 92-104].

For example, FAT10 promotes aneuploidy by interacting with the mitotic spindle checkpoint protein MAD2 during mitosis [68]. In addition, Zhang et al. reported that FAT10 promotes HCC development by mediating p53 degradation and may serve as a prognostic marker [62]. In hepatocellular carcinoma (HCC), FAT10 enhances cell proliferation, invasion, migration, and adhesion through the NF-κB-CXCR4/7 axis [105]. FAT10 and HOXB9 are overexpressed in HCC. FAT10 stabilizes β-catenin by inhibiting its ubiquitination and degradation, thereby upregulating HOXB9 via the β-catenin/TCF4 pathway, which drives the invasion and metastasis of HCC [64].

In pancreatic cancer (PC), FAT10 competes with ubiquitin to stabilize FOXM1, enhancing PC cell proliferation, epithelial-mesenchymal transition (EMT), and gemcitabine resistance [98]. Yuan et al. found that increased FAT10 expression correlates with poor prognosis in glioma and promotes tumor aggressiveness, making it a potential prognostic biomarker [104].

Taken together, FAT10 is implicated in diverse disease processes and holds promise as a therapeutic target and prognostic indicator.

The aims of the studies

Based on the background above, we have developed a comprehensive understanding of FAT10's structure, characteristics, and functions. Notably, FAT10 is inducible by pro-inflammatory cytokines, is selectively expressed in immune cells, participates in post-translational modifications, and modulates proteasomal degradation. Despite this knowledge, several key questions remain unanswered.

To address current knowledge gaps, this study will focus on the following aspects of FAT10 biology:

Chapter 1

Investigate the role of FAT10 phosphorylation in regulating its degradation pathway.

Chapter 2

Explore whether FAT10 influences IL-12 expression in DCs, given that FAT10

is expressed in DCs, which secrete IL-12 to promote Th1 differentiation.

Chapter 3

Identify potential E3 ligases for FAT10, beyond the currently known Parkin, using a FAT10-based probe.

Through these focused investigations, we aim to further elucidate the biochemical and immunological functions of FAT10 and contribute valuable insights to future research in the field.

Chapter 1
Phosphorylated FAT10 is more efficiently conjugated to substrates, does not bind to NUB1L, and does not alter degradation by the proteasome

1.1 Abstract

Background: FAT10 is a member of the ubiquitin-like modifier family. Similar to ubiquitin, FAT10 has a distinct enzyme cascade consisting of E1-activating, E2-conjugating, and possibly several E3-ligating enzymes, which will covalently link FAT10 to substrate proteins in order to target them directly for proteasomal degradation. FAT10 was reported to be phosphorylated by IKKβ during infection with influenza A virus. **Methods**: To assess the difference between the FAT10-dependent degradation of phosphorylated FAT10 and the non-phosphorylated FAT10 wild type (FAT10 WT), a mutated FAT10 that mimicked phosphorylation (FAT10 D) was constructed by replacing several serine residues and one threonine residue with aspartic or glutamic acid. The FAT10 degradation or conjugation was compared between the phospho-mimetic FAT10 and the wild-type FAT10 with respect to the dependence of the E3 ligase TRIM25, the UBL-UBA protein NUB1L, and the proteasomal ubiquitin receptor RPN10. **Results**: The phospho-mimetic FAT10 was more efficiently conjugated to substrate proteins as compared to the wild-type FAT10, particularly if TRIM25 was co-expressed. Additionally, the phospho-mimetic FAT10 was not bound by NUB1L. However, this did not affect FAT10 D or FAT10 WT degradation. No differences were found in the binding affinity of phospho-mimetic FAT10 to RPN10. **Conclusions**: In brief, the phospho-mimetic FAT10 shows enhanced conjugation efficiency, but phosphorylation does not alter its degradation by the proteasome. This reveals that phosphorylation may fine-tune FAT10's interactions with specific interaction partners without disrupting its core function of proteasomal degradation.

Keywords: *FAT10; phospho-mimetic FAT10; FAT10ylation; degradation; TRIM25; NUB1L; RPN10*

1.2 Introduction

Human leukocyte antigen (HLA)-F adjacent transcript 10 (FAT10) is a member

of the ubiquitin-like modifier family, encoded in the major histocompatibility complex (MHC) class I region [106]. FAT10, a 165 aa multifunctional protein [67], consists of two tandemly arranged ubiquitin-like (UBL) domains (N- and C-domains) linked by a flexible linker (KPSDE) [107]. The N- and C-terminal UBL domains of FAT10 share 29% and 36% sequence identity with ubiquitin, respectively [108]. Similar to the ubiquitin cascade, FAT10 has a specific enzymatic cascade for directing its conjugates to proteasomal degradation [72, 73], —a process termed "FAT10ylation" [109]. Several enzymes participate in the cascade, including the bispecific E1-activating enzyme UBA6 [110-112], the bispecific E2-conjugating enzyme USE1 [47, 110, 113], and putative E3 ligases such as Parkin [114-116]. So far, several proteins have been shown to interact with FAT10 through covalent or non-covalent interaction. Examples of covalently interacting proteins include p62, proliferating cell nuclear antigen (PCNA) [60] Parkin [114], and HUWE1 [63]. FAT10 plasticity destabilizes substrates significantly and creates partially unstructured regions in the substrate to enhance degradation [117]. Some reported non-covalently interacting proteins include histone deacetylase 6 (HDAC6), β-catenin [64, 118], and Mfn2 [114]. These proteins play important roles in several biological processes related to FAT10 [105], and are possibly implicated in the role of FAT10 in disease development. Additionally, numerous studies have demonstrated a correlation between FAT10 and cancer [61, 92-101].

FAT10 is predominantly expressed in the immune system, e.g., the thymus, lymph nodes, and spleen, whereas ubiquitin is expressed ubiquitously [78, 119-121]. RIG-I [122] plays a key role in the innate immune response to RNA viruses. FAT10 inhibits RIG-I activation and impairs the type I interferon signaling cascade. Two E3 ligases—TRIM25 and ZNF598—are notable for their roles in the signaling pathway. TRIM25 stabilizes FAT10 bound to RIG-I and ZNF598 promotes the interaction between FAT10 and RIG-I [65, 119]. Moreover, FAT10 is phosphorylated by IκB kinase β (IKKβ) in response to the pro-inflammatory cytokine tumor necrosis factor (TNF) and during influenza A virus infection at multiple serine (S) and threonine (T) residues (S62, S64, T77, S95, and S109) [76]. Additionally, the induction of type I IFN is decreased by phosphorylation of FAT10 [76]. Nevertheless, the effect of phosphorylation of FAT10 in the proteasomal degradation pathway remains unclear.

FAT10 targets substrates for degradation by the 26S proteasome, a multienzyme complex which comprises the 19S regulatory particle (RP, also called PA700) and a 20S cylindrical core particle (CP) [56, 123]. NEDD8 ultimate buster-1 long (NUB1L) and RPN10 are key proteins in FAT10 degradation. NUB1L, an alternative splicing variant of NUB1, harbors three ubiquitin-associated (UBA) domains, as compared to the two UBA domains of NUB1, and one ubiquitin-like domain (UBL) [124, 125]. NUB1L accelerates

FAT10 degradation [44, 126]. NUB1L utilizes FAT10's intrinsic instability to trap its N-terminal ubiquitin-like domain in an unfolded state, facilitating degradation [127]. UBL-UBA domain proteins, such as RAD23, bind polyubiquitin and the proteasome and are an additional layer of regulated proteasomal degradation [128]. The UBA domains of NUB1L do not bind mono- or polyubiquitin but interact with the N-terminal UBL domain of FAT10, while the UBL domain of NUB1L binds to the von Willebrand A (VWA) domain of RPN10 [129]. RPN10 is a subunit of 19S RP and was the first reported polyubiquitin receptor [49, 130, 131]. FAT10 can on its own directly bind to the VWA domain of RPN10 to facilitate FAT10 degradation [53]. However, it is unknown how phosphorylated FAT10 interacts with NUB1L or RPN10 in the FAT10 degradation pathway.

Prompted by a previous study [76], we constructed a phospho-mimetic FAT10, which was used in this study. We aimed to elucidate the role of the phospho-mimetic FAT10 variant in the FAT10 degradation pathway, particularly with respect to its interaction with NUB1L.

1.3 Material and methods

1.3.1 Cell culture and cell lines

Human HEK293T cells were cultured in DMEM (Gibco, 61965026, USA) supplemented with 10% fetal bovine serum (Gibco, Darmstadt, Germany) and 1% penicillin-streptomycin (Gibco, 15140122, USA). Tetracycline-regulated, NUB1L-overexpressing HEK293 cells were maintained under similar culture conditions [55, 132]. All cells were sourced from our laboratory's cell repository.

1.3.2 Plasmid constructs

All clones were generated using the original plasmids listed in Tables S1.1 and S1.2. The original plasmids, such as pcDNA3.1-His-3xFLAG-FAT10 (FAT10 WT), pCMV-FLAG-TRIM25, and Human s5a, were obtained from our laboratory's plasmid repository. Oligonucleotide primers were designed to be complementary to the opposite strands of the vector with the desired mutation. All primers are listed in Tables S1.1 and S1.2. For site-directed mutagenesis, the QuikChange Lightning Multi Site-Directed Mutagenesis Kit (Agilent, 210513, Germany) and the Q5 Site-Directed Mutagenesis Kit (NEB, E0552S, USA) manual. As for normal plasmid construction, the extension of

primers by Phusion High-Fidelity DNA Polymerase (NEB, M0530S, USA) generated a desired PCR product. Products and vectors were ligated using the Quick Ligation Kit (NEB, M2200S, USA) following digestion with specific enzymes. The ligated constructs were transformed into competent E. coli, and isolated plasmids from bacterial colonies were sequenced.

1.3.3 Transient transfection of plasmids

Plasmids were transiently transfected into HEK293T cells using Polyethyleneimine (PEI; Polysciences, 23966, USA) at a 1:3 ratio of DNA to reagent dissolved in serum-free DMEM medium for 24 h.

1.3.4 Cycloheximide chase (CHX) experiments

CHX experiments were performed as described previously [107]. In brief, cells were treated with 50 μM cycloheximide and divided into aliquots, one of which was harvested immediately, while the remaining aliquots were harvested at indicated time points.

1.3.5 Immunoprecipitation and Immunoblotting

Immunoprecipitation and immunoblotting experiments were performed as previously described [107]. The antibodies used are listed in Table S1.3. In brief, cells were lysed and centrifuged, and the cleared supernatants were transferred into new reaction tubes. Then, 20 μL of protein G beads was added to each of the antibodies. After overnight incubation, the samples were centrifuged, the supernatants were separated, and the beads with bound proteins were washed five times and then subjected to boiling in SDS sample buffer. Next, SDS gel electrophoresis and immunoblotting followed by incubation with primary and secondary antibodies was performed.

1.3.6 Radiolabeling and pulse-chase experiments

Radiolabeling and pulse–chase experiments were performed as previously described [55]. In brief, cells were starved for one hour in methionine- and cysteine-free medium. After starvation, the cells were pulsed for one hour with S35 Meth/Cys in medium. After the pulse, the radioactive medium was removed by washing the cells three times. The cells were resuspended in normal medium divided into aliquots and harvested at indicated time points. After lysis, immunoprecipitation and SDS gel electrophoresis gels were dried and exposed to phosphor imaging plates.

1.3.7 Statistical analysis

All statistical analyses were performed using GraphPad Prism software (version 8.0). Error bars represent means ± SDs unless otherwise stated. The two-tailed unpaired Student's t-test and one-way ANOVA with Tukey's multiple-comparison test were used to compare data sets with two or more continuous variables, respectively.

1.4 Results

1.4.1 Phospho-mimetic FAT10 is more efficiently conjugated than wild-type FAT10

Phosphorylation of FAT10 at multiple sites (S62, S64, T77, S95, and S109) has been previously reported [76], and the positions of the sites are schematically shown in Figure 1.1A. Serine (S) and threonine (T) carry a negative charge after phosphorylation. To simulate such a charge, we generated a phospho-mimetic FAT10 mutant (FAT10 D), with S62, S64, S95, and S109 mutated to aspartic acid (D) and T77 mutated to glutamic acid (E). To investigate the impact of these modifications on FAT10's role in protein degradation, we transiently transfected HEK293T cells with either wild-type FAT10 (FAT10 WT) or FAT10 D. The expression of FAT10, as well as its conjugate formation, was analyzed by immunoprecipitation and immunoblotting. The result indicated that FAT10 D, despite its lower expression rate, formed at least as many conjugates as FAT10 WT, yielding a higher conjugate-to-monomer ratio (Figure 1.1B,C). The lower expression rate of FAT10 D was not due to a faster degradation rate because FAT10 D was degraded at the same rate as FAT10 WT (Figure 1.1D,E). Notably, when cells were treated with the proteasome inhibitor MG-132, it was evident that FAT10 D exhibited a significantly higher conjugation efficiency than FAT10 WT (Figure 1.1D,F). Thus, it was suggested that phospho-mimetic FAT10 is more quickly or more efficiently conjugated to target proteins than wild-type FAT10.

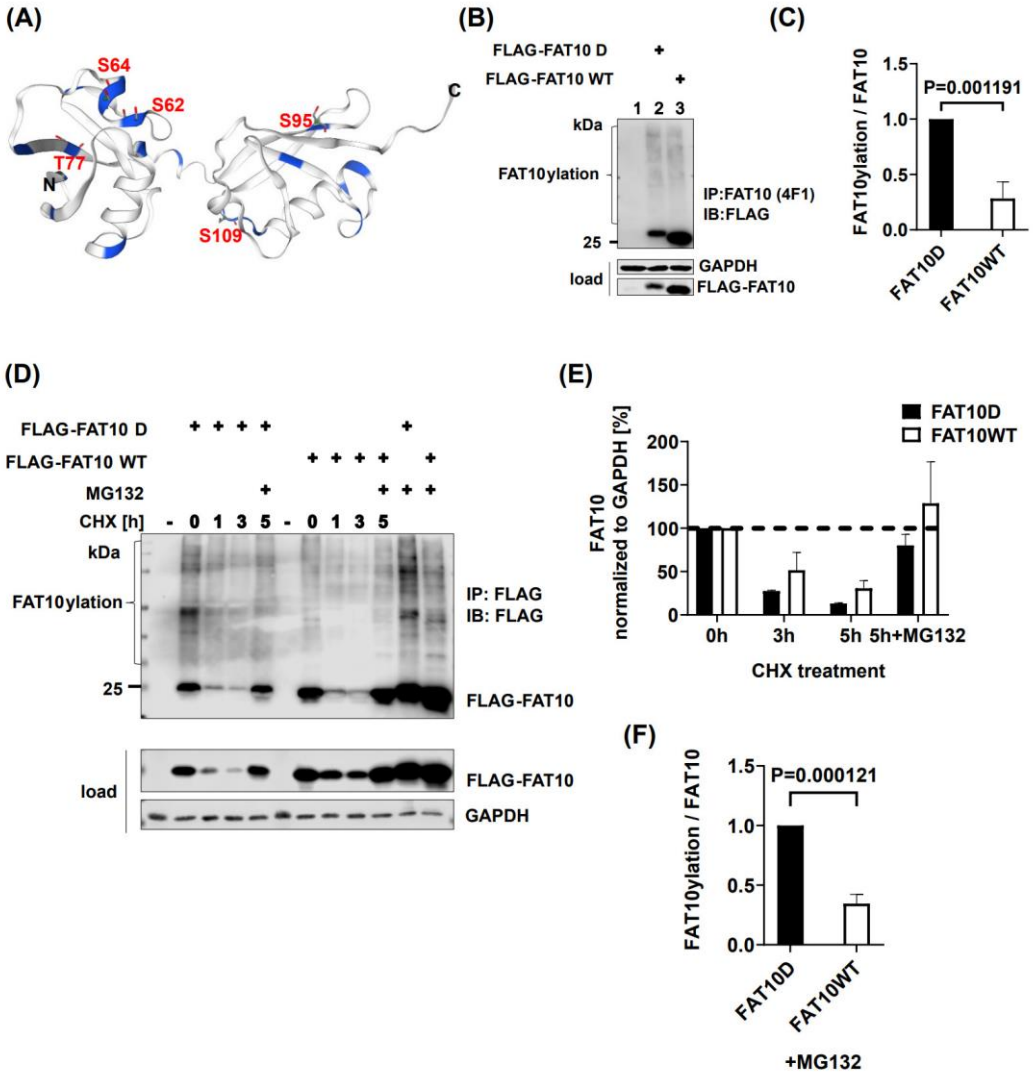

Figure 1.1. The phospho-mimetic FAT10 is more efficiently conjugated than wild-type FAT10. (**A**) FAT10 structure built in SWISS-MODEL. Blue represents all serine and threonine residues which might be phosphorylated. (**B**) HEK293T cells were transiently transfected with FLAG-FAT10 D or FLAG-FAT10 WT. One day later, cells were lysed, followed by FAT10 immunoprecipitation using a monoclonal FAT10-reactive antibody (4F1). SDS-PAGE and immunoblot analysis were performed with the indicated antibodies. (**C**) Quantification of the ECL signals from three independent experiments, as shown in (**B**). Values of FAT10ylation were normalized to the respective FLAG-FAT10 (WT or D) expression levels in the immunoprecipitates. The value of FLAG-FAT10 D was set to 1, and all other values were calculated accordingly. An unpaired Student's t-test was used for statistical analysis. Error bars represent means ± SDs. (**D**) HEK293T cells were transiently transfected with constructs expressing the indicated forms of FLAG-FAT10, followed by a cycloheximide (CHX) chase for 5 h. Where indicated, cells were additionally treated for 5 h with MG132 (10 μM). The immunoprecipitation and immunoblot analyses were performed with the indicated antibodies. GAPDH was used as a loading control. (**E**) Quantification of the ECL signals of the lysates (loads) from three independent experiments, as shown in (**D**). Levels were normalized to the respective levels of the housekeeping gene GAPDH. Values at 0 h were set to unity, and the other values were calculated accordingly. (**F**) Quantification of the ECL signals obtained

from cells only treated with MG132 in three independent experiments, as shown in (**D**). Values of FAT10ylation were normalized to the respective FLAG-FAT10 (WT or D) expression levels in the immunoprecipitates. The value of FLAG-FAT10 D was set to 1, and all other values were calculated accordingly. An unpaired Student's t-test was used for statistical analysis. Error bars represent means ± SDs.

1.4.2 TRIM25 contributes to FAT10 conjugation, without changing the degradation

TRIM25, an E3 ubiquitin/ISG15 ligase, elicits RIG-I activation by inducing K63 polyubiquitination. A previous study demonstrated that FAT10 was recruited to RIG-I-TRIM25 to form an inhibitory complex, where FAT10 was stabilized by TRIM25 [65]. This prompted us to ask if there is any difference between FAT10 D and FAT10 WT concerning interaction with TRIM25. FAT10 and TRIM25 plasmids were co-transfected into HEK293T cells, and a cycloheximide chase was performed as described for Figure 1.1. FAT10 and potential conjugates were immune-precipitated and analyzed. As depicted in Figure 1.2, the co-expression led to a much better conjugation of FAT10 D as compared to FAT10 WT. There was no detectable influence of TRIM25 on the degradation rate of FAT10.

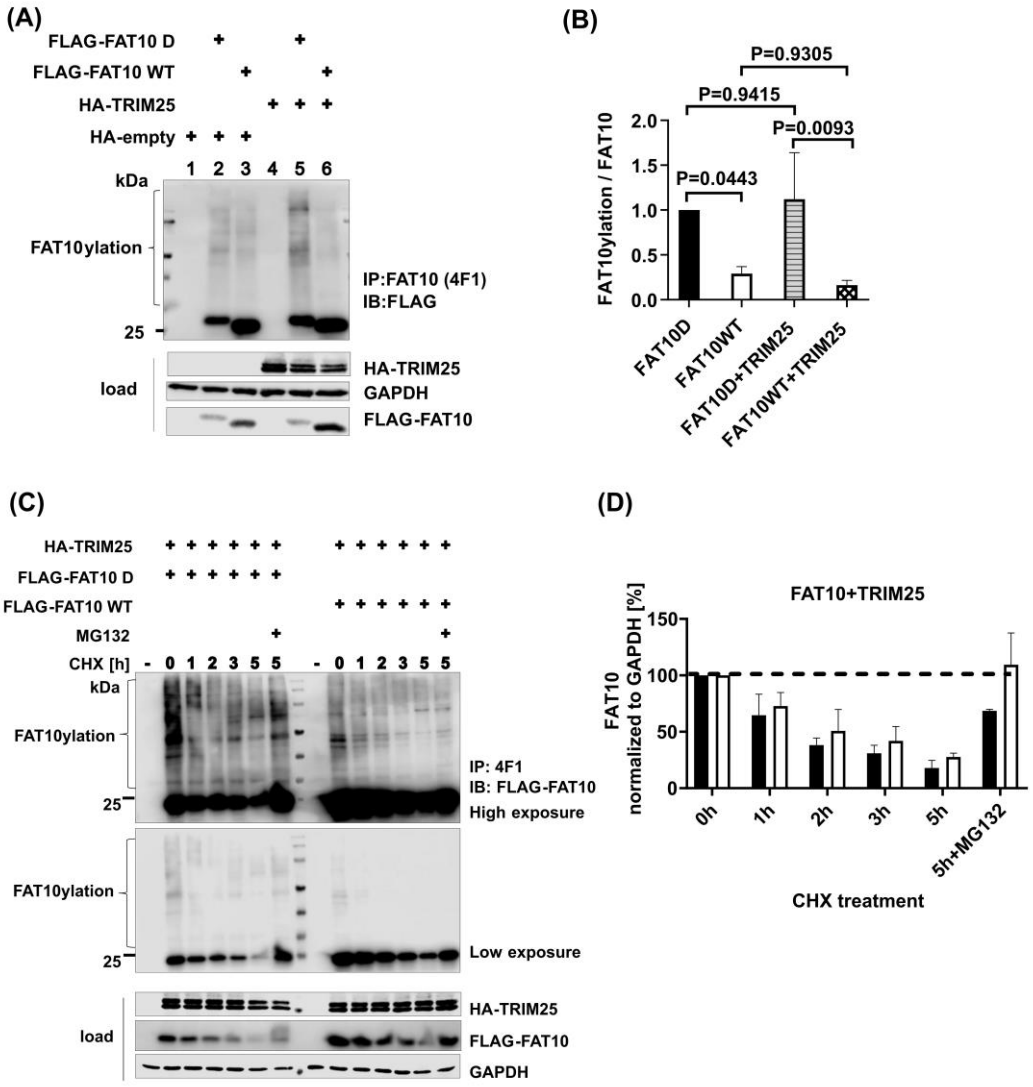

Figure 1.2. TRIM25 contributes to FAT10 expression but does not impact FAT10 degradation. (**A**) HEK293T cells were transiently co-transfected with TRIM25 and FAT10 expression plasmids. One day later, cells were lysed, followed by 4F1-immunoprecipitation, SDS-PAGE, and immunoblot analysis with the indicated antibodies. Quantification of the ECL signals from three independent experiments, as shown in (**B**). Values of FAT10ylation were normalized to the respective FLAG-FAT10 (WT or D) expression levels in the immunoprecipitates. The value of FLAG-FAT10 D was set to 1, and all other values were calculated accordingly. A one-way ANOVA with Tukey's multiple-comparison test was applied. Error bars represent means ± SDs. (**C**) HEK293T cells were transiently transfected with expression constructs for the indicated proteins, followed by a cycloheximide (CHX) chase for 5 h. Where indicated, cells were additionally treated for 5 h with MG132 (10 μM). Cells were lysed, followed by 4F1-immunoprecipitation, SDS-PAGE, and immunoblot analysis with the indicated antibodies. GAPDH was used as a loading control. Quantification of the ECL signals of the lysates (loads) from three independent experiments, as shown in (**D**). Levels were normalized to the respective levels of the housekeeping gene GAPDH. Values at 0 h were set to unity, and the other values were calculated accordingly.

1.4.3 The phospho-mimetic FAT10 alleviates the binding of NUB1L

FAT10 was reported to interact with the UBA domains of NUB1L [44]. To investigate whether FAT10 phosphorylation affects this interaction, we co-transfected HEK293T cells with either FAT10 WT or FAT10 D and NUB1L. Co-expression of NUB1L with FAT10 D or FAT10 WT resulted in a significant reduction in detectable FAT10 (Figure 1.3A,B). It was reported that NUB1L can bind to FAT10 and accelerate its degradation [55]. This observation is compatible with NUB1L-mediated accelerated FAT10 degradation. To investigate this in more detail, we first intended to detect binding of FAT10 D or FAT10 WT to NUB1L. Only in the case of FAT10 WT did co-expression and IP result in a co-precipitated band of NUB1L (Figure 1.3C). Apparently, FAT10 D lost its ability to interact with NUB1L. There are reports that phosphorylation of ubiquitin and NEDD8 at a single residue (S65 in both cases) [133, 134] changed their structure and function. We reported evidence of the phosphorylation of FAT10 at different sites [76] among them serine 64. To investigate whether a single phosphorylation site in FAT10 is sufficient to diminish the FAT10–NUB1L interaction, single and multiple mutants were generated and analyzed. As can be seen in Figure 1.4, the mutation of threonine 77 to glutamic acid had the most significant effect and was sufficient to almost prevent the binding of FAT10 to NUB1L. We reported previously that the interaction between NUB1L and FAT10 is not required for the accelerated degradation of FAT10 by NUB1L [126]. We analyzed the degradation rates of FAT10 WT and D in the presence of NUB1L in a cycloheximide chase experiment. As can be seen in Figure 1.5A,B, there was no significant difference in the rates of degradation of FAT10 WT and FAT10 D in the presence of NUB1L. To exclude any influence that the translation blocker cycloheximide might have on cellular processes, we performed a site-by-site radioactive pulse–chase experiment on FAT10 WT and FAT10 D with and without NUB1L. There was no obvious difference detectable in the rates of degradation of FAT10 WT and FAT10 D in the presence or absence of NUB1L (Figure 1.5C,D). However, the degradation of both FAT10 D and FAT10 WT was about 2-fold faster in the presence of NUB1L. This confirms our previous report about the independence of accelerated degradation and binding of FAT10 and NUB1L.

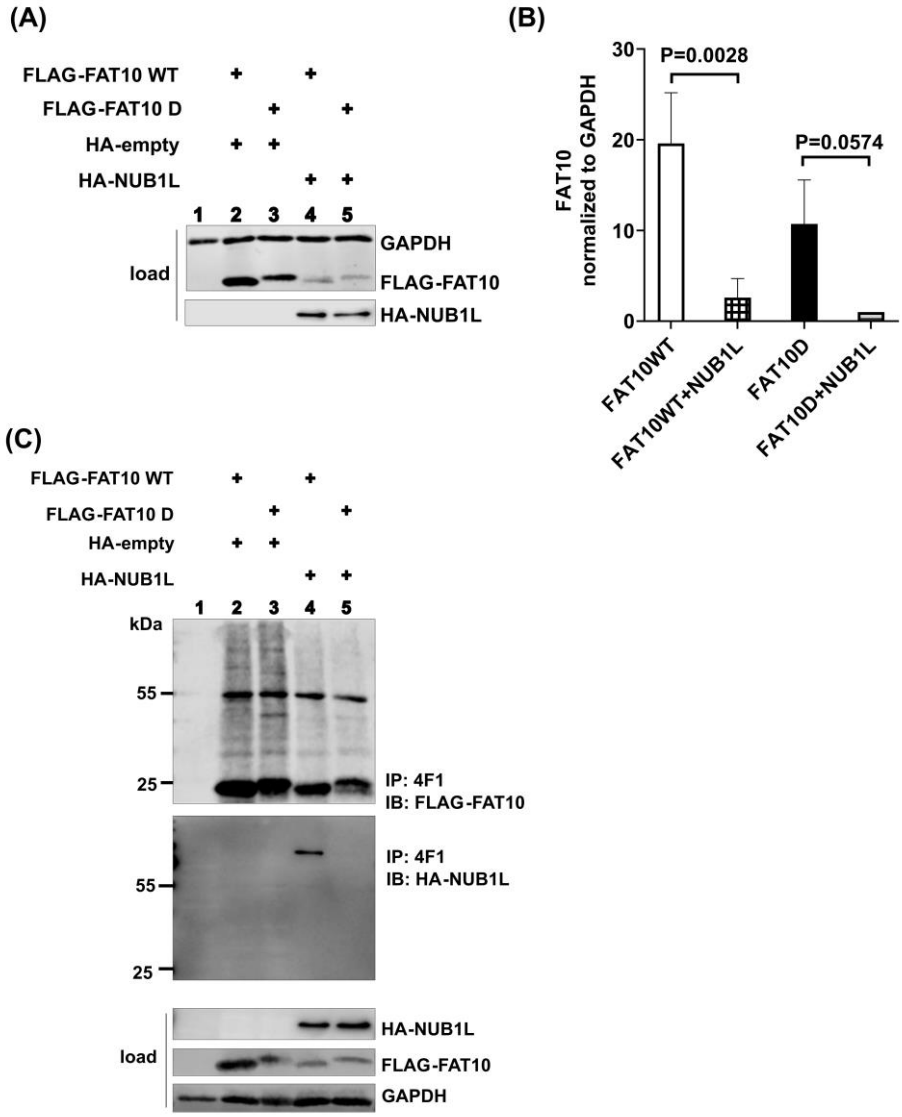

Figure 1.3. Phospho-mimetic FAT10 alleviates the binding of NUB1L. (**A**) HEK293T cells were transiently co-transfected with NUB1L and FAT10. One day later, cells were lysed, followed by SDS-PAGE and immunoblot analysis with the indicated antibodies. GAPDH was used as a loading control. (**B**) Quantification of the ECL signals of the lysates (loads) from three independent experiments, as shown in (**A**). Levels were normalized to the respective levels of the housekeeping gene GAPDH. The value of FLAG-FAT10 D was set to 1, and all other values were calculated accordingly. Statistical analysis was performed by one-way ANOVA with Tukey's multiple-comparison test. Error bars represent means ± SDs. (**C**) HEK293T cells were transiently co-transfected with NUB1L and FAT10 expression plasmids. One day later, cells were lysed, followed by immunoprecipitation (4F1 + protein A beads), SDS-PAGE, and immunoblot analysis with the indicated antibodies. GAPDH was used as a loading control.

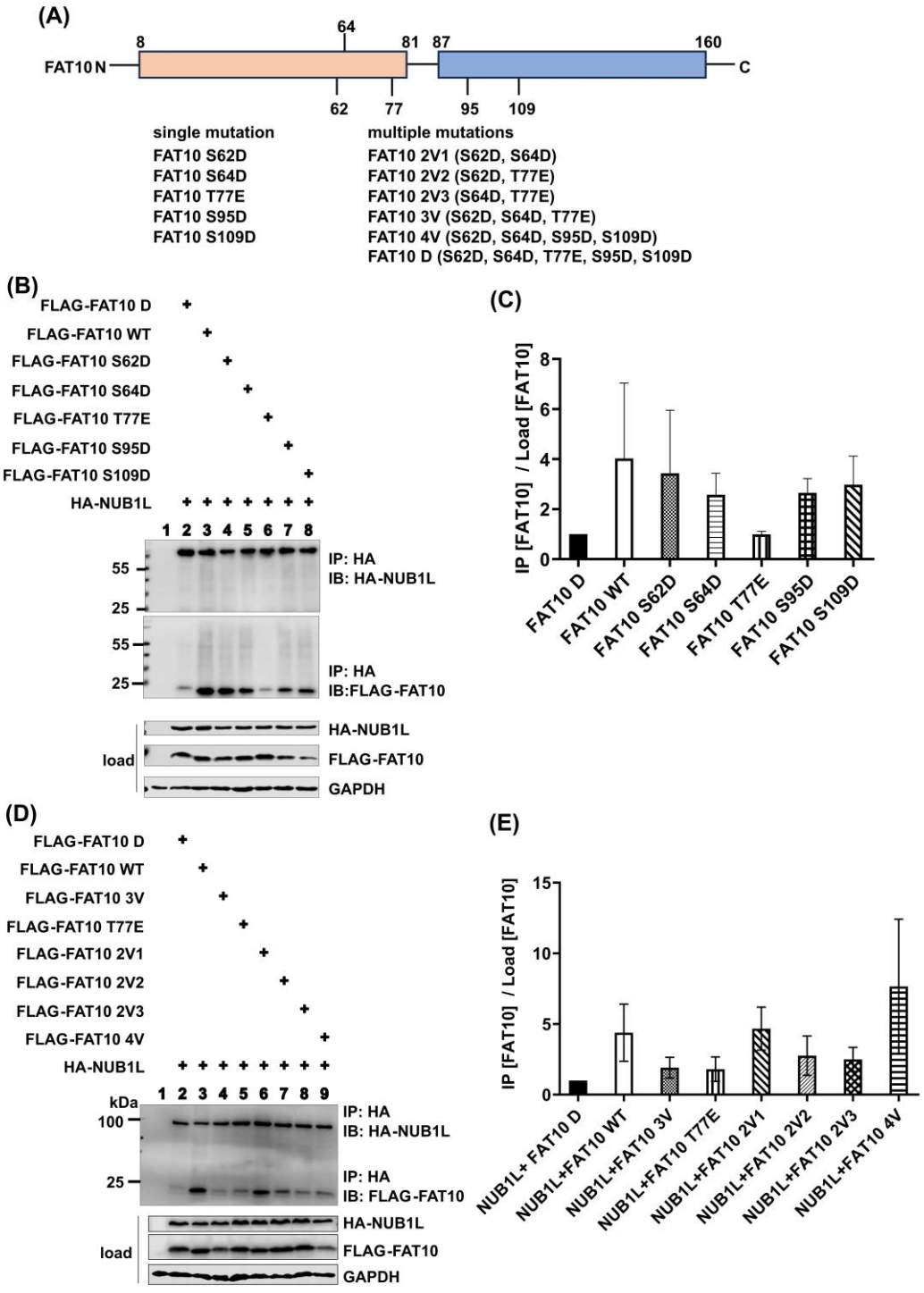

Figure 1.4. FAT10 threonine 77 is important in mediating FAT10–NUB1L interactions. (**A**) Scheme showing the protein domain of FAT10 and different mutations. (**B**,**D**) HEK293T cells were transiently co-transfected with NUB1L and FAT10. One day later, cells were lysed, followed by HA-immunoprecipitation, SDS-PAGE, and immunoblot analysis performed with the indicated antibodies. GAPDH was used as a loading control. (**C**,**E**) Quantification of the ECL signals from three independent experiments, as shown in (**B**) or (**D**). The ratio values represent FLAG-FAT10 expression levels in the immunoprecipitates relative to the respective FLAG-FAT10 expression levels in the lysates (loads). The value of FLAG-FAT10 D was set to 1,

and all other values were calculated accordingly.

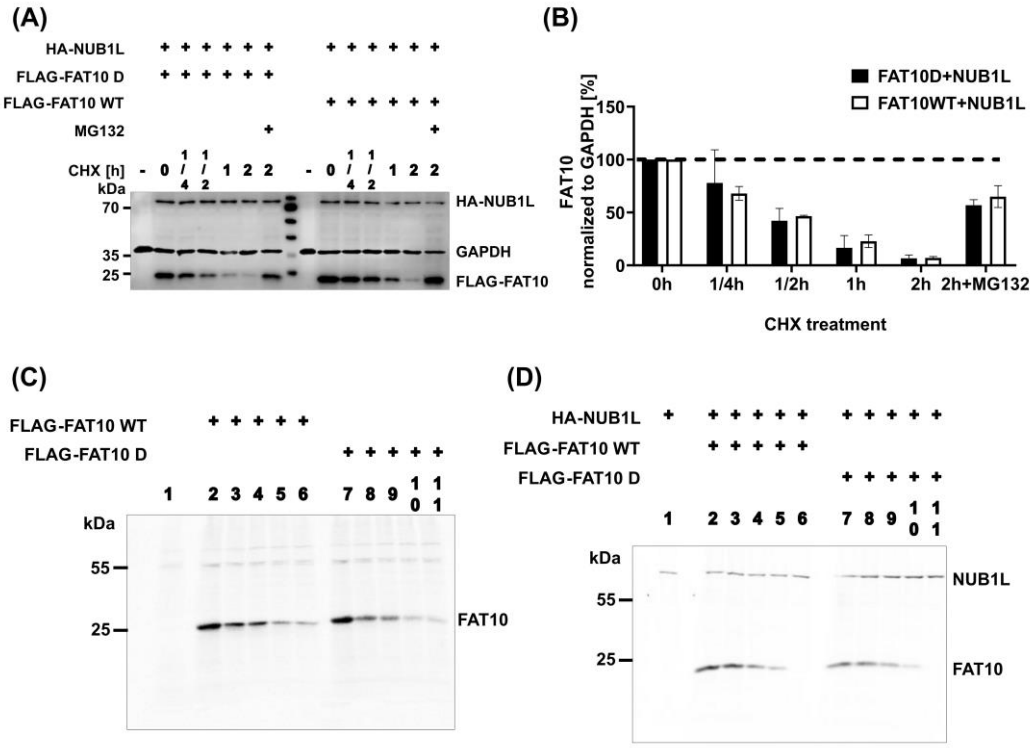

Figure 1.5. FAT10 D exhibits comparable degradation kinetics to FAT10 WT. (**A**) HEK293T cells were transiently transfected with constructs expressing the indicated plasmids, followed by a cycloheximide (CHX) chase for 5 h. Where indicated, cells were additionally treated for 5 h with MG132 (10 μM). Cells were lysed, followed by SDS-PAGE and immunoblot analysis with the indicated antibodies. GAPDH was used as a loading control. (**B**) Quantification of the ECL signals of the lysates (loads) from three independent experiments, as shown in (**A**). Levels were normalized to the respective levels of the housekeeping gene GAPDH. Values at 0 h were set to unity, and the other values were calculated accordingly. A stable cell line (overexpressing NUB1L) was transiently transfected with FAT10 D or FAT10 WT and treated with (**D**) or without (**C**) tetracycline. Following this, cells were subjected to a radioactive pulse–chase experiment.

1.4.4 The phospho-mimetic FAT10 does not change the binding of RPN10

FAT10 not only binds with its N-terminal UBL domain to the UBA domains of NUB1L, but it also interacts with the VWA domain of RPN10 via its C-terminal UBL domain for protein degradation [53]. We examined whether the phospho-mimetic mutations altered FAT10's interaction with RPN10. Co-transfection of HEK293T cells with FAT10 WT or FAT10 D and RPN10, followed by immunoprecipitation, showed no significant difference in the interaction between FAT10 WT or FAT10 D and RPN10 (Figure 1.6). This

indicates that despite the alleviated interaction with NUB1L, FAT10 D can still bind to RPN10 to mediate protein degradation, suggesting that phosphorylation of FAT10 does not impair its degradation function.

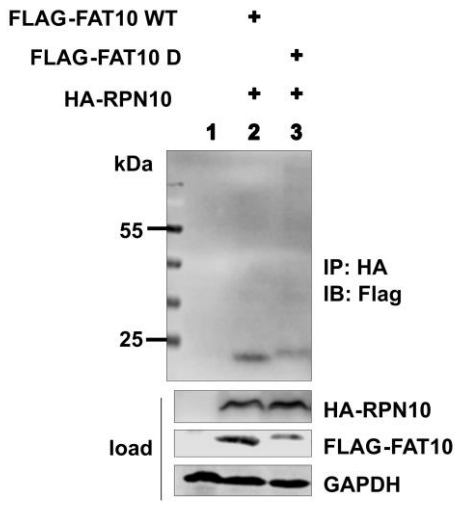

Figure 1.6. The phospho-mimetic FAT10 D does not change the binding of RPN10. HEK293T cells were transiently co-transfected with RPN10 and FAT10. One day later, cells were lysed, followed by immunoprecipitation (HA beads), SDS-PAGE, and immunoblot analysis with the indicated antibodies. GAPDH was used as a loading control.

1.5 Discussion

Previous reports have shown that not only ubiquitin [133, 135], SUMO [136] and NEDD8 [134] can be phosphorylated, but also FAT10 can be phosphorylated by IKKβ upon TNF stimulation and during influenza A virus infection [76]. Phosphorylation of FAT10 has been shown to limit IFN-I production during inflammation. Phosphorylation of ubiquitin and NEDD8 occurs on serine 65 [133, 134], enabling interactions with specific binding proteins. Phospho-ubiquitin activates the E3 ligase Parkin, leading to faster conjugation of ubiquitin from the loaded E2 UBCH7, while phospho-NEDD8 leads to activation of HSP70 [133, 134]. We constructed a phospho-mimetic FAT10 (FAT10 D, S62D, S64D, T77E, S95D, and S109D) by substituting serine and threonine residues with aspartic acid and glutamic acid, respectively (Figure 1.1A). We chose this approach because it was also used in the phospho-ubiquitin–parkin study [133]. FAT10 D, despite its lower expression, yielded at least the same amount of conjugated FAT10 as FAT10 WT, leading to a much higher conjugate-to-monomer ratio (Figure 1.1B,C). The rate of degradation was not different between FAT10 D and FAT10 WT (Figure

1.1D,E).

In the type I interferon signaling cascade, TRIM25 is beneficial for stabilizing FAT10 [65]. Phosphorylated FAT10 has been shown to reduce TRAF3 ubiquitination, hindering interferon regulatory factor 3 (IRF3) phosphorylation and downstream IFN-I induction [76]. To assess the interaction with TRIM25 after FAT10 is phosphorylated, FAT10 D and WT and TRIM25 were co-transfected into HEK293T cells. As can be seen in Figure 1.2A,B, the difference in the conjugate formation of FAT10 D and FAT10 WT was even more pronounced in the presence of TRM25. This seems to be analogous to phospho-ubiquitin, which also activates an E3, Parkin [133]. The rate of degradation was not changed in the presence of TRIM25 (Figure 1.2C,D). Additionally, the E1 and E2 enzymes of FAT10 were transfected with FAT10 and TRIM25 into UBA6 KO and USE1 KO cells. The results revealed that UBA6 and USE1 are indispensable for FAT10ylation (Figure S1.1).

Studies have shown that FAT10 targets substrates for degradation by the 26S proteasome and that NUB1L accelerates the process [44, 56, 123-126]. NUB1L can bind FAT10 via its UBA domains; however, for accelerated FAT10 degradation, the UBL domain of NUB1L is sufficient and the binding of FAT10 is dispensable [126]. In the current study, HEK293T cells were co-transfected with FAT10 and NUB1L. Transfection with NUB1L resulted in a reduction in detectable FAT10, independently whether FAT10 WT or FAT10 D was analysed. (Figure 1.3A,B). We tested whether FAT10 D could still be co-immunoprecipitated with NUB1L but failed to detect an interaction between FAT10 D and NUB1L, unlike FAT10 WT, which bound NUB1L (Figure 1.3C). To exclude the possibility that FAT10 D was somehow differently folded, we used FAT10 variants with only a single amino acid changed to mimic phosphorylation, as well as some combinations (Figure 1.4A). The experiments identified Thr77 as a key residue for this interaction (Figure 1.4B–E). As soon as Thr 77 carried a negative charge, the interaction with NUB1L was strongly diminished. This is analogous to ubiquitin and NEDD8, where a single-site phosphorylation is sufficient to change an interaction [134]. NUB1L was reported to accelerate the degradation of FAT10 [55], and this was independent of FAT10 binding to NUB1L [126]. The analysis of the half-lives of FAT10 D and FAT10 WT in cycloheximide chase experiments did not reveal any differences. To exclude any effect of the translational inhibitor cycloheximide, we used a radioactive pulse–chase labeling approach with and without NUB1L. As shown in Figure 1.5C,D, FAT10 and FAT10 D behaved indistinguishably. Their half-lives were the same, and the acceleration by NUB1L was the same as well. This confirms the data reported by Schmidtke [126] on the independence of the accelerated degradation from the binding. Furthermore, the results are in agreement with

reports about other UBL-UBA domain proteins, such as Rad23 and Dsk2 [137, 138]. These proteins bind polyubiquitinated proteins and act as soluble polyubiquitin carriers to the 26S proteasome, defining a new layer of substrate specificity [128]. Reported functions of the UBL-UBA proteins include inhibition of excess polyubiquitination, prevention of deubiquitination, activation of the 26 S complex, and positioning of the substrate in a favorable position for degradation. The fact that NUB1L prefers the binding of unphosphorylated FAT10 may point towards a new level of regulation. NUB1L leads to faster degradation of FAT10 and its conjugates. Overexpression of FAT10 is toxic in some cell lines [71], so NUB1L may reduce the toxicity of FAT10 by removing it. However, conjugation of FAT10 is also required. The phosphorylation of FAT10 may prevent it from binding to NUB1L, leaving it available for conjugation. After conjugation, the substrate is still removed more quickly in the presence of NUB1L. The UBL domain of NUB1L interacts with the von Willebrand A (VWA) domain of the proteasomal subunit RPN10 for FAT10 degradation [129]. FAT10 itself can directly interact with the VWA domain of RPN10 to enable its degradation [53]. The interaction between FAT10 and RPN10 was not affected by the phospho-mimetic mutations (Figure 1.6), suggesting that FAT10's degradation pathway remains intact even with altered NUB1L binding, explaining why there was no difference in the degradation of FAT10 D as compared to FAT10 WT. This was also proof that FAT10 D was correctly folded, as the binding to RPN10 and degradation by the proteasome were indistinguishable from those of FAT10 WT. There have been at least three reports in recent years providing evidence that FAT10 induces cancer by the stabilization of different proteins [98, 139, 140]. The mechanism is possibly the prevention of ubiquitylation by blocking lysine residues in the respective proteins. Apparently, degradation via the ubiquitin pathway is faster with respect to the FAT10 pathway. That is why an upregulated conjugation with FAT10 without faster degradation may be important in cancer development. More FAT10ylated protein means fewer substrates available for ubiquitylation and therefore a stabilization of certain proteins, which may contribute to cancer development.

In conclusion, while phospho-mimetic FAT10 exhibits increased conjugation efficiency, it does not alter the overall degradation process of itself or its conjugates. This suggests that phosphorylation may fine-tune FAT10's interactions with specific partners without disrupting its core function in proteasomal degradation.

1.6 Supplementary information

Table S1.1. Site-directed mutagenesis

Constructed plasmids	Primers	Templates
FAT10 D (S62D, S64D, T77E, S95D, S109D)	F1: 5′-GATCTTAAAGCCACGGAGAGACCTCGATTCTTATGGCATTGAC AAAG-3′ F2: 5′-GAAGACCATCCACCTTGAGCTGAAAGTGGTGAAGCCCAG-3′ F3: 5′-CCCTTGTTTCTTGTGGAGGATGGTGATGAGGCAAAGAGGC-3′ F4: 5′-CTCCAGGTGCGAAGGGACAGCTCAGTGGCACAAG-3′	pcDNA3.1-His-3xFLAG-FAT10 (FAT10 WT)
FAT10 S62D	F: 5′- GCC ACG GAG AGA CCT CTC ATC TTA TG-3′ R: 5′- TTT AAG ATC TTG GAG CCC-3′	
FAT10 S64D	F: 5′- GAG AAG CCT CGA TTC TTA TGG CAT TGA C-3′ R: 5′- CGT GGC TTT AAG ATC TTG-3′	
FAT10 T77E	F: 5′- GAAGACCATCCACCTTGAGCTGAAAGTGGTGAAGCCCAG -3′ R: 5′- TCT TTG TCA ATG CCA TAA GAT GAG-3′	
FAT10 S95D	F: 5′- CCCTTGTTTCTTGTGGAGGATGGTGATGAGGCAAAGAGGC -3′ R: 5′- CAG CTC CTC ATC ACT GGG CT-3′	
FAT10 S109D	F: 5′- CTCCAGGTGCGAAGGGACAGCTCAGTGGCACAAG -3′ R: 5′- GAG GTG CCT CTT TGC CTC ATC -3′	
FAT10 2V1 (S62, 64D)	F: 5′- GATCTTAAAGCCACGGAGAGACCTCGATTCTTATGGCATTGACAA AG -3′ R: 5′- TTGGAGCCCAGCAAAAGA-3′	
FAT10 2V2 (S62D, T77E)	F: 5′- GAAGACCATCCACCTTGAGCTGAAAGTGGTGAAGCCCAG -3′ R: 5′- TCT TTG TCA ATG CCA TAA GAT GAG-3′	FAT10 S62D
FAT10 2V3 (S64D, T77E)	F: 5′- GAAGACCATCCACCTTGAGCTGAAAGTGGTGAAGCCCAG -3′ R: 5′- TCT TTG TCA ATG CCA TAA GAT GAG-3′	FAT10 S64D
FAT10 3V (S62D, S64D, T77E)	F: 5′- GAAGACCATCCACCTTGAGCTGAAAGTGGTGAAGCCCAG -3′ R: 5′- TCT TTG TCA ATG CCA TAA GAT GAG-3′	FAT10 2V1 (S62, 64D)
FAT10 4V (S62D, S64D, S95D, S109D)	F: 5′- CATCCACCTTACCCTGAAAGTGGTGA-3′ R: 5′- GTCTTCTCTTTGTCAATGC-3′	FAT10 D (S62D, S64D, T77E, S95D, S109D)

Table S1.2. Normal construction

Constructed plasmid	Primers	Original plasmid and restriction sites
HA-TRIM25	F: 5′-GAAACGGTACCTATGGCAGAGCTGTGC-3′ R: 5′-GTTTCTCTAGACCTACTTGGGGGAGCA-3′	pCMV-FLAG-TRIM25 and pcDNA-HA-hFAT10 Kpn I and Xba I
HA-RPN10	F: 5'-GAA ACG GTA CCT ATG GTG TTG GAA-3' R: 5'-GTT TCT CTA GAC TCA CTT CTT GTC-3'	Human s5a and pcDNA-HA-hFAT10 Kpn I and Xba I

Table S1.3. Regents

Reagents or kit	Company	Cat No.
EZview™ Red Protein A Affinity Gel	Millipore	P6486
EZview™ Red Anti-HA Affinity Gel	Millipore	E6779
EZview™ Red ANTI-FLAG® M2 Affinity Gel	Millipore	F2426
Monoclonal ANTI-FLAG® M2 antibody produced in mouse	Sigma-Aldrich	F1804
Monoclonal ANTI-FLAG® M2-Peroxidase (HRP) antibody produced in mouse	Sigma-Aldrich	A8592
Anti-GAPDH antibody produced in rabbit	Sigma-Aldrich	G9545
Anti-HA−Peroxidase antibody, Mouse monoclonal	Sigma-Aldrich	H6533
Monoclonal ANTI- FAT10 antibody produced in mouse (4F1)	Our laboratory	-
IRDye® 800CW Goat anti-Rabbit IgG Secondary Antibody	LICOER	926-32211
IRDye® 800CW Goat anti-Mouse IgG Secondary Antibody	LICOER	926-32210
IRDye® 680RD Goat anti-Rabbit IgG Secondary Antibody	LICOER	926-68071
IRDye® 680RD Goat anti-Mouse IgG Secondary Antibody	LICOER	926-68070
cOmplete™, EDTA-free Protease Inhibitor Cocktail	Roche	4693132001
β-mercaptoethanol	ROTH	4227.3
DMEM, high glucose, GlutaMAX™ Supplement	Gibco	61965026
Fetal Bovine Serum	Gibco	10270106
Penicillin-Streptomycin	Gibco	15140122
Polyethyleneimine (PEI)	Polysciences	23966
QuikChange Lightning Multi Site-Directed Mutagenesis Kit	Agilent	210513
Q5® Site-Directed Mutagenesis Kit	NEB	E0552S
Phusion® High-Fidelity DNA Polymerase	NEB	M0530S
Quick Ligation™ Kit	NEB	M2200S
Intercept® (TBS) Blocking Buffer	LICOER	927-60001
MG-132	Sigma-Aldrich	474787
Cycloheximide (CHX)	Sigma-Aldrich	239763
SuperSignal™ Western Blot Substrate Bundle, Pico PLUS	Thermo Scientific	A43840
All applications are based on the manufacturing processes of the company.		

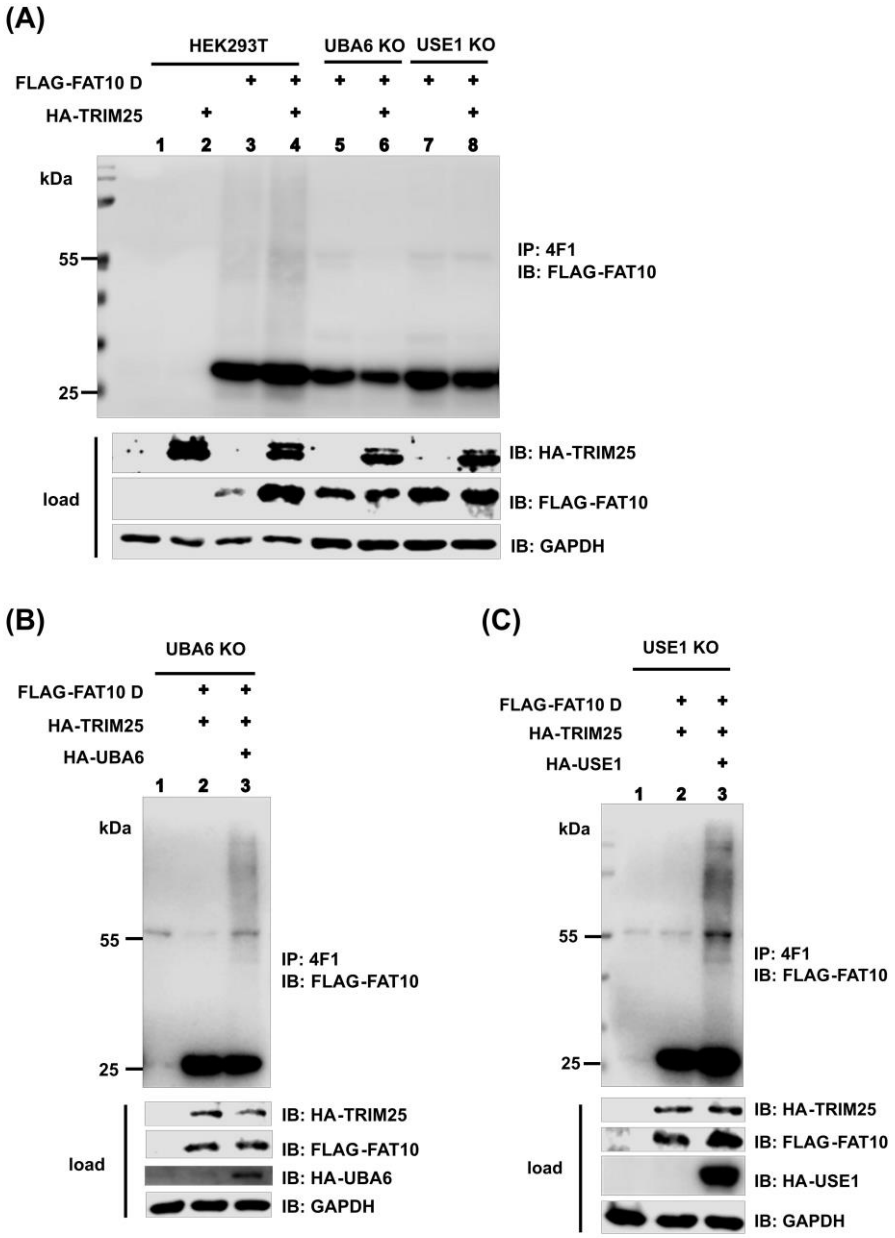

Figure S1.1. UBA6 and USE1 are indispensable for FAT10ylation. (**A**) HEK293T, UBA6 KO and USE1 KO cells were transiently transfected with TRIM25 and/or FAT10 D expression plasmids. One day later, cells were lysed, followed by 4F1-immunoprecipitation, SDS-PAGE, and immunoblot analysis with the indicated antibodies. GAPDH was used as a loading control. (**B**) UBA6 KO cells were transiently transfected with FAT10 D, TRIM25 and/or UBA6 expression plasmids. One day later, cells were lysed, followed by 4F1-immunoprecipitation, SDS-PAGE, and immunoblot analysis with the indicated antibodies. GAPDH was used as a loading control. (**C**) USE1 KO cells were transiently transfected with FAT10 D, TRIM25 and/or USE1 expression plasmids. One day later, cells were lysed, followed by 4F1-immunoprecipitation, SDS-PAGE, and immunoblot analysis with the indicated antibodies. GAPDH was used as a loading control

Chapter 2
The ubiquitin-like modifier FAT10 does not affect IL-12 expression and signaling

2.1 Abstract

The ubiquitin-like modifier FAT10 is strongly expressed in dendritic cells (DCs) and upregulated during inflammation. Interleukin (IL)-12 plays a critical role in promoting $CD4^+$ T cell differentiation into Th1 cells and in IFN-γ induction in T cells. Previously, it was shown that FAT10 is required for IFN-γ expression of activated T cells. In this study, we investigated whether FAT10 influences IL-12 expression or IL-12 induced signaling and thereby contributes to the reduced IFN-γ expression. Presence or absence of FAT10 did not alter IL-12 expression in DC2.4 cells and in bone marrow derived DCs. Furthermore, FAT10 had no influence on the differentiation of naïve T helper cells to Th1 cells under Th1 polarizing conditions. Additionally, FAT10 did not alter STAT4 phosphorylation in IL-12 receptor stimulated T cells. Taken together, FAT10 neither influences IL-12 expression in DCs nor affects IL-12 receptor signaling in T cells. Hence, the previously observed influence of FAT10 on IFN-γ secretion is not mediated by IL-12.

Keywords: *FAT10, UBD, IL-12, STAT signaling, Th1 differentiation*

2.2 Introduction

Whereas ubiquitin is expressed ubiquitously, human leukocyte antigen (HLA)-F adjacent transcript 10 (FAT10) is mainly expressed in tissues of the immune system such as lymph nodes or thymus [77, 141]. Furthermore, FAT10 expression can be induced in a synergistic manner by IFN-γ and TNF [80], or during the maturation of dendritic cells (DCs) [77]. FAT10 is encoded in the major histocompatibility complex (MHC) locus [106, 142], and is the only ubiquitin-like modifier that directly targets its substrates for degradation by the 26S proteasome in a ubiquitin-independent manner [73, 143]. Hitherto, several proteins have been identified as interacting partners of FAT10, including the autophagy adaptor p62 [57], histone deacetylase 6 (HDAC6) [69], AP-1 transcription factor subunit (Jun) [59], proliferating cell nuclear

antigen (PCNA) [60], β-catenin [118], mitofusin 2 (Mfn2) [114], FAT10 E3 ligase parkin [114], and the HECT-type ubiquitin E3 ligase HUWE1 [63]. Each of these proteins plays a critical role in different biological processes, underscoring the potential significance of FAT10 in diverse cellular functions. Interestingly, phosphorylation of FAT10 seems to fine-tune FAT10's interactions with specific interaction partners, indicated by a more efficient conjugation to substrates of phosphorylated FAT10 [144]. Apart from different cellular functions, FAT10 is involved in different immunological processes [86, 119]. Due to its selective expression in medullary thymic epithelial cells, it influences T cell selection [141]. Furthermore, FAT10 might play a role in the MHC class I antigen presentation pathway [83, 84, 86]. Moreover, FAT10 contributes to intracellular defense against bacteria by decorating autophagy-targeted *Salmonella* [89]. FAT10 knockout mice are viable and fertile, indicating that the lack of FAT10 does not interfere with essential housekeeping tasks [78]. However, lymphocytes of FAT10-deficient mice showed increased spontaneous apoptotic cell death. Infection of mice with influenza virus or lymphocytic choriomeningitis virus rapidly induces FAT10 mRNA expression [91]. Splenocytes from LCMV-infected FAT10-deficient mice exhibited diminished IFN-γ secretion and IL-12 p40 mRNA expression, while displaying enhanced production of type I interferons compared to their FAT10-proficient counterparts. Following viral infection, FAT10 fine-tunes the balance of interferons by reducing the production of type I interferons and increasing the levels of type II interferons [91].

Interleukin-12 (IL-12) is mainly secreted by dendritic cells (DCs), B cells, monocytes, and macrophages [145], and belongs to the IL-12 family, including other cytokines such as IL-23, IL-27, and IL-35 [146]. IL-12 consists of two subunits, IL-12p35 and IL-12p40, which are covalently linked to form the bioactive IL-12p70 [145]. The predominantly proinflammatory cytokine, plays a critical role in the development of T helper (Th)1 cells [146]. The signaling pathway of IL-12 involves the signal transducer activator of transcription (STAT) family, including STAT1, STAT4, and STAT5 [147]. Among these, STAT4 plays a key role in IL-12 receptor induced signaling.

In this study, we investigate whether altered IL-12 expression or signaling contribute to the previously observed reduced IFN-γ secretion of FAT10-deficient mouse $CD8^+$ T cells.

2.3 Material and methods

2.3.1 Mice

C57BL/6 mice were originally purchased from Charles River Laboratories (Sulzfeld, Germany). FAT10$^{-/-}$ mice [78] were kindly provided by A. Canaan and S. M. Weissman (Yale University School of Medicine, New Haven, CT). Mice were housed in a pathogen-free environment. They were matched by sex and age, and used when they were between 6 to 10 weeks of age. Mouse organ collection was approved by the Regierungspräsidium Freiburg ethics review board (approval number T-24/02TFA). Mice were euthanized using CO_2 inhalation, in accordance with approved animal care protocols. No experiments on living mice were performed.

2.3.2 Cells

DC2.4 is a dendritic cell line (a kind gift from Dr. K. Rock, University of Massachusetts Medical School, Worcester, MA) and cultured in RPMI 1640 medium (Gibco, 61870010, USA), supplemented with 10 % Fetal Bovine Serum (FBS, Gibco, 10270106, USA), 1x Penicillin-Streptomycin (Gibco, 15140122, USA). FAT10 expressing DC2.4 cells were generated by infecting DC2.4 cells with the lentiviral particles encoding murine 3xFLAG-FAT10. After three days of cultivation, the cells were selected with 5 µg/ml puromycin (Gibco, A1113802, USA).

To generate bone marrow-derived DCs (BMDCs), bone marrow from the femur and tibia of 10-weeks-old C57BL/6 wild-type mice and FAT10$^{-/-}$ mice was harvested. Isolated bone marrow cells were cultured in 10 cm dishes in RPMI 1640 medium, supplemented with 10 % FBS, 1x penicillin/streptomycin, 50 µM β-mercaptoethanol (β-Me, ROTH, 4227.3, Germany), and 20 ng/ml recombinant murine GM-CSF (peprotech, 315-03, USA) for 10 days.

2.3.3 Lentivirus production

Production of lentiviruses was exactly performed as previously described [148]. In brief, lentiviral particles were produced by transient co-transfection of the expression vector 3xFlag-FAT10, the envelope vector pMD2.G, and the packaging vector psPAX2 into HEK293T cells using polyethylenimine (PEI, Polysciences, 23966, USA). For this purpose, HEK293T cells were cultured in Iscove's Modified Dulbecco's Medium (IMDM) containing GlutaMAX (Gibco, 31980022, USA) supplemented with 10% FCS, 1x Penicillin-Streptomycin. Supernatant containing lentiviral particles was harvested 48 h and 72 h

post-transfection. The lentiviral particles were stored at - 80 ℃.

2.3.4 Th1 cell differentiation

$CD4^+$ T cells were magnetically isolated from the spleens according to the manufacturer´s protocol (CD4 (L3T4) MicroBeads, Miltenyi Biotec, 130-117-043, Germany). Th1 differentiation was performed as previously described [149]. Shortly, purified cells were activated with plate-bound anti-mouse CD3ε antibody (BioLegend, 100302, Clone 145-2C11, USA) and anti-mouse CD28 antibody (BioLegend, 102102, Clone 37.51, USA) for 3 days in the presence of 10 ng/ml IL-12, 10 ng/ml IL-2, and 10 µg/ml anti-IL-4 (CytoBox Th1; Miltenyi Biotec, 130-107-761, Germany).

2.3.5 Intracellular cytokine staining and flow cytometry

Polarized $CD4^+$ T cells were restimulated for 5 h with 25 ng/ml phorbol 12-myristate 13-acetate (PMA) and 500 ng/ml ionomycin in the presence of 10 µg/ml brefeldin A. After surface staining with PE anti-mouse CD4 Antibody (BioLegend, 100408, Clone GK1.5, USA), cells were fixed with 70 µl 4% paraformaldehyde, washed with permeabilization buffer (Invitrogen), and stained with FITC anti-mouse IFN-γ antibody (BioLegend, 505805, Clone XMG1.2, USA). The samples were measured and analyzed on Accuri C6 flow cytometers (BD Biosciences, Franklin Lakes, New Jersey, USA).

2.3.6 Immunoblotting

Cells were lysed in lysis buffer (20 mM Tris-HCl pH 7.6, 50 mM NaCl, 10 mM $MgCl_2$, 1% NP40, 1x EDTA-free Protease Inhibitor Cocktail (Roche, 4693132001, Switzerland), 1x PhosSTOP (Roche, 4906845001, Switzerland), incubated on ice for 30 min and centrifuged for 15 min at 13,000 x g. Total cell lysates were boiled with 4× SDS sample buffer (250 mM Tris-HCl pH 6.8, 40% glycerol, 8% SDS, 0.004% bromophenol blue) supplemented with 20% β-mercaptoethanol at 95 ℃ for 5 min. Equal amounts of cell lysates were separated by SDS-PAGE and transferred onto a nitrocellulose membrane. Protein was analyzed by the following antibodies: anti-pSTAT1 antibody (Cell Signaling, 7649S), anti-STAT1 antibody (Cell Signaling, 9172S, USA), and anti-pSTAT4 antibody (Cell Signaling, 4134S, USA). Anti-GAPDH antibody (Sigma-Aldrich, G9545, Germany) served as loading control. IRDye680RD goat anti-mouse (LICOR, 926-68070, USA) or anti-rabbit (LICOR, 926-68071, USA) and IRDye800CW goat anti-rabbit (LICOR, 926-32211, USA) or anti-mouse (LICOR, 926-32210, USA) were used as secondary antibodies. The LI-COR Odyssey Imager (LI-COR Biosciences, Lincoln, Nebraska, USA) and

the Image Studio Lite Version 5.2 were used for analyzing signals.

2.3.7 Real-time RT-PCR

Total RNA was extracted (RNeasy Mini Kit, QIAGEN, 74106) from cells, followed by reverse transcription (cDNA Synthesis Kit, Biozym, 331470L, Germany). Then, real-time RT-PCR (Biozym Blue S´Green Kit, 331416XL, Germany) was executed in a Biometra TProfessional Thermocycler (Analytik Jena, Germany). The quantitative value of each sample was normalized to mouse GAPDH, which was used as reference gene. Further information on primer pairs and reagents can be found in Supplementary table S2.1 and S2.2.

2.3.8 ELISA

The secretion of IL-12 was measured according to the protocol provided by the manufacturer (ELISA MAX™ Deluxe Set Mouse IL-12 (p70), BioLegend, 433604, USA).

2.3.9 Statistical analysis

Statistical analysis was conducted using Prism software (GraphPad, version 8.0). For comparisons involving two continuous variables, a two-tailed unpaired Student's t-test was used, while for comparisons involving more than two continuous variables, one-way ANOVA followed by Tukey's multiple comparison test was applied. The data are presented as individual scattered points along with the mean ± standard deviation (SD).

2.4 Results

2.4.1 FAT10 does not influence IL-12 expression in DC2.4 cells.

Mah et al. showed that in the absence of FAT10 IFN-γ secretion of TCR stimulated splenocytes derived from LCMV-infected mice is strongly reduced [91]. Furthermore, these splenocytes expressed less mRNA for IL-12 p40 but secreted more IFN-α and IFN-β. Il-12 secreted by DCs is driving the differentiation of naïve T helper cells into Th1 cells and contributes to the proper activation of cytotoxic T cells. In this study, we intend to investigate the effect of FAT10 on IL-12 expression and signaling. In a first step, the effect of FAT10 on IL-12 expression was investigated in the murine dendritic

cell-like cell line DC2.4. Since there are no antibodies available recognizing mouse FAT10 protein, FAT10 expression levels had to be analyzed on mRNA level using real-time RT-PCR. Non-stimulated DC2.4 cells barley express FAT10 mRNA (Figure 2.1A). Stimulation of DC2.4 with IFN-γ or IFN-γ/TNF strongly induced FAT10 mRNA, whereas LPS alone had no effect on FAT10 expression. Analysis of IL-12 mRNA levels in these stimulated cells, revealed a strong IL-12 mRNA induction (Figure 2.1B). Hence, DC2.4 is a suitable cell line to investigate the effect of FAT10 on IL-12. DC2.4 cells were stably transfected with FAT10 (Figure 2.1C). Stimulation with LPS strongly induced IL-12 mRNA in DC2.4 wild type and FAT10 overexpressing cells. However, there was no difference in IL-12 mRNA level in FAT10 overexpressing DC2.4 cells compared to wild type DC2.4 cells.

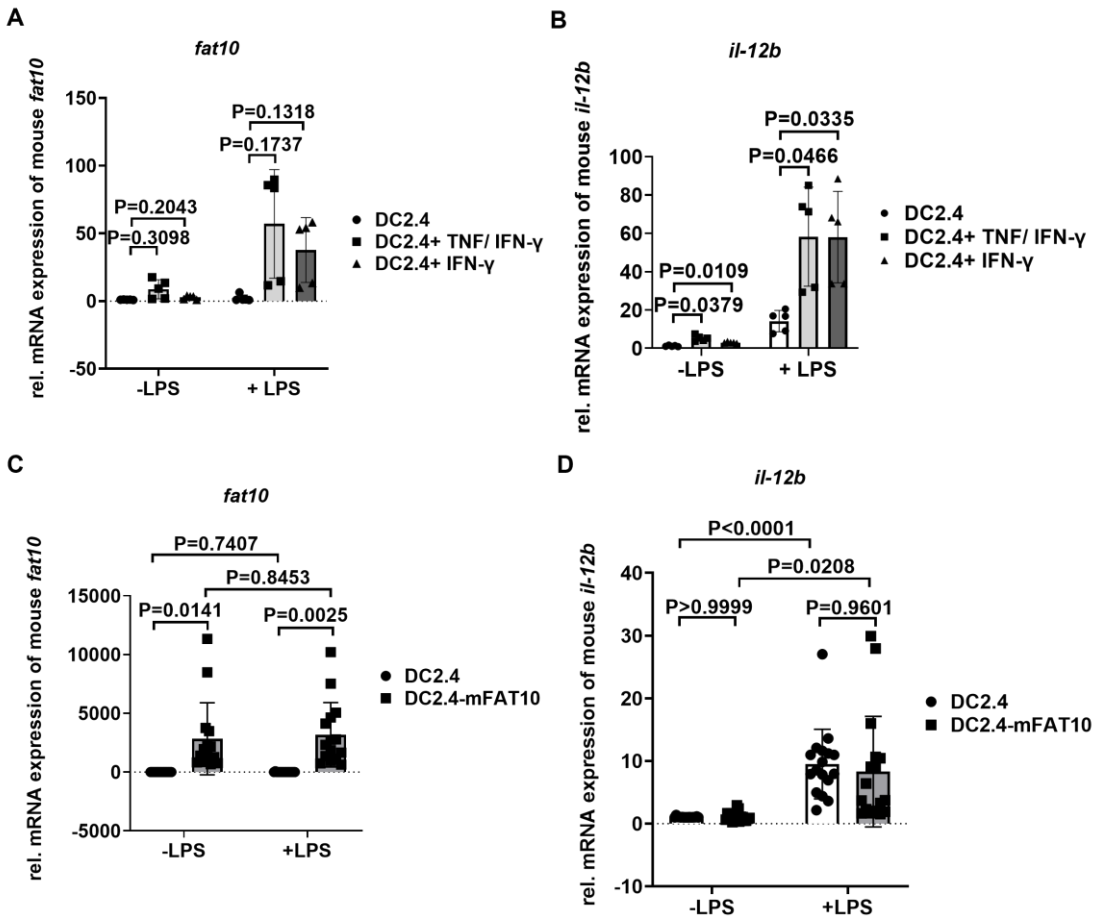

Figure 2.1. The Impact of FAT10 on IL-12 expression in DC2.4 cells. (**A, B**) DC2.4 cells were treated with TNF (400 U/ml) /IFN-γ (200 U/ml), IFN-γ (200 U/ml) in combination with (indicated +LPS) or without (indicated -) LPS (2 μg/ml) for 1 day. The mRNA level of FAT10 (A) and IL-12 (B) were detected by real-time RT-PCR. (**C, D**) DC2.4 cells and DC2.4-mFAT10 cells (stably expressing mouse FAT10) were treated with (indicated +LPS) or without (indicated -) LPS (2 μg/ml) for 1 day. The mRNA level of FAT10 (**C**) and IL-12 (**D**) were detected by real-time RT-PCR. (**A-D**) The y-axis depicts relative mRNA levels normalized to GAPDH. Data was analyzed by one-way ANOVA with Tukey's multiple comparisons test. P

values are indicated. Data are depicted as mean ± SDs. Each symbol in the graph represents an individual experiment. A, B: n=5; C: n=17, D: n=15.

2.4.2 FAT10 has no significant effect on IL-12 expression in bone marrow-derived dendritic cells

To further explore the effect of FAT10 on IL-12, we conducted experiments using bone marrow-derived dendritic cells (BMDCs) from C57BL/6 wild type mice and FAT10$^{-/-}$ mice. To up-regulate FAT10, in vitro generated BMDCs were stimulated with IFN-γ for one day to induce FAT10 expression. TNF was not included in this stimulation setup to prevent IL-12 expression during FAT10 induction. This was followed by an additional day of LPS stimulation to induce IL-12 expression. Indeed, in this experimental set-up we observed a strong induction of FAT10 (Figure 2.2A) and IL-12 (Figure 2.2B). However, FAT10 wild type and FAT10-deficient BMDCs induced similar levels of IL-12 mRNA. Next, we analyzed IL-12 secretion into the supernatant of IFN-γ/LPS stimulated wild type and FAT10-deficient BMDCs by ELISA. Similar to mRNA levels, FAT10 did not affect IL-12 secretion in BMDCs. (Figure 2.2C).

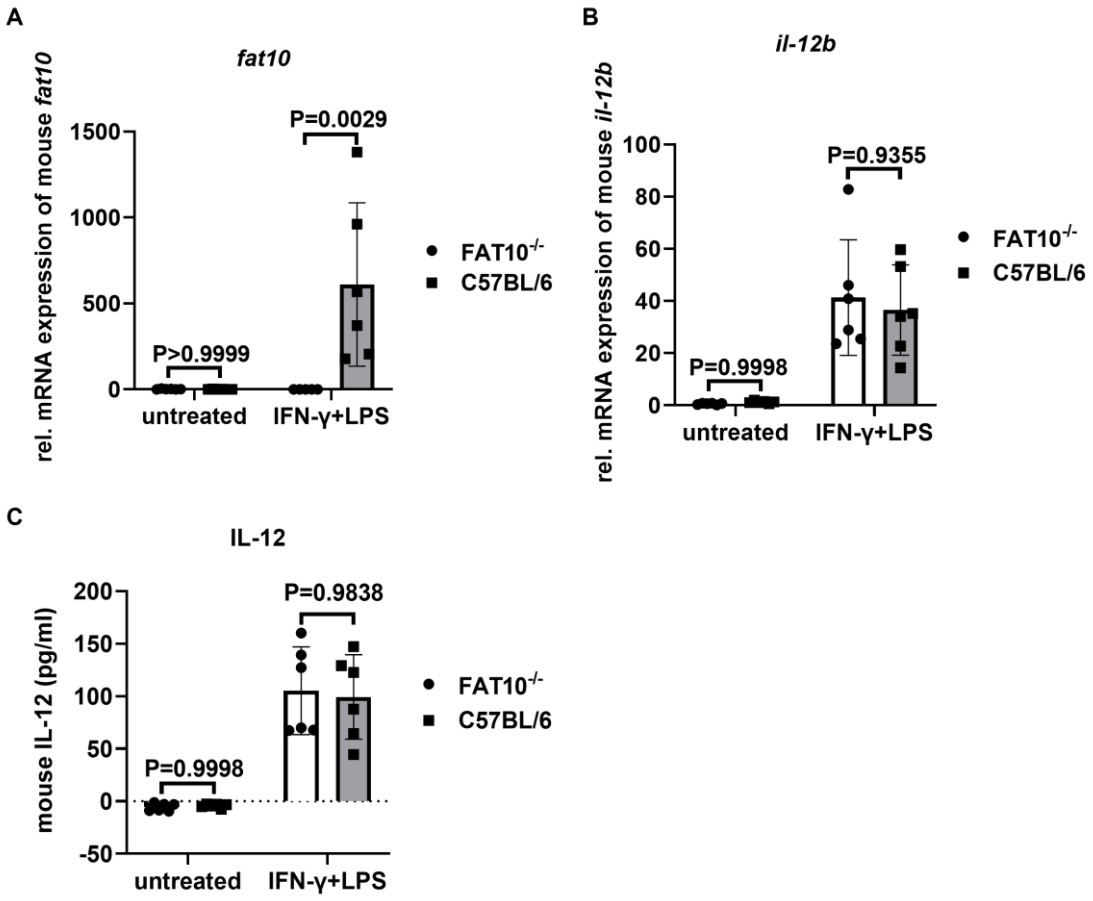

Figure 2.2. No impact of FAT10 on IL-12 expression in BMDCs. (**A-C**) BMDCs were generated from C57BL/6 wild type mice or FAT10$^{-/-}$ mice. BMDCs were treated with IFN-γ (200 U/ml) for 1 day, followed by LPS (1 μg/ml) treatment for 1 further day (indicated IFN-γ + LPS) or were left untreated (indicated untreated). (**A, B**) The mRNA level of FAT10 (**A**) and IL-12 (**B**) were detected by real-time RT-PCR. The y-axis depicts relative mRNA levels normalized to GAPDH. (**C**) The secretion of IL-12 into the supernatant was measured by ELISA. (**A-C**) Data was analyzed by one-way ANOVA with Tukey's multiple comparisons test. P values are indicated. Data are depicted as mean ± SDs. Each symbol in the graph represents BMDCs derived from an individual mouse. n=6 per group.

2.4.3 FAT10 does not affect Th1 cell differentiation

IL-12 is essential for Th1 cell differentiation, which plays a crucial role in protective cell-mediated immunity against various intracellular pathogens [150, 151]. In vitro, Th1 cells can be generated in the presence of IL-12. If FAT10 plays a crucial role in response to IL-12 stimulation, this should affect differentiation of FAT10-deficient Th1 cells. CD4^{+} T cells were magnetically isolated from the spleens of C57BL/6 wild type mice and FAT10$^{-/-}$ mice and cultured under Th1-polarizing conditions for 72 hours. IFN-γ is the signature cytokine of Th1 cells. Therefore, efficiency of Th1 differentiation was analyzed by intracellular IFN-γ staining of CD4^{+} T cells. No significant differences in Th1 differentiation between C57BL/6 wild type and FAT10$^{-/-}$ CD4^{+} T cells could be observed (Figure 2.3), indicating that FAT10 does not play an important role in the Th1 skewing process.

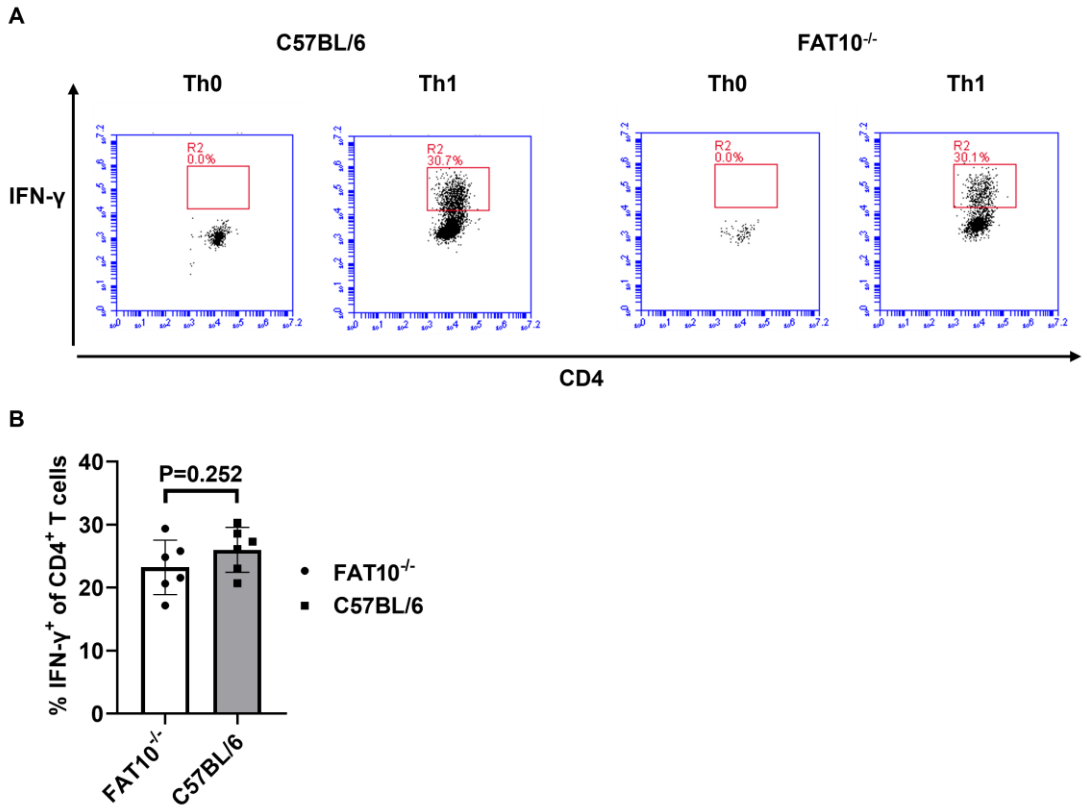

Figure 2.3. FAT10 does not affect Th1 differentiation. $CD4^+$ T cells were magnetically purified from the spleen of C57BL/6 wild type mice or $FAT10^{-/-}$ mice. Purified cells were cultured under Th0 or Th1 skewing condition for 72 h. Cells were restimulated with PMA/ionomycin in the presence of brefeldin A for 4 h, stained for CD4 and intracellular IFN-γ, and analyzed by flow cytometry. (**A**) Representative dot plots. (**B**) Bar graph depicting percentage of IFN-γ + CD4 cells. Data are depicted as mean ± SDs of $CD4^+$ cells isolated from 6 different mice per group (n=6) statistically analyzed by unpaired Student's *t*-test.

2.4.4 FAT10 does not modulate STAT signaling pathway

Although the absence of FAT10 had no crucial role on Th1-polarizing condition, we further investigated the effect of FAT10 in IL-12 receptor signaling. IL-12 activates $CD4^+$ T cells to produce IFN-γ via the STAT signaling pathway [152]. After IL-12 interacts with its receptor subunits IL-12Rβ1 and IL-12Rβ2, it triggers two signaling pathways: the Janus kinase (JAK) and STAT pathways [153, 154]. STAT4 serves as the primary downstream signaling target of IL-12, whereas IL-12 has less influence on STAT1, STAT3, and STAT5 molecules [150]. Therefore, we only investigated STAT4 and STAT1. Murine naïve T cells barely express FAT10 [81].Therefore, magnetically isolated $CD4^+$ T were stimulated with TNF/IFN-γ for 1 day. Analysis of STAT1 phosphorylation by western blot revealed that this

treatment induced the pSTAT1 (Figure 2.4A). Hence, this experimental set-up could not be used to investigate activation of STAT1 after IL-12R stimulation. Nevertheless, we observed no influence of FAT10 on STAT1 phosphorylation after TNF/IFN-γ stimulation (Figure 2.4A,B). After IL-12R stimulation, STAT4 is phosphorylated, and dimerization enables subsequent nuclear translocation. Magnetically isolated CD4⁺ T cells were treated with TNF/IFN-γ to induce FAT10 for 24 h [81]. Interestingly, this treatment did not induce STAT4 phosphorylation (Figure 2.4C). TNF/IFN-γ pre-treated cells were stimulated with IL-12 for 2h. Phosphorylation of STAT4 was analyzed by western blot. Within 2h, pSTAT4 could be detected. However, no difference in STAT4 phosphorylation could be observed between C57BL/6 wild type and FAT10-deficient CD4⁺ T cells (Figure 2.4D). These results suggest that FAT10 does not modulate the STAT signaling pathway in CD4⁺ T cells.

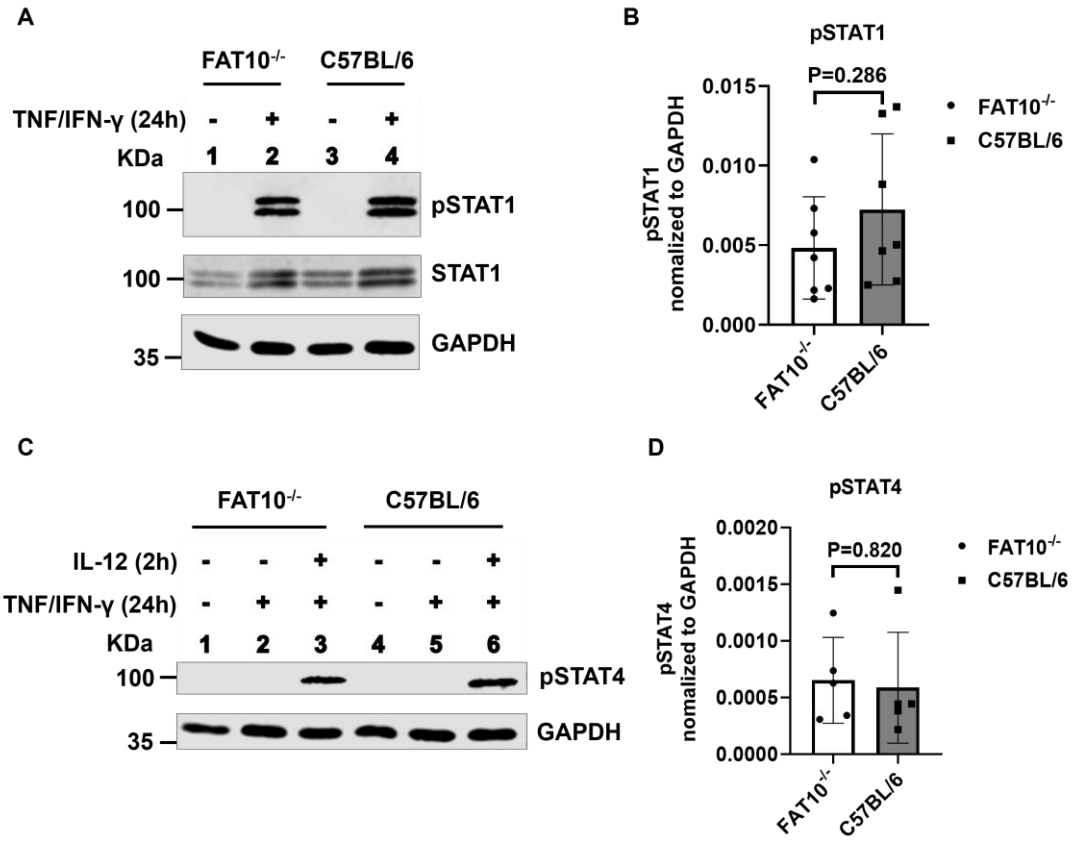

Figure 2.4. FAT10 does not modulate the IL-12 signaling pathway. (**A-D**) CD4⁺ T cells were magnetically purified from spleens of C57BL/6 wild type mice or FAT10$^{-/-}$ mice. (**A, B**) CD4⁺ T cells were treated with TNF (400 U/ml) /IFN-γ (200 U/ml) (indicated +) for 1 day or were left untreated (indicated -). pSTAT1, STAT1, and GAPDH were analyzed by western blot. (**B**) Quantification of pSTAT1 normalized to GAPDH. Data are depicted as mean ± SDs derived from 7 different experiments (n=7). (**C, D**) CD4⁺ T cells were treated with TNF (400U/ml) /IFN-γ (200 U/ml) for 1 day or left untreated, followed by a treatment with IL-12 (10 ng/ml) for 2 h. Treatment regime is indicated. pSTAT4 and GAPDH were analyzed by western blot. (**D**) Quantification of pSTAT4 normalized to GAPDH. Data are depicted as mean ± SDs

derived from 5 different experiments (n=5).

2.5 Discussion

FAT10 is the only ubiquitin-like modifier targeting proteins for degradation by the proteasome [143]. By this mean it can potentially control any processes, such as signaling or transcription, within cells. Since FAT10 is expressed in lymphoid tissues and can be strongly induced in an inflammatory environment, such processes might play a crucial role in inflammation. Indeed, phosphorylated FAT10 is essential for the efficient inhibition of IFN-β secretion upon TNF stimulation and during influenza A virus infection [76]. Phosphorylated FAT10 has been demonstrated to significantly interact with OTUB1, leading to a reduction in whole ubiquitylation levels and suppression of IFN-I induction through modulation of TRAF3 signaling. Furthermore, during influenza A virus infection, the presence of FAT10 leads to a reduction in the total ubiquitination of the E3 ligase TRIM21. The degradation of TRIM21 mediated by FAT10 decreased IFN-β production [155]. DCs initiate all antigen-specific immune responses and are considered as the master regulators of the immune response [156]. FAT10 is strongly expressed in human monocyte-derived dendritic cells [77]. Notably, FAT10 mRNA expression is increased during the later stages of dendritic cell maturation. DCs stimulated with LPS exhibited enhanced FAT10 expression and an accumulation of FAT10 conjugates [82]. IL-12 is primarily secreted by monocytes, macrophages, B cells and DCs [145]. IL-12 secreted by DCs is crucial for proper activation of cytotoxic T cells and T helper cells and for promoting Th1 differentiation [157]. Interestingly, $FAT10^{-/-}$ mice exhibit higher IL-12p40 expression in the spleen compared to $FAT10^{+/-}$ mice three days post LCMV infection [91]. This raised the question whether FAT10 is involved in regulating IL-12 expression in DCs or influencing IL-12 receptor signaling in T cells.

The murine DC cell line DC2.4 is an established model to study DC functions [158]. DC maturation stimuli, such as LPS, poly (I:C), IL-1β, and R848 can induce IL-12 production [158-160]. In a first step, we investigated whether LPS can induce IL-12 mRNA in DC2.4. Indeed, LPS induced IL-12p40 mRNA 24 h post stimulation (Figure 2.1B). IL-12p35 mRNA induction could not consistently and reliably be detected in our set-up, which might slightly limit the interpretation of our results. Whereas LPS barely induced FAT10, IFN-γ or TNF/IFN-γ strongly upregulated FAT10 expression in DC2.4 cells (Figure 2.1A). Interestingly, IFN-γ or TNF/IFN-γ treatment strongly enhanced LPS induced IL-12p40 mRNA expression. To study the effect of FAT10 on IL-12p40

mRNA induction in DC2.4 cells, DC2.4 cells stably overexpressing FAT10 were generated (Figure 2.1C). Notably, wild type DC2.4 cells barely express FAT10. LPS stimulation induced a strong induction of IL-12p40 mRNA in wild type and FAT10 overexpressing DC2.4 cells. However, absence of FAT10 (wild type DC2.4 cells) or overexpression of FAT10 had no influence on IL-12p40 mRNA expression. These results were confirmed in primary bone marrow derived dendritic cells derived from wild type C57BL/6 mice and FAT10-deficient mice (Figure 2.2). Although FAT10 was strongly up-regulated in wild type LPS/IFN-γ stimulated BMDCs (Figure 2.2A), no influence of FAT10 on IL-12 mRNA (Figure 2.2B) or protein (Figure 2.2C) levels could be observed in BMDCs. Taken together, these data strongly indicate that FAT10 does not play a significant role in IL-12 expression in murine DCs (Figures 2.1,2.2).

Mah et al. reported a reduced IFN-γ production of TCR-stimulated FAT10-deficient splenocytes [91]. The authors speculated that altered IL-12 expression could account for the diminished IFN-γ production in the absence of FAT10. However, we demonstrated that IL-12 expression is not altered in presence or absence of FAT10 (Figures 2.1,2.2). IL-12 stimulation of T cells strongly contributes to IFN-γ expression of activated T cells [161]. Hence, an altered IL-12 signaling in T cells might also lead to the reduced IFN-γ expression observed by Mah et al. [91]. Since IL-12 stimulates $CD4^+$ T cell differentiation into Th1 cells via the STAT signaling pathway, the influence of FAT10 on Th1 differentiation was investigated. Wild type and FAT10-deficient $CD4^+$ T cells were polarized in Th1 skewing condition. Both wild type and $FAT10^{-/-}$ $CD4^+$ cells differentiated to IFN-γ producing Th1 cells. However, no influence of FAT10 on Th1 differentiation was observed (Figure 2.3). This indicates that the absence of FAT10 in T cells does not influence IL-12R signaling induced by the Th1 skewing cytokine IL-12. Although the requirement of IL-12 for Th1 differentiation is well established, we can not completely exclude that IL-12 is required at all for Th1 differentiation in our in vitro Th1 differentiation set-up, which might limit the interpretation of our results. Nevertheless, IL-12 receptor signaling was further investigated in T cells (Figure 2.4). However, IL-12 induced signaling in $CD4^+$ T cells manifested in similar phosphorylation of STAT4 in FAT10-proficient and FAT10-deficient cells, showing that FAT10 does not influence IL-12R signaling in $CD4^+$ T cells.

Taken together, we found no indications that FAT10 alters IL-12 expression in DCs nor IL-12 induced signaling in T cells. Therefore, we conclude that a different mechanism is responsible for the previously observed reduction of IFN-γ secretion in FAT10-deficient splenocytes [91].

2.6 Supplementary information

Table S2.1. Primer pairs for used for real-time RT PCR.

mRNA	Forward (5′ to 3′)	Reverse (5′ to 3′)
(mouse) fat10	GGGATTGACAAGGAAACCACTA	TTCACAACCTGCTTCTTAGGG
(mouse) il-12 p40	GGGTGTAACCAGAAAGGTGC	AGGGAACACATGCCCACTTG
(mouse) gapdh	GTGTTCCTACCCCCAATGT	TGTCATCATACTTGGCAGGTTTC

Table S2.2. Reagents.

Reagents	Company	Cat No.
Recombinant murine IFN-γ	peprotech	315-05
Recombinant murine TNF	peprotech	315-01A
Purified anti-mouse CD3ε antibody	BioLegend	100302
Purified anti-mouse CD28 antibody	BioLegend	102102
CD4 (L3T4) MicroBeads, mouse	Miltenyi Biotec	130-117-043
CytoBox Th1, mouse (IL-12, IL-2, anti-IL4)	Miltenyi Biotec	130-107-761
Lipopolysaccharides (LPS)	Sigma-Aldrich	L4391
PMA	Sigma-Aldrich	P8139
Brefeldin A	Sigma-Aldrich	B7651
Ionomycin	Sigma-Aldrich	I9657
ELISA MAX™ Deluxe Set Mouse IL-12 (p70)	BioLegend	433604
Phospho-stat4 (Tyr693) (D2E4) rabbit mAb	Cell Signaling	4134S
Phospho-stat1 (Tyr701) (D4A7) rabbit mAb	Cell Signaling	7649S
Polyethyleneimine (PEI)	Polysciences	23966
Stat1 antibody	Cell Signaling	9172S
Anti-GAPDH antibody produced in rabbit	Sigma-Aldrich	G9545
Recombinant murine GM-CSF	peprotech	315-03
FITC anti-mouse IFN-γ Antibody	BioLegend	505805
PE anti-mouse CD4 antibody	BioLegend	100408
RPMI 1640 medium	gibco	61870010
Fetal bovine Serum	gibco	10270106
Penicillin/streptomycin	gibco	15140122
β-mercaptoethanol	ROTH	4227.3
IRDye® 800CW goat anti-rabbit IgG secondary antibody	LICORbio	926-32211
IRDye® 800CW goat anti-mouse IgG secondary antibody	LICORbio	926-32210
IRDye® 680RD goat anti-Rabbit IgG Secondary Antibody	LICORbio	926-68071
IRDye® 680RD goat anti-mouse IgG secondary antibody	LICORbio	926-68070
Permeabilization buffer	Invitrogen	00-8333-56
PhosSTOP™	Roche	4906845001
cOmplete™, EDTA-free protease inhibitor cocktail	Roche	4693132001
Biozym cDNA synthesis kit	Biozym	331470L
Biozym Blue S'Green qPCR kit separate ROX	Biozym	331416XL
RNeasy mini kit	QIAGEN	74106
All applications are based on the manufacturing processes of the company.		

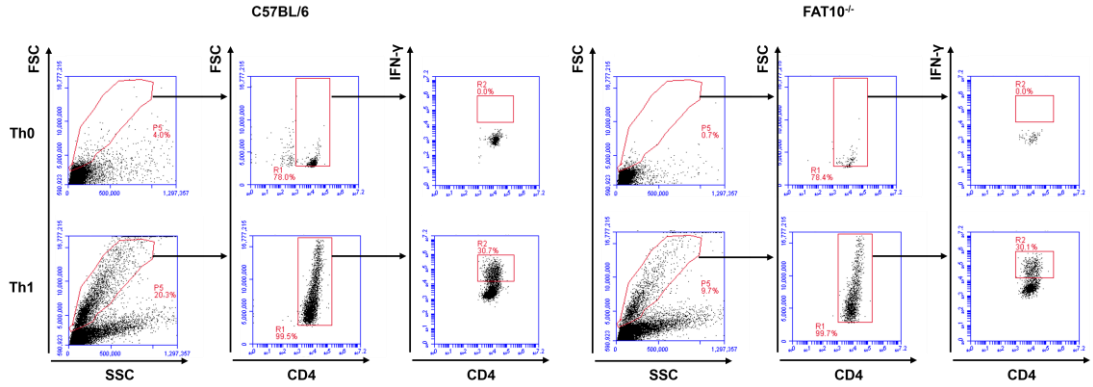

Figure S2.1. Flow cytometry gating strategy of Figure 2.3.

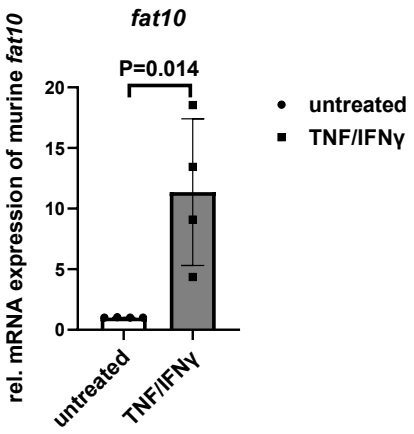

Figure S2.2. The *fat10* gene expression in C57BL/6 mice of Figure 2.4. $CD4^+$ T cells were magnetically purified from spleens of C57BL/6 wild type mice. $CD4^+$ T cells were treated with TNF (400 U/ml) /IFN-γ (200 U/ml) (indicated +) for 1 day or were left untreated (indicated -). The mRNA level of FAT10 were detected by real-time RT-PCR. The y-axis depicts relative mRNA levels normalized to GAPDH. Data are depicted as mean ± SDs derived from 4 different experiments (n=4).

Chapter 3
Making FAT10 with a reactive C-terminus for E3 ligase screening

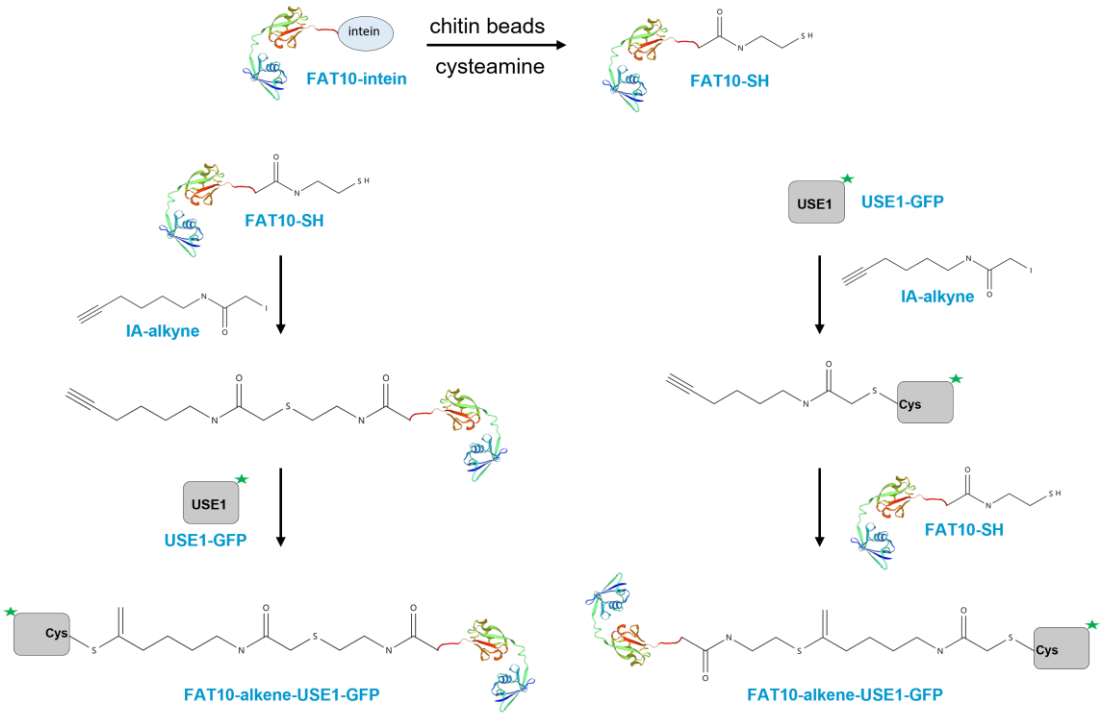

3.1 Abstract

Background: FAT10, a ubiquitin-like modifier, targets proteins to the 26S proteasome for degradation, similar and in addition to ubiquitin. However, FAT10 utilizes its own enzyme cascade, including E1 (UBA6), E2 (USE1), and various E3 ligases. To date, Parkin is the only identified E3 ligase for FAT10, but about 800 different E3-enzymes were reported for ubiquitin. In this study, we aimed to generate a branched FAT10-USE1 conjugate with a reactive C-terminus for the purpose of screening potential E3 ligases. Our method is simple, cost effective and does not require expensive lab equipment. We were able to avoid organic solvents and extreme pH or salt conditions. **Methods:** The proteins were expressed at a low temperature for 7–8 hours and purified using affinity resin. Conjugation was achieved through a radical thiol–yne coupling reaction. The resulting products were analyzed by Coomassie Brilliant Blue staining and Western blotting. **Results:** FAT10-SH was successfully purified using a Strep-Tactin column and chitin resin, while

USE1-GFP was purified via Ni-affinity chromatography. Notably, FAT10-alkene-USE1-GFP conjugates were successfully generated using IA-alkyne, but not STP-alkyne. **Conclusion:** In this study, we developed novel FAT10-based probes suitable for E3 ligase screening, which may facilitate future investigations into FAT10 biology. The method can be easily adapted to other ubiquitin like modifiers.

Keywords: *FAT10, USE1-GFP, Ni-affinity chromatography, Strep-Tactin, thiol–yne coupling reaction, IA-alkyne, E3 ligase screening*

3.2 Introduction

Human leukocyte antigen-F adjacent transcript 10 (FAT10) is a member of the ubiquitin-like modifier family and is encoded within the MHC class I locus [106]. It contains two ubiquitin-like domains—an N-terminal domain and a C-terminal domain—jointed by a short linker (KPSDE) [43]. FAT10 is predominantly expressed in the immune system and is strongly upregulated by tumor necrosis factor (TNF) and interferon-gamma (IFN-γ) [162, 163]. FAT10 was reported to play a role in certain carcinomas and proposed as a tumor marker [93, 96, 98-100, 164]. FAT10 utilizes its own enzyme cascade to directly target proteins, including itself, for degradation by the 26S proteasome [143]—a process known as FAT10ylation. Similar to the ubiquitination pathway, FAT10ylation involves three key enzymes: an E1 activating enzyme, an E2 conjugating enzyme, and an E3 ligase. UBA6 has been identified as the E1 activating enzyme [165, 166] and USE1 as the E2 conjugating enzyme [47]. Both are bispecific, functioning in both the ubiquitin and FAT10 pathways. First, FAT10 is activated by an E1 activating enzyme, forming a thioester bond between the C-terminal glycine of FAT10 and the catalytic cysteine in the adenylation domain of E1 via a covalent interaction. Subsequently, FAT10 is transferred to an E2 conjugating enzyme, forming a thioester bond between its C-terminal domain and the active-site cysteine of E2. Finally, with the assistance of an E3 ligase, an isopeptide bond is formed between the C-terminal glycine of FAT10 and a lysine residue on the substrate protein [43]. The E3 ligase, which plays an essential and non-redundant role in substrate recognition and transfer, remains less well characterized in the context of FAT10. Thus far, Parkin has been identified as an E3 ligase for FAT10 [114]. For ubiquitin, for instance, about 800 different E3 enzymes were identified [167, 168]. Therefore, it is likely that other E3 ligases for FAT10 exist, the identification of which would help to understand the function of FAT10 in cancer.

To date, numerous studies have reported the mechanisms of ubiquitination [169-173]. Additionally, activity-based probes (ABPs) have been developed to investigate the enzymatic activity of E3 [174-176] or DUB [177]. Several approaches were used to identify components of the ubiquitin conjugation and de-conjugation pathway. A method using intein chemistry for such analysis was reported by Wilkinson [178]. Several such reports were published which modified the C-terminus of ubiquitin to enable reactions with the active sites of cascade enzymes. However the methods described sometimes required HPLC purification of intermediates or final products [174, 178], used low pH [179], used organic solvents [180], or used cupper click reactions [181], all of those conditions will lead to denaturation of FAT10 and loss of function. Some of the published reactions required the synthesis of components [181-183] or used expensive methods for analysis [180, 182-184]. We would like to avoid all of the mentioned conditions and components. Some reports made advantage of the thiol–yne coupling reaction [182-185] as the enzymes involved have a thiol in the active center. Because the product of the thiol–yne coupling reaction can react with thiols to form a stable bisthioether bond [181, 182]. This is a promising approach if we link an alkyne to FAT10 C-terminus and let it react with the active site cysteine of USE1. If the active site cysteine of an E3 comes close, it can form a stable bisthioether bond. Such an approach was used in [181], but with help of a cupper click reaction. We also employed a reverse strategy by attaching a linker to the active-site cysteine of USE1, enabling the alkyne to react with a thiol at the FAT10 C-terminus, which was generated using intein technology. So we generated two branched FAT10-USE1 conjugates, with the thiol-reactive group in a different position to maximize chances to react with an E3. We also tried to link an alkyne to any of the lysines of USE1 in order to make the branch mimicking an isopeptide bond and trap an isopeptidase, but failed to link FAT10 to it.

3.3 Material and methods

3.3.1 Plasmid

The plasmids for expression of Strep-FAT10-intein and pET28-USE1-GFP have been previously described [47, 56].

3.3.2 Induction of protein

Induction of protein was performed as previously described [56]. The

bacterial culture was shaken at 180 rpm at 37 ℃. When the OD600 of the bacteria reached 0.5, 1 mM IPTG (ROTH, 2316.4, Germany) was added to induce protein expression. Meanwhile, the bacteria were shaken at 180 rpm at 37 ℃ for 7 to 8 hours. Lastly, the bacteria were harvested by centrifugation at 5000 rpm for 10 minutes and then stored at -20 ℃.

3.3.3 Extraction of protein

Protein extraction followed the protocol described in [56]. The bacteria were resuspended in 10 mL of buffer. Then, 1 mg/mL lysozyme (Fluka, 62971, USA), 0.1 mg/mL DNase I (Roche, 3724778103, Switzerland), and 1x EDTA-free Protease Inhibitor Cocktail (Roche, 4693132001, Switzerland) were added to the mixture and incubated on ice for 1 hour. Next, the bacteria were sonicated, followed by centrifugation at 18,000 rpm at 4 ℃ for 1 hour. The supernatant was collected and sonicated again. Lastly, the supernatant was filtered using a 0.22 μm filter (TPP, 99722, Switzerland).

3.3.4 Purification of FAT10-SH

Purification of FAT10 was performed as described by Brockmann et al. [56]. The lysate was applied to the Strep-Tactin column (iba, 2-5998-000, Germany), following the manufacturer's instructions. Subsequently, the appropriate amount of chitin resin was added to the desalted FAT10-intein and incubated at 4 ℃ with rocking for 5 hours. The supernatant was then discarded. Then, a suitable volume of 50 mM cysteamine (Sigma-Aldrich, 30070, USA) was added to the resin and incubated at 4 ℃ overnight with rocking. Lastly, the supernatant was desalted using a Nap-10 column with PBS, yielding the desired FAT10-SH protein.

3.3.5 Purification of USE1-GFP

The lysate was applied to Ni-NTA agarose (Macherey-Nagel, 745400, Germany), following the company manual. The purified USE1-GFP was concentrated using a 30 kDa centrifugal filter and desalted with a Nap-10 (cytiva, 17085401, USA) column, yielding the desired USE1-GFP.

3.3.6 The reaction of compounds

The purified protein (50 μL, 2 mg/mL in PBS) was treated with 1 μM iodoacetamide alkyne (IA-alkyne, MCE, HY-136205, USA) or 1 μM pentynoic acid STP ester (STP-alkyne, lumiprobe, 40720, Germany) and incubated at room temperature for 1 hour. The reaction was quenched by desalting via a

NAP-5 column according to instruction by the manufacterer. Next, FAT10-alkyne or USE1-GFP-alkyne was reacted with USE1-GFP or FAT10 via a TYC reaction under 365 nm UV light irradiation in the presence of 1,5 mM reduced glutathione (GSH, Sigma-Aldrich, G4251, USA) and 5 mM VA-044 (FUJIFILM, 225-02111, Japan) for 4 hours. The resulting product was first purified using 50µl Ni-IDA resin (Macherey-Nagel, 745210, Germany), followed by further purification using a 100 µl Strep-Tactin column. The eluted fraction were collected and analyzed by Western blotting.

3.3.7 Coomassie Brilliant Blue staining and silver staining

The SDS-PAGE gels were soaked in Coomassie Brilliant Blue (Abcam, ab119211, UK) for 1 to 2 hours. Afterwards, the SDS-PAGE gels were submerged in ultrapure water for at least 1 hour or overnight. We used the silver staining kit (Thermo Scientific, 24612, USA) according to the manufacturer's instructions.

3.3.8 Western blotting

The sample was boiled in SDS sample buffer. SDS-PAGE gel electrophoresis was then performed, followed by transferring the SDS-PAGE gel onto a nitrocellulose membrane using the Trans-Blot Turbo Transfer System at 25 V for 10 minutes. The membrane was blocked with Intercept (TBS) Blocking Buffer (LICOR, 927-60001, USA) at room temperature for 1 hour, then incubated with the primary antibody at 4 ℃ overnight. Afterward, the membrane was washed with TBS-T for 5 minutes, repeating this step three times. Next, the membrane was incubated with the secondary antibody at room temperature for 1 hour, followed by another round of washing with TBS-T for 5 minutes, repeated three times. Finally, signal detection was performed using an ODYSSEY XF processor (LICOR, model 2800, USA).

3.4 Results

3.4.1 Expression of FAT10-intein and USE1-GFP proteins

In this study, we aim to generate the FAT10-USE1 conjugate. First, the expression of FAT10 and USE1-GFP proteins was carried out. The FAT10 and USE1-GFP plasmids were separately transferred into B834 competent cells. After 7–8 hours of induction with IPTG, the expression of FAT10 (Figure 3.1A) and USE1-GFP (Figure 3.1B) was analyzed using Coomassie Brilliant Blue

staining and Western blotting.

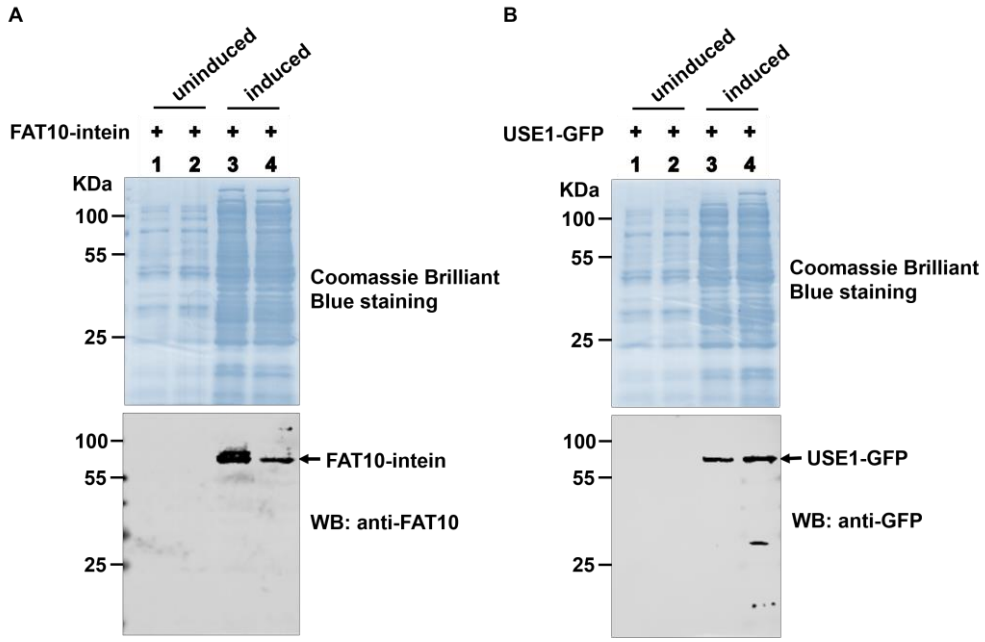

Figure 3.1. Expression of FAT10-intein and USE1-GFP proteins. (**A**) FAT10-intein expression was induced with 1 mM IPTG for 7–8 hours and analyzed by Western blotting. (**B**) USE1-GFP expression was induced with 1 mM IPTG for 7–8 hours and analyzed by Western blotting.

3.4.2 Purification of FAT10-SH protein

The lysate of FAT10-intein-chitin binding was applied to a 1 mL Strep-tag column, following the manufacturer's manual. The protein was eluted with buffer BXT. The results showed that FAT10-intein was successfully purified. Afterward, chitin resin was added to the purified FAT10-intein protein. FAT10-SH was removed from the chitin resin using 50 mM cysteamine. The results showed that FAT10-SH was successfully separated from the chitin resin (Figure 3.2).

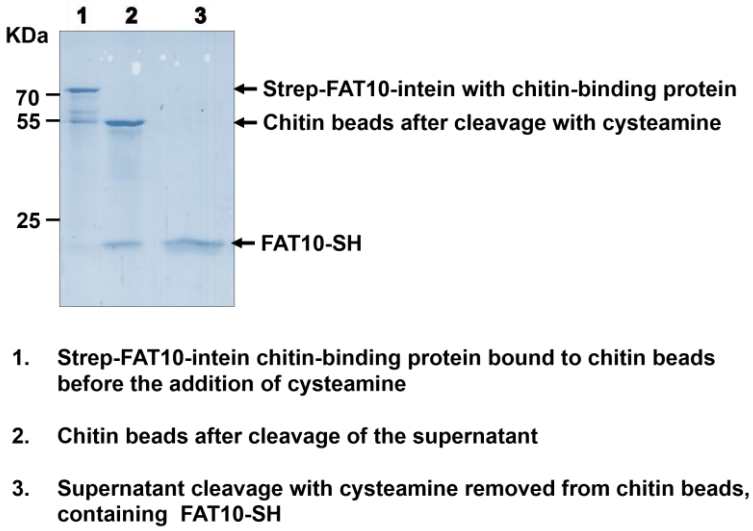

Figure 3.2. Purification of FAT10-SH protein. FAT10-SH was eluted from chitin beads with 50 mM cysteamine and analyzed by Coomassie Brilliant Blue staining.

3.4.3 Purification of USE1-GFP protein

The lysate of USE1-GFP was applied to Ni-NTA agarose, following the manufacturer's manual. Additionally, we purified USE1. As shown in Figure 3.3, the purification of USE1-GFP was more efficient than that of USE1 alone. GFP not only serves as a reporter gene but also facilitates protein purification.

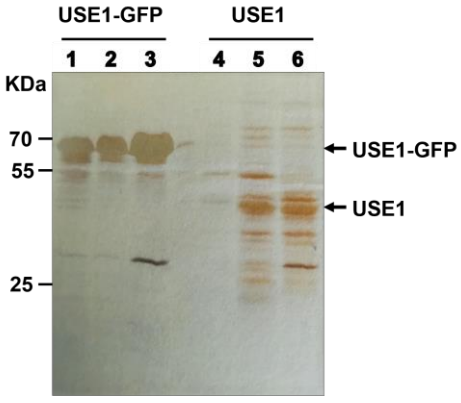

Figure 3.3. Purification of USE1-GFP and USE1 protein. Shown are three subsequent elution fractions from Ni-NTA agarose, each 1.5 times the volume of the batch. USE1-GFP and USE1 was analyzed by silver staining.

3.4.4 The generation of FAT10 and USE1 conjugates

Conjugation was carried out after all proteins had been prepared. Initially, FAT10 or USE1-GFP were incubated with IA-alkyne or STP-alkyne at room temperature for 1 hour, after which the reaction was quenched by by passing the proteins through a NAP-5 column. Subsequently, a radical TYC reaction was performed by irradiating a mixture of either FAT10-alkyne or USE1-GFP-alkyne with USE1-GFP or FAT10, VA-044, and GSH under 365 nm UV light for 4 hours. The product was first purified using Ni-IDA resin, removing all smal components and proteins without Hexa-His tag, e.g. unreacted FAT10. Final purification was achieved using a Strep-Tactin column. All componets without the strep tag, e.g. USE1-GFP which did not react with FAT10 were removed. As all proteins bound on the column must have a Strep tag and a Hexa-His tag, which is only the case for Strep-FAT10-Hexa-His-USE1-GFP conjugates. Flow-through and eluted fractions from the Strep-Tactin column were collected and analyzed by western blotting. As shown in Figure 3.4B, the GFP Western blot revealed a difference of approximately 15 kDa in molecular mass between the flow-through of the Strep-Tactin column and the eluate, which is consistent with the expected size increase resulting from the addition of FAT10 to USE1-GFP. The USE1-GFP is, expectetly, in the low through, whereas the FAT10-USE1-GFP is in the eluate. The higher molecular band in lane 2 and 4 reacted positive with an anti-FAT10 antibody, no reaction was observed in the other lanes. Therefore, FAT10-alkene-USE1-GFP conjugates were detected in reactions involving either FAT10-IA-alkyne + USE1-GFP or USE1-GFP-IA-alkyne + FAT10-SH, but not in the USE1-GFP-STP-alkyne + FAT10-SH condition. These findings indicate that FAT10 binds to the catalytic center of USE1-GFP with considerable affinity, in a manner consistent with its native degradation pathway. Additionally, when any lysine of USE1-GFP is modified with an alkyne group, it does not react with FAT10-SH. This is probably because the affinity of FAT10 to the active center of USE1 is high, whereas FAT10 has no affinity to the surface of USE1 to react with exposed lysines, at least not under the consentration applied and the condition tested (Figure 3.4).

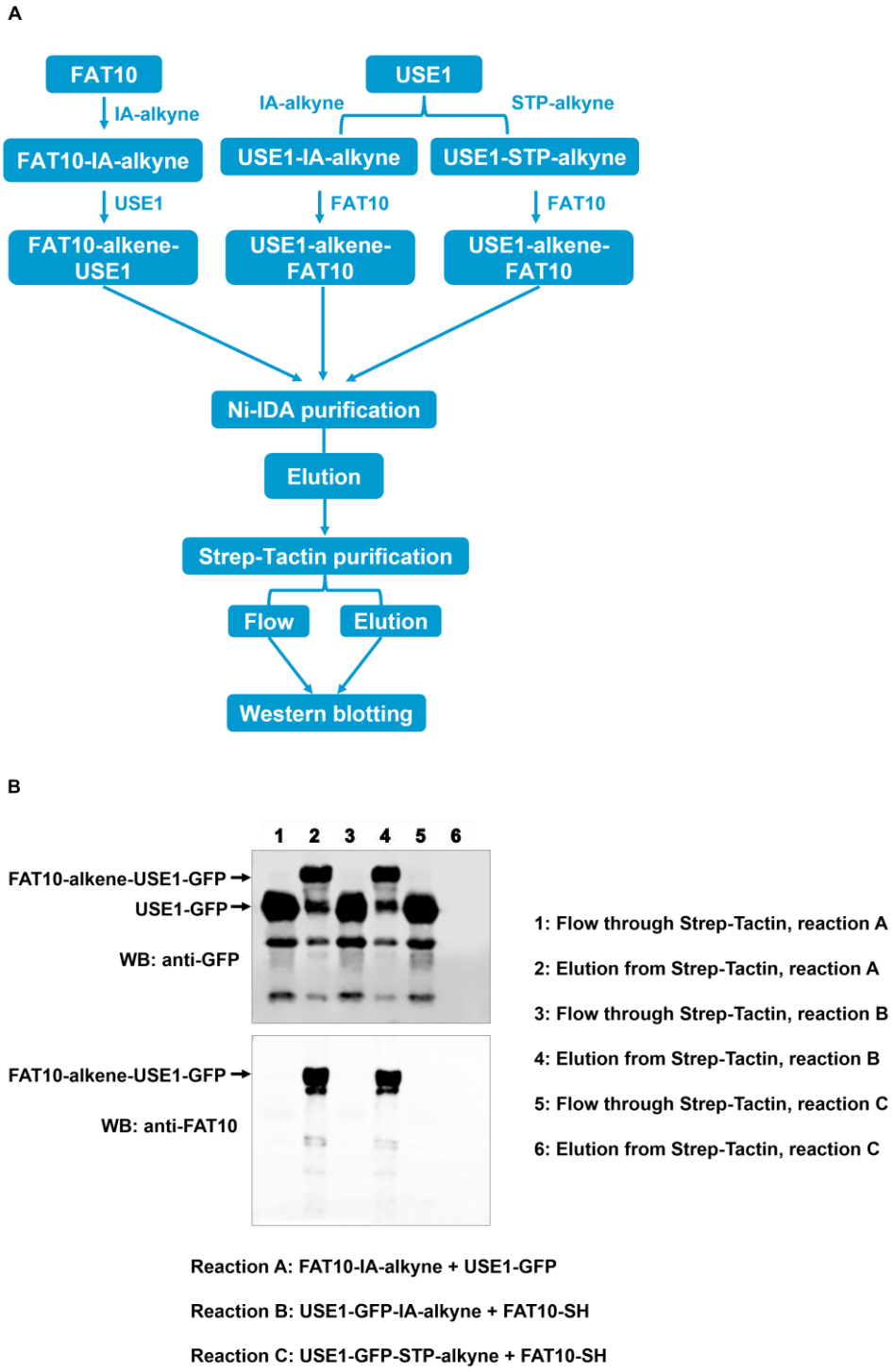

Figure 3.4. Formation of the FAT10-alkene-USE1-GFP conjugate. The conjugate was purified using Ni-IDA resin, followed by purification with a Strep-Tactin column. (**A**) Workflow for the generation of the conjugates. (**B**) Lanes 1, 3, and 5 correspond to the flow-through collection after loading of the Strep-Tactin column, while lanes 2, 4, and 6 represent the eluted fractions containing the purified protein. FAT10-alkene-USE1-GFP was analyzed by Western blotting.

3.5 Discussion

FAT10, unlike ubiquitin—which is ubiquitously expressed—is restricted to the immune system [108], and is upregulated in various cancers [93, 96, 98-100, 164]. FAT10ylation is a unique protein degradation pathway—FAT10 employs its own enzymatic cascade [47, 165, 166]. In this process, FAT10 is covalently attached to substrate proteins and co-degraded with them by the 26S proteasome [143]. To date, Parkin is the only known E3 ligase mediating FAT10ylation [114]. In this study, we aimed to generate FAT10-USE1-GFP conjugates, as this is more promising as compared to just a C-terminal reactive group on FAT10 only, to facilitate the screening of potential E3 ligases involved in FAT10ylation. Just a modified C-terminus on FAT10 is more likely to react with an E1 and E2, forming stable conjugates with these, and will not be able to react with an E3. This was also the rationale in [181]. The advantages of our conjugates are the simple preparation on the bench top without expensive equipment. The avoidance of any hard condition, the use of cost effective commercially available components, and the easy and fast final purification via two consecutive affinity chromatographies, which leave only the conjugate of FAT10 and USE1-GFP in the eluate, as it is the only one having both affinity tags. We used two strategies for the generation of the conjugates which link the C-terminus of FAT10 to USE1-GFP active site cysteine. We assume it is the active site cysteine without formal confirmation, because it is the most reactive one. Other publication, which did in depth analysis via mass spectrometry [180, 181, 184, 185] always found reaction with the active site cysteine only. The affinity of the UBL-modifier to the active center is much higher than to any other part of the protein, which keeps the reactive groups long enough together to react. One report notes that the length of the linker has an influence on the reaction efficacy [185], whereas another report did not see such a dependency [184]. The low concentration and affinity are probably the reason why we did not see any reaction between the alkyne labeled lysine of USE1-GFP and FAT10-SH, at least not with our conditions, because there is no binding of the surface of USE1-GFP and the C-terminus of FAT10-SH. Rather the active center of USE1-GFP might bind the FAT10-SH C-terminus, preventing it from reacting with the alkyne. We generated two different FAT10-USE1-GFP conjugates, with the difference being the position of the reactive group. It is possible that the position will have an influence on the reaction with a potential E3, so it is better to use different probes. As there is only one known E3 for FAT10, but several hundred for ubiquitin, we are confident that our tool will enable the identification of several E3 enzymes for FAT10, should suitable patient material available. Our method of generation of branched FAT10-E2 conjugates with two different positions of a thiol-reactive group can as well be easily adapted to any other ubiquitin like modifier, and any other enzyme of

the conjugation cascade, as well as to isopeptidases, many of them have a cysteine in the active center. This is of great advantage if the budget is limited an access to expensive equipment is impossible.

3.6 Supplementary information

Table S3.1. Regents and materials

Reagents or kit	Company	Cat No.
Cysteamine	Sigma-Aldrich	30070
Kanamycin	ROTH	T832.2
Ampicillin sodium salt	ROTH	K029.1
Tryptone/Peptone ex casein	ROTH	8952.2
TWEEN® 20	Sigma-Aldrich	P7949
Triton™ X-100	Sigma-Aldrich	X100
Trizma® base	Sigma-Aldrich	T1503
Glycine	ROTH	3908.2
Sodium chloride	ROTH	3957.2
Yeast Extract	ROTH	2363.4
InstantBlue® Coomassie Protein Stain (ISB1L)	Abcam	ab119211
β-mercaptoethanol	ROTH	4227.3
Acrylamide/Bis Solution, 37.5:1	SERVA	10688.01
Strep-Tactin®XT 4Flow® high capacity resin	iba	2-5030-002
Strep-Tactin®XT 4Flow® Starter Kit	iba	2-5998-000
Pentinsäure-STP-Ester	lumiprobe	40720
IA-Alkyne	MCE	HY-136205
Chitin Resin	NEB	S6651S
Anti-GFP	Roche	11814460001
Anti-His Tag Antibody	Sigma-Aldrich	05-531
IRDye® 800CW Goat anti-Mouse IgG Secondary Antibody	LICORbio	926-32210
IRDye® 680RD Goat anti-Mouse IgG Secondary Antibody	LICORbio	926-68070
Amicon® Ultra Centrifugal Filter, 3 kDa MWCO	Millipore	UFC500308
Amicon® Ultra Centrifugal Filter, 30 kDa MWCO	Millipore	UFC903024
Amicon® Ultra Centrifugal Filter, 30 kDa MWCO	Millipore	UFC803024
Pierce™ BCA Protein Assay Kits	Thermo Scientific™	23225
1,4-Dithioerythritol	Sigma-Aldrich	D8255
cOmplete™, EDTA-free Protease Inhibitor Cocktail	Roche	4693132001
Intercept® (TBS) Blocking Buffer	LICOR	927-60001
IPTG	ROTH	2316.4
Lysozyme	Fluka	62971
DNase I	Roche	3724778103
syringe filter 22	TPP	99722
PETRI DISH, PS, 94/16 MM, WITHOUT VENTS	greiner	632180
Screw cap tube, 15 ml, (LxØ): 120 x 17 mm, PP, with print	SARSTEDT	62.554.502
Screw cap tube, 50 ml, (LxØ): 114 x 28 mm, PP, with print	SARSTEDT	62.547.254
Agar	Millipore	1016141000
NAP-5 Columns Sephadex G-25 DNA Grade	cytiva	17085302
NAP-10 Columns Sephadex G-25 DNA Grade	cytiva	17085401
2-Propanol ≥99.7%, AnalaR NORMAPUR® ACS, Reag. Ph. Eur. analytical reagent	VWR Chemicals	20842.312
Trans-Blot Turbo 5x Transfer Buffer	BIO-RAD	10026938
Magnesium chloride hexahydrate	ROTH	2189.1

Ethylenediamine tetraacetic acid disodium salt dihydrate	ROTH	8043.2
Ethanol	ROTH	9065.3
VA-044	FUJIFILM	225-02111
L-Glutathione reduced (GSH)	Sigma-Aldrich	G4251
Protino Ni-IDA Resin für His-Tag-Proteinreinigung	Macherey-Nagel	745210
Protino Ni-NTA Agarose für His-Tag-Proteinreinigung	Macherey-Nagel	745400
Pierce™ Silver Stain Kit	Thermo Scientific	24612
All applications are based on the manufacturing processes of the company.		

General discussion

While the three research projects presented in this dissertation emphasize different aspects of FAT10 biology, they are unified by a common objective: to elucidate the function of FAT10. Specifically, we investigated the contribution of phosphorylated FAT10 to protein degradation pathways, the relationship between FAT10 and IL-12 secretion, and the development of a FAT10-based probe to identify potential E3 ligases. Together, these studies provide a multidimensional perspective on the biological activities of FAT10. As research has advanced, FAT10 has been implicated in a wide array of processes, including antigen presentation[57, 83-86], autophagy[63, 87, 88], antibacterial [89] and antiviral responses[65, 90, 91], and tumorigenesis [61, 92-104]. In certain cancers, FAT10 stabilizes proteins by inhibiting ubiquitination at lysine residues [98, 139, 140] and has been proposed as a prognostic biomarker [62, 104]. These findings underscore the need for further systematic investigation into FAT10's biological roles. Accordingly, we aimed to address several knowledge gaps through our experimental work.

In Chapter 1, we examined the role of phosphorylated FAT10 in protein degradation. Phosphorylation of FAT10 has been shown to limit type I interferon production during inflammatory responses. The modification occurs at four serine residues and one threonine residue [76]. We therefore constructed a phosphomimetic FAT10 mutant (FAT10D) by substituting Ser62, Ser64, Ser95, and Ser109 with aspartate and Thr77 with glutamate. As shown in Figures 1.1 and 1.2, although the expression level of FAT10 D was lower than FAT10 WT, FAT10 D's conjugation appeared to be more abundant than that of FAT10 WT. However, the degradation rate of FAT10 D did not differ significantly from that of FAT10 WT. NUB1L is known to bind FAT10 and accelerate its degradation [44, 56, 126]. As shown in Figure 1.3, the interaction between FAT10 D and NUB1L was weakened. Moreover, the results indicate that Thr77 is a critical residue for this interaction (Figure 1.4). This resembles the behavior of ubiquitin and NEDD8, where a single phosphorylation event can significantly alter protein–protein interactions [134]. However, both exhibited similar half-lives, and NUB1L similarly accelerated their degradation. This is in agreement with the findings of Schmidtke, who reported that NUB1L enhances FAT10 degradation independently of its binding to FAT10 [126]. Additionally, FAT10 can directly interact with the VWA domain of RPN10 to facilitate its degradation [53]. The interaction between FAT10 and RPN10 was unaffected by phospho-mimetic mutations (Figure 1.6). Therefore, even when binding to NUB1L is altered, the FAT10 degradation pathway remains intact. These findings suggest that FAT10

phosphorylation fine-tunes interactions with specific adaptor proteins without compromising its essential role in proteasomal targeting.

In Chapter 2, we investigated the relationship between FAT10 and IL-12 secretion by DCs. DCs are crucial initiators of antigen-specific immune responses and key regulators of immune homeostasis [156]. Notably, FAT10 is robustly expressed in human monocyte-derived DCs [77] and is upregulated following LPS stimulation, alongside the accumulation of FAT10-conjugated substrates [82]. IL-12, predominantly secreted by monocytes, macrophages, B cells, and DCs [145]. Previous observations indicated that FAT10-deficient mice exhibited reduced IL-12p40 expression in the spleen following LCMV infection [91], prompting the hypothesis that FAT10 might regulate IL-12 production or signaling. We first investigated whether LPS stimulation could induce IL-12 mRNA expression in DC2.4 cells. As shown in Figure 2.1, IL-12p40 mRNA expression was induced in both DC2.4 and DC2.4-FAT10 cells after 24 hours of LPS stimulation, however, no significant difference was observed between the two cell lines, suggesting that FAT10 does not influence IL-12p40 mRNA expression in DC2.4 cells. This result was further confirmed in BMDCs isolated from wild-type C57BL/6 and FAT10-deficient mice (Figure 2.2). Since IL-12 promotes $CD4^+$ T cell differentiation into Th1 cells via the STAT signaling pathway [146, 147, 157] , we also examined whether FAT10 influences Th1 differentiation and downstream signaling. However, no effects of FAT10 on Th1 differentiation (Figure 2.3) or on downstream signaling events (Figure 2.4) were observed. In summary, our results indicate that FAT10 has no effect on the regulation of IL-12 expression in dendritic cells or IL-12-induced signaling in T cells.

In Chapter 3, we aimed to construct FAT10-USE1-GFP conjugates designed to serve as functional probes for the identification of E3 ligases involved in FAT10ylation. Notably, FAT10 expression is elevated in various types of cancer [93, 96, 98-100, 164]. FAT10ylation constitutes a distinct PTM pathway, involving a dedicated enzymatic cascade comprising an E1 activating enzyme, an E2 conjugating enzyme, and an E3 ligase [47, 165, 166]. During this process, FAT10 is covalently attached to substrate proteins and co-degraded with them by the 26S proteasome [143]. In this study, we developed FAT10-USE1-GFP conjugates via C-terminal thiol-reactive modification of FAT10, allowing selective binding to candidate E3 ligases with high affinity. Compared to previously reported strategies [181], our approach is notably more straightforward and time-efficient, while avoiding harsh reaction conditions and the need for expensive instrumentation. Previous mass spectrometry-based studies [180, 181, 184, 185] have demonstrated that USE1 reacts specifically at its active site cysteine. As shown in Figure 3.4, the C-terminus of FAT10 is covalently linked to the cysteine residue in USE1-GFP,

consistent with reactivity at the catalytic site. Furthermore, we did not observe any reaction between the alkyne-labeled lysine of USE1-GFP and FAT10-SH, likely due to the low affinity and concentration of the reactants under our conditions, or due to the preferential interaction of the FAT10-SH C-terminus with the active center of USE1-GFP, which may prevent the alkyne from reacting. Currently, only one E3 ligase has been identified for FAT10 [114], in stark contrast to the hundreds known for ubiquitin [167]. Therefore, we are confident that the FAT10-USE1-GFP conjugates generated in this study will serve as valuable tools for uncovering additional E3 ligases specific to FAT10, especially when suitable patient-derived material becomes available.

These investigations advance our understanding of FAT10 at the molecular, immunological, and methodological levels.

Nevertheless, significant challenges remain. Although our investigations cover broad aspects of FAT10 biology, they are not without limitations in depth. For example, future studies could employ dynamic in vivo tracking of phospho-mimetic FAT10 to examine its expression patterns, intracellular trafficking, and stability under physiological conditions. Furthermore, while our findings exclude a direct role for FAT10 in IL-12 secretion, the underlying mechanisms responsible for altered cytokine profiles in FAT10-deficient immune cells remain unclear and merit further exploration. It is also important to consider the influence of environmental factors, such as inflammation or infection, on FAT10 function in immune regulation. Additionally, while we successfully generated a FAT10-based probe, the identification and functional characterization of novel E3 ligases require further systematic investigation.

In conclusion, this dissertation offers novel insights into the functional landscape of FAT10, contributing to both biochemical and immunological research and providing a foundation for future mechanistic investigations.

References

1. Schlesinger DH, Goldstein G, Niall HD: **The complete amino acid sequence of ubiquitin, an adenylate cyclase stimulating polypeptide probably universal in living cells**. *Biochemistry* 1975, **14**(10):2214-2218.

2. Swatek KN, Komander D: **Ubiquitin modifications**. *Cell Res* 2016, **26**(4):399-422.

3. Rona G, Pagano M: **Mixed ubiquitin chains regulate DNA repair**. *Genes Dev* 2019, **33**(23-24):1615-1616.

4. Chen ZJ, Sun LJ: **Nonproteolytic functions of ubiquitin in cell signaling**. *Mol Cell* 2009, **33**(3):275-286.

5. van der Veen AG, Ploegh HL: **Ubiquitin-like proteins**. *Annu Rev Biochem* 2012, **81**:323-357.

6. Cappadocia L, Lima CD: **Ubiquitin-like Protein Conjugation: Structures, Chemistry, and Mechanism**. *Chem Rev* 2018, **118**(3):889-918.

7. Kerscher O, Felberbaum R, Hochstrasser M: **Modification of proteins by ubiquitin and ubiquitin-like proteins**. *Annu Rev Cell Dev Biol* 2006, **22**:159-180.

8. Rogov VV, Nezis IP, Tsapras P, Zhang H, Dagdas Y, Noda NN, Nakatogawa H, Wirth M, Mouilleron S, McEwan DG *et al*: **Atg8 family proteins, LIR/AIM motifs and other interaction modes**. *Autophagy Rep* 2023, **2**(1).

9. Wesch N, Kirkin V, Rogov VV: **Atg8-Family Proteins-Structural Features and Molecular Interactions in Autophagy and Beyond**. *Cells* 2020, **9**(9).

10. Noda NN, Satoo K, Fujioka Y, Kumeta H, Ogura K, Nakatogawa H, Ohsumi Y, Inagaki F: **Structural basis of Atg8 activation by a homodimeric E1, Atg7**. *Mol Cell* 2011, **44**(3):462-475.

11. Geng J, Klionsky DJ: **The Atg8 and Atg12 ubiquitin-like conjugation systems in macroautophagy. 'Protein modifications: beyond the usual suspects' review series**. *EMBO Rep* 2008, **9**(9):859-864.

12. Radoshevich L, Murrow L, Chen N, Fernandez E, Roy S, Fung C, Debnath J: **ATG12 conjugation to ATG3 regulates mitochondrial homeostasis and cell death**. *Cell* 2010, **142**(4):590-600.

13. Hanada T, Noda NN, Satomi Y, Ichimura Y, Fujioka Y, Takao T, Inagaki F, Ohsumi Y: **The Atg12-Atg5 conjugate has a novel E3-like activity for protein lipidation in autophagy**. *J Biol Chem* 2007, **282**(52):37298-37302.

14. Keulers TG, Koch A, van Gisbergen MW, Barbeau LMO, Zonneveld MI, de Jong MC, Savelkouls KGM, Wanders RG, Bussink J, Melotte V *et al*: **ATG12 deficiency results in intracellular glutamine depletion, abrogation of tumor hypoxia and a favorable prognosis in cancer**. *Autophagy* 2022, **18**(8):1898-1914.

15. Mirzalieva O, Juncker M, Schwartzenburg J, Desai S: **ISG15 and ISGylation in Human Diseases**. *Cells* 2022, **11**(3).

16. Dzimianski JV, Scholte FEM, Bergeron E, Pegan SD: **ISG15: It's Complicated**. *J Mol Biol* 2019, **431**(21):4203-4216.

17. Perng YC, Lenschow DJ: **ISG15 in antiviral immunity and beyond**. *Nat Rev Microbiol* 2018, **16**(7):423-439.

18. Jeon YJ, Yoo HM, Chung CH: **ISG15 and immune diseases**. *Biochim Biophys Acta* 2010, **1802**(5):485-496.

19. Kono M, Yamasaki K, Nakamura M: **Investigating the regulatory mechanism of glucose metabolism by ubiquitin-like protein MNSFbeta**. *Mol Biol Rep* 2024, **51**(1):1053.

20. Nakamura M, Fukuma Y, Notsu K, Kono M: **Quercetin and HSC70 coregulate the anti-inflammatory action of the ubiquitin-like protein MNSFbeta**. *Mol Biol Rep* 2022, **49**(2):1213-1222.

21. Nakamura M, Nakagawa M, Watanabe J: **Ubiquitin-like protein MNSFbeta negatively regulates T cell function and survival**. *Immunol Invest* 2015, **44**(1):1-12.

22. Lu X, Malley KR, Brenner CC, Koroleva O, Korolev S, Downes BP: **A MUB E2 structure reveals E1 selectivity between cognate ubiquitin E2s in eukaryotes**. *Nat Commun* 2016, **7**:12580.

23. Dowil RT, Lu X, Saracco SA, Vierstra RD, Downes BP: **Arabidopsis membrane-anchored ubiquitin-fold (MUB) proteins localize a specific subset of ubiquitin-conjugating (E2) enzymes to the plasma membrane**. *J Biol Chem* 2011, **286**(17):14913-14921.

24. Downes BP, Saracco SA, Lee SS, Crowell DN, Vierstra RD: **MUBs, a family of ubiquitin-fold proteins that are plasma membrane-anchored by prenylation**. *J Biol Chem* 2006, **281**(37):27145-27157.

25. Papakyriacou I, Kutkaite G, Rubies Bedos M, Nagarajan D, Alford LP, Menden MP, Mao Y: **Loss of NEDD8 in cancer cells causes vulnerability to immune checkpoint blockade in triple-negative breast cancer**. *Nat Commun* 2024, **15**(1):3581.

26. Fu DJ, Wang T: **Targeting NEDD8-activating enzyme for cancer therapy: developments, clinical trials, challenges and future research directions**. *J Hematol Oncol* 2023, **16**(1):87.

27. Baek K, Krist DT, Prabu JR, Hill S, Klugel M, Neumaier LM, von Gronau S, Kleiger G, Schulman BA: **NEDD8 nucleates a multivalent cullin-RING-UBE2D ubiquitin ligation assembly**. *Nature* 2020, **578**(7795):461-466.

28. Schwechheimer C: **NEDD8-its role in the regulation of Cullin-RING ligases**. *Curr Opin Plant Biol* 2018, **45**(Pt A):112-119.

29. Watson IR, Irwin MS, Ohh M: **NEDD8 pathways in cancer, Sine Quibus Non**. *Cancer Cell* 2011, **19**(2):168-176.

30. Wu Q, Jiang Y, You C: **The SUMO components in rheumatoid arthritis**. *Rheumatology (Oxford)* 2022, **61**(12):4619-4630.

31. Yau TY, Sander W, Eidson C, Courey AJ: **SUMO Interacting Motifs: Structure and Function**. *Cells* 2021, **10**(11).

32. Chang HM, Yeh ETH: **SUMO: From Bench to Bedside**. *Physiol Rev* 2020, **100**(4):1599-1619.

33. Han ZJ, Feng YH, Gu BH, Li YM, Chen H: **The post-translational modification, SUMOylation, and cancer (Review)**. *Int J Oncol* 2018, **52**(4):1081-1094.

34. Xia L, He Y, Sui Y, Feng X, Qian X, Liu Y, Qi Z: **UBL5 and Its Role in Viral**

Infections. *Viruses* 2024, **16**(12).

35. Chanarat S: **UBL5/Hub1: An Atypical Ubiquitin-Like Protein with a Typical Role as a Stress-Responsive Regulator**. *Int J Mol Sci* 2021, **22**(17).

36. McNally T, Huang Q, Janis RS, Liu Z, Olejniczak ET, Reilly RM: **Structural analysis of UBL5, a novel ubiquitin-like modifier**. *Protein Sci* 2003, **12**(7):1562-1566.

37. Kolathur KK, Mallya S, Barve S, Bojja SL, Wagle MM: **Moonlighting functions of the ubiquitin-like protein, Hub1/UBL-5**. *Int J Biochem Cell Biol* 2023, **162**:106445.

38. Komatsu M, Inada T, Noda NN: **The UFM1 system: Working principles, cellular functions, and pathophysiology**. *Mol Cell* 2024, **84**(1):156-169.

39. Yang S, Moy N, Yang R: **The UFM1 conjugation system in mammalian development**. *Dev Dyn* 2023, **252**(7):976-985.

40. Daniel J, Liebau E: **The ufm1 cascade**. *Cells* 2014, **3**(2):627-638.

41. Cairo LV, Hong X, Muller MBD, Yuste-Checa P, Jagadeesan C, Bracher A, Park SH, Hayer-Hartl M, Hartl FU: **Stress-dependent condensate formation regulated by the ubiquitin-related modifier Urm1**. *Cell* 2024, **187**(17):4656-4673 e4628.

42. Termathe M, Leidel SA: **Urm1: A Non-Canonical UBL**. *Biomolecules* 2021, **11**(2).

43. Aichem A, Groettrup M: **The ubiquitin-like modifier FAT10 - much more than a proteasome-targeting signal**. *J Cell Sci* 2020, **133**(14).

44. Schmidtke G, Aichem A, Groettrup M: **FAT10ylation as a signal for proteasomal degradation**. *Biochim Biophys Acta* 2014, **1843**(1):97-102.

45. Aichem A, Anders S, Catone N, Rossler P, Stotz S, Berg A, Schwab R, Scheuermann S, Bialas J, Schutz-Stoffregen MC *et al*: **The structure of the ubiquitin-like modifier FAT10 reveals an alternative targeting mechanism for proteasomal degradation**. *Nat Commun* 2018, **9**(1):3321.

46. Gavin JM, Chen JJ, Liao H, Rollins N, Yang X, Xu Q, Ma J, Loke HK, Lingaraj T, Brownell JE *et al*: **Mechanistic studies on activation of ubiquitin and di-ubiquitin-like protein, FAT10, by ubiquitin-like modifier activating enzyme 6, Uba6**. *J Biol Chem* 2012, **287**(19):15512-15522.

47. Aichem A, Pelzer C, Lukasiak S, Kalveram B, Sheppard PW, Rani N, Schmidtke G, Groettrup M: **USE1 is a bispecific conjugating enzyme for ubiquitin and FAT10, which FAT10ylates itself in cis**. *Nat Commun* 2010, **1**:13.

48. Bialas J, Boehm AN, Catone N, Aichem A, Groettrup M: **The ubiquitin-like modifier FAT10 stimulates the activity of deubiquitylating enzyme OTUB1**. *J Biol Chem* 2019, **294**(12):4315-4330.

49. Deveraux Q, Ustrell V, Pickart C, Rechsteiner M: **A 26 S protease subunit that binds ubiquitin conjugates**. *J Biol Chem* 1994, **269**(10):7059-7061.

50. Jiang TX, Zhao M, Qiu XB: **Substrate receptors of proteasomes**. *Biol Rev Camb Philos Soc* 2018, **93**(4):1765-1777.

51. Wang Q, Young P, Walters KJ: **Structure of S5a bound to monoubiquitin provides a model for polyubiquitin recognition**. *J Mol Biol* 2005, **348**(3):727-739.

52. van Nocker S, Sadis S, Rubin DM, Glickman M, Fu H, Coux O, Wefes I, Finley D, Vierstra RD: **The multiubiquitin-chain-binding protein Mcb1 is a component of the 26S proteasome in Saccharomyces cerevisiae and plays a nonessential,**

substrate-specific role in protein turnover. *Mol Cell Biol* 1996, **16**(11):6020-6028.

53. Rani N, Aichem A, Schmidtke G, Kreft SG, Groettrup M: **FAT10 and NUB1L bind to the VWA domain of Rpn10 and Rpn1 to enable proteasome-mediated proteolysis**. *Nat Commun* 2012, **3**:749.

54. Raasi S, Varadan R, Fushman D, Pickart CM: **Diverse polyubiquitin interaction properties of ubiquitin-associated domains**. *Nat Struct Mol Biol* 2005, **12**(8):708-714.

55. Hipp MS, Raasi S, Groettrup M, Schmidtke G: **NEDD8 ultimate buster-1L interacts with the ubiquitin-like protein FAT10 and accelerates its degradation**. *J Biol Chem* 2004, **279**(16):16503-16510.

56. Brockmann F, Catone N, Wunsch C, Offensperger F, Scheffner M, Schmidtke G, Aichem A: **FAT10 and NUB1L cooperate to activate the 26S proteasome**. *Life Sci Alliance* 2023, **6**(8).

57. Aichem A, Kalveram B, Spinnenhirn V, Kluge K, Catone N, Johansen T, Groettrup M: **The proteomic analysis of endogenous FAT10 substrates identifies p62/SQSTM1 as a substrate of FAT10ylation**. *J Cell Sci* 2012, **125**(Pt 19):4576-4585.

58. Bialas J, Groettrup M, Aichem A: **Conjugation of the ubiquitin activating enzyme UBE1 with the ubiquitin-like modifier FAT10 targets it for proteasomal degradation**. *PLoS One* 2015, **10**(3):e0120329.

59. Aichem A, Sailer C, Ryu S, Catone N, Stankovic-Valentin N, Schmidtke G, Melchior F, Stengel F, Groettrup M: **The ubiquitin-like modifier FAT10 interferes with SUMO activation**. *Nat Commun* 2019, **10**(1):4452.

60. Chen Z, Zhang W, Yun Z, Zhang X, Gong F, Wang Y, Ji S, Leng L: **Ubiquitin-like protein FAT10 regulates DNA damage repair via modification of proliferating cell nuclear antigen**. *Mol Med Rep* 2018, **17**(6):7487-7496.

61. Ji F, Jin X, Jiao CH, Xu QW, Wang ZW, Chen YL: **FAT10 level in human gastric cancer and its relation with mutant p53 level, lymph node metastasis and TNM staging**. *World J Gastroenterol* 2009, **15**(18):2228-2233.

62. Zhang Y, Zuo Z, Liu B, Yang P, Wu J, Han L, Han T, Chen T: **FAT10 promotes hepatocellular carcinoma (HCC) carcinogenesis by mediating P53 degradation and acts as a prognostic indicator of HCC**. *J Gastrointest Oncol* 2021, **12**(4):1823-1837.

63. Mueller S, Bialas J, Ryu S, Catone N, Aichem A: **The ubiquitin-like modifier FAT10 covalently modifies HUWE1 and strengthens the interaction of AMBRA1 and HUWE1**. *PLoS One* 2023, **18**(8):e0290002.

64. Yuan R, Wang K, Hu J, Yan C, Li M, Yu X, Liu X, Lei J, Guo W, Wu L *et al*: **Ubiquitin-like protein FAT10 promotes the invasion and metastasis of hepatocellular carcinoma by modifying beta-catenin degradation**. *Cancer Res* 2014, **74**(18):5287-5300.

65. Nguyen NT, Now H, Kim WJ, Kim N, Yoo JY: **Ubiquitin-like modifier FAT10 attenuates RIG-I mediated antiviral signaling by segregating activated RIG-I from its signaling platform**. *Sci Rep* 2016, **6**:23377.

66. Wang G, Kouwaki T, Okamoto M, Oshiumi H: **Attenuation of the Innate Immune Response against Viral Infection Due to ZNF598-Promoted Binding of FAT10 to RIG-I**. *Cell Rep* 2019, **28**(8):1961-1970 e1964.

67. Theng SS, Wang W, Mah WC, Chan C, Zhuo J, Gao Y, Qin H, Lim L, Chong SS, Song

J *et al*: **Disruption of FAT10-MAD2 binding inhibits tumor progression**. *Proc Natl Acad Sci U S A* 2014, **111**(49):E5282-5291.

68. Liu YC, Pan J, Zhang C, Fan W, Collinge M, Bender JR, Weissman SM: **A MHC-encoded ubiquitin-like protein (FAT10) binds noncovalently to the spindle assembly checkpoint protein MAD2**. *Proc Natl Acad Sci U S A* 1999, **96**(8):4313-4318.

69. Kalveram B, Schmidtke G, Groettrup M: **The ubiquitin-like modifier FAT10 interacts with HDAC6 and localizes to aggresomes under proteasome inhibition**. *J Cell Sci* 2008, **121**(Pt 24):4079-4088.

70. Venne AS, Kollipara L, Zahedi RP: **The next level of complexity: crosstalk of posttranslational modifications**. *Proteomics* 2014, **14**(4-5):513-524.

71. Raasi S, Schmidtke G, Groettrup M: **The ubiquitin-like protein FAT10 forms covalent conjugates and induces apoptosis**. *J Biol Chem* 2001, **276**(38):35334-35343.

72. Buchsbaum S, Bercovich B, Ciechanover A: **FAT10 is a proteasomal degradation signal that is itself regulated by ubiquitination**. *Mol Biol Cell* 2012, **23**(1):225-232.

73. Hipp MS, Kalveram B, Raasi S, Groettrup M, Schmidtke G: **FAT10, a ubiquitin-independent signal for proteasomal degradation**. *Mol Cell Biol* 2005, **25**(9):3483-3491.

74. Bilbrough T, Piemontese E, Seitz O: **Dissecting the role of protein phosphorylation: a chemical biology toolbox**. *Chem Soc Rev* 2022, **51**(13):5691-5730.

75. Khoury GA, Baliban RC, Floudas CA: **Proteome-wide post-translational modification statistics: frequency analysis and curation of the swiss-prot database**. *Sci Rep* 2011, **1**.

76. Saxena K, Roverato ND, Reithmann M, Mah MM, Schregle R, Schmidtke G, Silbern I, Urlaub H, Aichem A: **FAT10 is phosphorylated by IKKbeta to inhibit the antiviral type-I interferon response**. *Life Sci Alliance* 2024, **7**(1).

77. Lukasiak S, Schiller C, Oehlschlaeger P, Schmidtke G, Krause P, Legler DF, Autschbach F, Schirmacher P, Breuhahn K, Groettrup M: **Proinflammatory cytokines cause FAT10 upregulation in cancers of liver and colon**. *Oncogene* 2008, **27**(46):6068-6074.

78. Canaan A, Yu X, Booth CJ, Lian J, Lazar I, Gamfi SL, Castille K, Kohya N, Nakayama Y, Liu YC *et al*: **FAT10/diubiquitin-like protein-deficient mice exhibit minimal phenotypic differences**. *Mol Cell Biol* 2006, **26**(13):5180-5189.

79. Lee CG, Ren J, Cheong IS, Ban KH, Ooi LL, Yong Tan S, Kan A, Nuchprayoon I, Jin R, Lee KH *et al*: **Expression of the FAT10 gene is highly upregulated in hepatocellular carcinoma and other gastrointestinal and gynecological cancers**. *Oncogene* 2003, **22**(17):2592-2603.

80. Raasi S, Schmidtke G, de Giuli R, Groettrup M: **A ubiquitin-like protein which is synergistically inducible by interferon-gamma and tumor necrosis factor-alpha**. *Eur J Immunol* 1999, **29**(12):4030-4036.

81. Schregle R, Mah MM, Mueller S, Aichem A, Basler M, Groettrup M: **The expression profile of the ubiquitin-like modifier FAT10 in immune cells suggests cell type-specific functions**. *Immunogenetics* 2018, **70**(7):429-438.

82. Ebstein F, Lange N, Urban S, Seifert U, Kruger E, Kloetzel PM: **Maturation of human dendritic cells is accompanied by functional remodelling of the**

ubiquitin-proteasome system. *Int J Biochem Cell Biol* 2009, **41**(5):1205-1215.

83. Ebstein F, Lehmann A, Kloetzel PM: **The FAT10- and ubiquitin-dependent degradation machineries exhibit common and distinct requirements for MHC class I antigen presentation**. *Cell Mol Life Sci* 2012, **69**(14):2443-2454.

84. Pach N, Basler M: **Cellular stress increases DRIP production and MHC Class I antigen presentation**. *Front Immunol* 2024, **15**:1445338.

85. Munz C: **Antigen Processing for MHC Class II Presentation via Autophagy**. *Front Immunol* 2012, **3**:9.

86. Basler M, Buerger S, Groettrup M: **The ubiquitin-like modifier FAT10 in antigen processing and antimicrobial defense**. *Mol Immunol* 2015, **68**(2 Pt A):129-132.

87. Wan R, Yuan P, Guo L, Shao J, Liu X, Lai W, Kong Q, Chen L, Ge J, Xu Z *et al*: **Ubiquitin-like protein FAT10 suppresses SIRT1-mediated autophagy to protect against ischemic myocardial injury**. *J Mol Cell Cardiol* 2021, **153**:1-13.

88. Zhang W, Du D, Lu H, Zhang D, Liu L, Li J, Chen Z, Yu X, Ye M, Wang W *et al*: **FAT10 mediates the sorafenib-resistance of hepatocellular carcinoma cells by stabilizing E3 ligase NEDD4 to enhance PTEN/AKT pathway-induced autophagy**. *Am J Cancer Res* 2024, **14**(4):1523-1544.

89. Spinnenhirn V, Farhan H, Basler M, Aichem A, Canaan A, Groettrup M: **The ubiquitin-like modifier FAT10 decorates autophagy-targeted Salmonella and contributes to Salmonella resistance in mice**. *J Cell Sci* 2014, **127**(Pt 22):4883-4893.

90. Zhang Y, Tang J, Yang N, Liu Q, Zhang Q, Zhang Y, Li N, Zhao Y, Li S, Liu S *et al*: **FAT10 Is Critical in Influenza A Virus Replication by Inhibiting Type I IFN**. *J Immunol* 2016, **197**(3):824-833.

91. Mah MM, Basler M, Groettrup M: **The ubiquitin-like modifier FAT10 is required for normal IFN-gamma production by activated CD8(+) T cells**. *Mol Immunol* 2019, **108**:111-120.

92. Ma C, Zhang Z, Cui Y, Yuan H, Wang F: **Silencing FAT10 inhibits metastasis of osteosarcoma**. *Int J Oncol* 2016, **49**(2):666-674.

93. Xue F, Zhu L, Meng QW, Wang L, Chen XS, Zhao YB, Xing Y, Wang XY, Cai L: **FAT10 is associated with the malignancy and drug resistance of non-small-cell lung cancer**. *Onco Targets Ther* 2016, **9**:4397-4409.

94. Xiang S, Shao X, Cao J, Yang B, He Q, Ying M: **FAT10: Function and Relationship with Cancer**. *Curr Mol Pharmacol* 2020, **13**(3):182-191.

95. Zhang K, Chen L, Zhang Z, Cao J, He L, Li L: **Ubiquitin-like protein FAT10: A potential cardioprotective factor and novel therapeutic target in cancer**. *Clin Chim Acta* 2020, **510**:802-811.

96. Zou Y, Du Y, Cheng C, Deng X, Shi Z, Lu X, Hu H, Qiu J, Jiang W: **FAT10 promotes the progression of bladder cancer by upregulating HK2 through the EGFR/AKT pathway**. *Exp Cell Res* 2021, **398**(1):112401.

97. Wang Y, Zhang H: **FAT10 is a Prognostic Biomarker and Correlated With Immune Infiltrates in Skin Cutaneous Melanoma**. *Front Mol Biosci* 2022, **9**:805887.

98. Zhu J, Zhao J, Luo C, Zhu Z, Peng X, Zhu X, Lin K, Bu F, Zhang W, Li Q *et al*: **FAT10 promotes chemotherapeutic resistance in pancreatic cancer by inducing epithelial-mesenchymal transition via stabilization of FOXM1 expression**. *Cell*

Death Dis 2022, **13**(5):497.

99. Cheng F, Yuan L, Wu Z, Li X, Xia W, Huang Z, Li Z, Mao S, Shen W: **Ubiquitin-Like Protein FAT10 Promote Colorectal Cancer Progression by Affecting the Ubiquitination of Capn4**. *Dig Dis Sci* 2023, **68**(8):3312-3323.

100. Chen X, Wu W, Jeong JH, Rokavec M, Wei R, Feng S, Schroth W, Brauch H, Zhong S, Luo JL: **Cytokines-activated nuclear IKKalpha-FAT10 pathway induces breast cancer tamoxifen-resistance**. *Sci China Life Sci* 2024, **67**(7):1413-1426.

101. Wang Q, Tan W, Zhang Z, Chen Q, Xie Z, Yang L, Tang C, Zhuang H, Wang B, Jiang J *et al*: **FAT10 induces immune suppression by upregulating PD-L1 expression in hepatocellular carcinoma**. *Apoptosis* 2024, **29**(9-10):1529-1545.

102. Liu L, Dong Z, Liang J, Cao C, Sun J, Ding Y, Wu D: **As an independent prognostic factor, FAT10 promotes hepatitis B virus-related hepatocellular carcinoma progression via Akt/GSK3beta pathway**. *Oncogene* 2014, **33**(7):909-920.

103. Yan DW, Li DW, Yang YX, Xia J, Wang XL, Zhou CZ, Fan JW, Wen YG, Sun HC, Wang Q *et al*: **Ubiquitin D is correlated with colon cancer progression and predicts recurrence for stage II-III disease after curative surgery**. *Br J Cancer* 2010, **103**(7):961-969.

104. Yuan J, Tu Y, Mao X, He S, Wang L, Fu G, Zong J, Zhang Y: **Increased expression of FAT10 is correlated with progression and prognosis of human glioma**. *Pathol Oncol Res* 2012, **18**(4):833-839.

105. Gao Y, Theng SS, Zhuo J, Teo WB, Ren J, Lee CG: **FAT10, an ubiquitin-like protein, confers malignant properties in non-tumorigenic and tumorigenic cells**. *Carcinogenesis* 2014, **35**(4):923-934.

106. Fan W, Cai W, Parimoo S, Schwarz DC, Lennon GG, Weissman SM: **Identification of seven new human MHC class I region genes around the HLA-F locus**. *Immunogenetics* 1996, **44**(2):97-103.

107. Aichem A, Boehm AN, Catone N, Schmidtke G, Groettrup M: **Analysis of modification and proteolytic targeting by the ubiquitin-like modifier FAT10**. *Methods Enzymol* 2019, **618**:229-256.

108. Bates EE, Ravel O, Dieu MC, Ho S, Guret C, Bridon JM, Ait-Yahia S, Briere F, Caux C, Banchereau J *et al*: **Identification and analysis of a novel member of the ubiquitin family expressed in dendritic cells and mature B cells**. *Eur J Immunol* 1997, **27**(10):2471-2477.

109. Wang T, Jiang J, Zhang X, Ke X, Qu Y: **Ubiquitin-like modification dependent proteasomal degradation and disease therapy**. *Trends Mol Med* 2024, **30**(11):1061-1075.

110. Chiu YH, Sun Q, Chen ZJ: **E1-L2 activates both ubiquitin and FAT10**. *Mol Cell* 2007, **27**(6):1014-1023.

111. Wang F, Zhao B: **UBA6 and Its Bispecific Pathways for Ubiquitin and FAT10**. *Int J Mol Sci* 2019, **20**(9).

112. Truongvan N, Li S, Misra M, Kuhn M, Schindelin H: **Structures of UBA6 explain its dual specificity for ubiquitin and FAT10**. *Nat Commun* 2022, **13**(1):4789.

113. Wu C, Liu Y, Gu X, Zhu T, Yang S, Sun W: **LMO2 blocks the UBA6-USE1 interaction and downstream FAT10ylation by targeting the ubiquitin fold domain of UBA6**. *Biochem Biophys Res Commun* 2016, **478**(3):1442-1448.

114. Roverato ND, Sailer C, Catone N, Aichem A, Stengel F, Groettrup M: **Parkin is an E3 ligase for the ubiquitin-like modifier FAT10, which inhibits Parkin activation and mitophagy**. *Cell Rep* 2021, **34**(11):108857.

115. Wang XL, Feng ST, Wang ZZ, Yuan YH, Chen NH, Zhang Y: **Parkin, an E3 Ubiquitin Ligase, Plays an Essential Role in Mitochondrial Quality Control in Parkinson's Disease**. *Cell Mol Neurobiol* 2021, **41**(7):1395-1411.

116. Caulfield TR, Fiesel FC, Springer W: **Activation of the E3 ubiquitin ligase Parkin**. *Biochem Soc Trans* 2015, **43**(2):269-274.

117. Negi H, Ravichandran A, Dasgupta P, Reddy S, Das R: **Plasticity of the proteasome-targeting signal Fat10 enhances substrate degradation**. *Elife* 2024, **13**.

118. Dominguez-Brauer C, Khatun R, Elia AJ, Thu KL, Ramachandran P, Baniasadi SP, Hao Z, Jones LD, Haight J, Sheng Y *et al*: **E3 ubiquitin ligase Mule targets beta-catenin under conditions of hyperactive Wnt signaling**. *Proc Natl Acad Sci U S A* 2017, **114**(7):E1148-E1157.

119. Mah MM, Roverato N, Groettrup M: **Regulation of Interferon Induction by the Ubiquitin-Like Modifier FAT10**. *Biomolecules* 2020, **10**(6).

120. Nakamura N: **Ubiquitin System**. *Int J Mol Sci* 2018, **19**(4).

121. Akutsu M, Dikic I, Bremm A: **Ubiquitin chain diversity at a glance**. *J Cell Sci* 2016, **129**(5):875-880.

122. Thoresen D, Wang W, Galls D, Guo R, Xu L, Pyle AM: **The molecular mechanism of RIG-I activation and signaling**. *Immunol Rev* 2021, **304**(1):154-168.

123. Wehmer M, Rudack T, Beck F, Aufderheide A, Pfeifer G, Plitzko JM, Forster F, Schulten K, Baumeister W, Sakata E: **Structural insights into the functional cycle of the ATPase module of the 26S proteasome**. *Proc Natl Acad Sci U S A* 2017, **114**(6):1305-1310.

124. Tanaka T, Kawashima H, Yeh ET, Kamitani T: **Regulation of the NEDD8 conjugation system by a splicing variant, NUB1L**. *J Biol Chem* 2003, **278**(35):32905-32913.

125. Vodicka P, Chase K, Iuliano M, Valentine DT, Sapp E, Lu B, Kegel-Gleason KB, Sena-Esteves M, Aronin N, DiFiglia M: **Effects of Exogenous NUB1 Expression in the Striatum of HDQ175/Q7 Mice**. *J Huntingtons Dis* 2016, **5**(2):163-174.

126. Schmidtke G, Kalveram B, Weber E, Bochtler P, Lukasiak S, Hipp MS, Groettrup M: **The UBA domains of NUB1L are required for binding but not for accelerated degradation of the ubiquitin-like modifier FAT10**. *J Biol Chem* 2006, **281**(29):20045-20054.

127. Arkinson C, Dong KC, Gee CL, Costello SM, Marqusee S, Martin A: **Nub1 traps unfolded FAT10 for ubiquitin-independent degradation by the 26S proteasome**. *bioRxiv* 2024.

128. Verma R, Oania R, Graumann J, Deshaies RJ: **Multiubiquitin chain receptors define a layer of substrate selectivity in the ubiquitin-proteasome system**. *Cell* 2004, **118**(1):99-110.

129. Tanji K, Tanaka T, Kamitani T: **Interaction of NUB1 with the proteasome subunit S5a**. *Biochem Biophys Res Commun* 2005, **337**(1):116-120.

130. Kawahara H: **Structures and functions of the 26S proteasome Rpn10 family**.

Yakugaku Zasshi 2002, **122**(9):615-624.

131. Saeki Y, Saitoh A, Toh-e A, Yokosawa H: **Ubiquitin-like proteins and Rpn10 play cooperative roles in ubiquitin-dependent proteolysis**. *Biochem Biophys Res Commun* 2002, **293**(3):986-992.

132. Shockett P, Difilippantonio M, Hellman N, Schatz DG: **A modified tetracycline-regulated system provides autoregulatory, inducible gene expression in cultured cells and transgenic mice**. *Proc Natl Acad Sci U S A* 1995, **92**(14):6522-6526.

133. Koyano F, Okatsu K, Kosako H, Tamura Y, Go E, Kimura M, Kimura Y, Tsuchiya H, Yoshihara H, Hirokawa T *et al*: **Ubiquitin is phosphorylated by PINK1 to activate parkin**. *Nature* 2014, **510**(7503):162-166.

134. Stuber K, Schneider T, Werner J, Kovermann M, Marx A, Scheffner M: **Structural and functional consequences of NEDD8 phosphorylation**. *Nat Commun* 2021, **12**(1):5939.

135. Kane LA, Lazarou M, Fogel AI, Li Y, Yamano K, Sarraf SA, Banerjee S, Youle RJ: **PINK1 phosphorylates ubiquitin to activate Parkin E3 ubiquitin ligase activity**. *J Cell Biol* 2014, **205**(2):143-153.

136. Matic I, Macek B, Hilger M, Walther TC, Mann M: **Phosphorylation of SUMO-1 occurs in vivo and is conserved through evolution**. *J Proteome Res* 2008, **7**(9):4050-4057.

137. Lowe ED, Hasan N, Trempe JF, Fonso L, Noble ME, Endicott JA, Johnson LN, Brown NR: **Structures of the Dsk2 UBL and UBA domains and their complex**. *Acta Crystallogr D Biol Crystallogr* 2006, **62**(Pt 2):177-188.

138. Liang RY, Chen L, Ko BT, Shen YH, Li YT, Chen BR, Lin KT, Madura K, Chuang SM: **Rad23 interaction with the proteasome is regulated by phosphorylation of its ubiquitin-like (UbL) domain**. *J Mol Biol* 2014, **426**(24):4049-4060.

139. Um H, Jeong H, Lee B, Kim Y, Lee J, Roh JS, Lee SG, Park HR, Robinson WH, Sohn DH: **FAT10 Induces cancer cell migration by stabilizing phosphorylated ABI3/NESH**. *Anim Cells Syst (Seoul)* 2023, **27**(1):53-60.

140. Dong D, Jiang W, Lei J, Chen L, Liu X, Ge J, Che B, Xi X, Shao J: **Ubiquitin-like protein FAT10 promotes bladder cancer progression by stabilizing survivin**. *Oncotarget* 2016, **7**(49):81463-81473.

141. Buerger S, Herrmann VL, Mundt S, Trautwein N, Groettrup M, Basler M: **The Ubiquitin-like Modifier FAT10 Is Selectively Expressed in Medullary Thymic Epithelial Cells and Modifies T Cell Selection**. *J Immunol* 2015, **195**(9):4106-4116.

142. Fan W, Liu YC, Parimoo S, Weissman SM: **Olfactory receptor-like genes are located in the human major histocompatibility complex**. *Genomics* 1995, **27**(1):119-123.

143. Schmidtke G, Kalveram B, Groettrup M: **Degradation of FAT10 by the 26S proteasome is independent of ubiquitylation but relies on NUB1L**. *FEBS Lett* 2009, **583**(3):591-594.

144. Cao J, Aichem A, Basler M, Alvarez Salinas GO, Schmidtke G: **Phosphorylated FAT10 Is More Efficiently Conjugated to Substrates, Does Not Bind to NUB1L, and Does Not Alter Degradation by the Proteasome**. *Biomedicines* 2024, **12**(12).

145. Gee K, Guzzo C, Mat NFC, Ma W, Kumar A: **The IL-12 family of cytokines in infection, inflammation and autoimmune disorders**. *Inflamm Allergy Drug Targets*

2009, **8**(1):40-52.

146. Vignali DA, Kuchroo VK: **IL-12 family cytokines: immunological playmakers**. *Nat Immunol* 2012, **13**(8):722-728.

147. Gollob JA, Murphy EA, Mahajan S, Schnipper CP, Ritz J, Frank DA: **Altered interleukin-12 responsiveness in Th1 and Th2 cells is associated with the differential activation of STAT5 and STAT1**. *Blood* 1998, **91**(4):1341-1354.

148. Schmidtke G, Schregle R, Alvarez G, Huber EM, Groettrup M: **The 20S immunoproteasome and constitutive proteasome bind with the same affinity to PA28alphabeta and equally degrade FAT10**. *Mol Immunol* 2019, **113**:22-30.

149. Oliveri F, Basler M, Rao TN, Fehling HJ, Groettrup M: **Immunoproteasome Inhibition Reduces the T Helper 2 Response in Mouse Models of Allergic Airway Inflammation**. *Front Immunol* 2022, **13**:870720.

150. Trinchieri G: **Interleukin-12 and the regulation of innate resistance and adaptive immunity**. *Nat Rev Immunol* 2003, **3**(2):133-146.

151. Sinigaglia F, D'Ambrosio D, Panina-Bordignon P, Rogge L: **Regulation of the IL-12/IL-12R axis: a critical step in T-helper cell differentiation and effector function**. *Immunol Rev* 1999, **170**:65-72.

152. Thierfelder WE, van Deursen JM, Yamamoto K, Tripp RA, Sarawar SR, Carson RT, Sangster MY, Vignali DA, Doherty PC, Grosveld GC *et al*: **Requirement for Stat4 in interleukin-12-mediated responses of natural killer and T cells**. *Nature* 1996, **382**(6587):171-174.

153. Zou J, Presky DH, Wu CY, Gubler U: **Differential associations between the cytoplasmic regions of the interleukin-12 receptor subunits beta1 and beta2 and JAK kinases**. *J Biol Chem* 1997, **272**(9):6073-6077.

154. Bacon CM, McVicar DW, Ortaldo JR, Rees RC, O'Shea JJ, Johnston JA: **Interleukin 12 (IL-12) induces tyrosine phosphorylation of JAK2 and TYK2: differential use of Janus family tyrosine kinases by IL-2 and IL-12**. *J Exp Med* 1995, **181**(1):399-404.

155. Saxena K, Inholz K, Basler M, Aichem A: **FAT10 inhibits TRIM21 to down-regulate antiviral type-I interferon secretion**. *Life Sci Alliance* 2024, **7**(9).

156. Mellman I: **Dendritic cells: master regulators of the immune response**. *Cancer Immunol Res* 2013, **1**(3):145-149.

157. Langrish CL, McKenzie BS, Wilson NJ, de Waal Malefyt R, Kastelein RA, Cua DJ: **IL-12 and IL-23: master regulators of innate and adaptive immunity**. *Immunol Rev* 2004, **202**:96-105.

158. He T, Tang C, Xu S, Moyana T, Xiang J: **Interferon gamma stimulates cellular maturation of dendritic cell line DC2.4 leading to induction of efficient cytotoxic T cell responses and antitumor immunity**. *Cell Mol Immunol* 2007, **4**(2):105-111.

159. Rouas R, Lewalle P, El Ouriaghli F, Nowak B, Duvillier H, Martiat P: **Poly(I:C) used for human dendritic cell maturation preserves their ability to secondarily secrete bioactive IL-12**. *Int Immunol* 2004, **16**(5):767-773.

160. Zhou J, Nouri-Shirazi M, Tang H, Shen Y, Zeng M: **R848/TLR7-Mediated Stronger CD8+ T Immunity Is Dependent on DC-NK Cell Interactions**. *Int Arch Allergy Immunol* 2022, **183**(8):860-875.

161. Watford WT, Moriguchi M, Morinobu A, O'Shea JJ: **The biology of IL-12:**

coordinating innate and adaptive immune responses. *Cytokine Growth Factor Rev* 2003, **14**(5):361-368.

162. Schnell L, Zubrod A, Catone N, Bialas J, Aichem A: **Tumor necrosis factor mediates USE1-independent FAT10ylation under inflammatory conditions**. *Life Sci Alliance* 2023, **6**(11).

163. Raasi S, Schmidtke G, de Giuli R, Groettrup M: **A ubiquitin-like protein which is synergistically inducible by interferon-γ and tumor necrosis factor-α**. *European Journal of Immunology* 1999, **29**(12):4030-4036.

164. Aichem A, Groettrup M: **The ubiquitin-like modifier FAT10 in cancer development**. *Int J Biochem Cell Biol* 2016, **79**:451-461.

165. Pelzer CG, Marcus **FAT10 activated by UBA6 and functioning in protein degredation**. 2010.

166. Groettrup M, Pelzer C, Schmidtke G, Hofmann K: **Activating the ubiquitin family: UBA6 challenges the field**. *Trends Biochem Sci* 2008, **33**(5):230-237.

167. Ciechanover A: **The unravelling of the ubiquitin system**. *Nat Rev Mol Cell Biol* 2015, **16**(5):322-324.

168. Liu Y, Duan C, Zhang C: **E3 Ubiquitin Ligase in Anticancer Drugdsla Resistance: Recent Advances and Future Potential**. *Front Pharmacol* 2021, **12**:645864.

169. Hershko A, Ciechanover A: **The ubiquitin system**. *Annu Rev Biochem* 1998, **67**:425-479.

170. Zinngrebe J, Montinaro A, Peltzer N, Walczak H: **Ubiquitin in the immune system**. *EMBO Rep* 2014, **15**(1):28-45.

171. Yau R, Rape M: **The increasing complexity of the ubiquitin code**. *Nat Cell Biol* 2016, **18**(6):579-586.

172. Varshavsky A: **The Ubiquitin System, Autophagy, and Regulated Protein Degradation**. *Annu Rev Biochem* 2017, **86**:123-128.

173. Burslem GM: **The chemical biology of ubiquitin**. *Biochim Biophys Acta Gen Subj* 2022, **1866**(3):130079.

174. Mathur S, Fletcher AJ, Branigan E, Hay RT, Virdee S: **Photocrosslinking Activity-Based Probes for Ubiquitin RING E3 Ligases**. *Cell Chem Biol* 2020, **27**(1):74-82 e76.

175. Xu L, Fan J, Wang Y, Zhang Z, Fu Y, Li Y-M, Shi J: **An activity-based probe developed by a sequential dehydroalanine formation strategy targets HECT E3 ubiquitin ligases**. *Chem Commun (Camb)* 2019, **55**(49):7109-7112.

176. Witting KF, Mulder MPC, Ovaa H: **Advancing our Understanding of Ubiquitination Using the Ub-Toolkit**. *J Mol Biol* 2017, **429**(22):3388-3394.

177. Gui W, Paudel P, Zhuang Z: **Activity-Based Ubiquitin Probes for Investigation of Deubiquitinases**. In: *Comprehensive Natural Products III*. 2020: 589-602.

178. Wilkinson KD, Gan-Erdene T, Kolli N: **Derivitization of the C-terminus of ubiquitin and ubiquitin-like proteins using intein chemistry: methods and uses**. *Methods Enzymol* 2005, **399**:37-51.

179. Farnung J, Tolmachova KA, Bode JW: **Installation of electrophiles onto the C-terminus of recombinant ubiquitin and ubiquitin-like proteins**. *Chem Sci* 2022,

14(1):121-129.

180. Xu L, Xu Y, Qu Q, Guan C-J, Chu G-C, Shi J, Li Y-M: **Efficient chemical synthesis for the analogue of ubiquitin-based probe Ub–AMC with native bioactivity**. *RSC Advances* 2016, **6**(53):47926-47930.

181. Pao KC, Stanley M, Han C, Lai YC, Murphy P, Balk K, Wood NT, Corti O, Corvol JC, Muqit MM *et al*: **Probes of ubiquitin E3 ligases enable systematic dissection of parkin activation**. *Nat Chem Biol* 2016, **12**(5):324-331.

182. Li Y, Pan M, Li Y, Huang Y, Guo Q: **Thiol-yne radical reaction mediated site-specific protein labeling via genetic incorporation of an alkynyl-L-lysine analogue**. *Org Biomol Chem* 2013, **11**(16):2624-2629.

183. Sommer S, Weikart ND, Linne U, Mootz HD: **Covalent inhibition of SUMO and ubiquitin-specific cysteine proteases by an in situ thiol-alkyne addition**. *Bioorg Med Chem* 2013, **21**(9):2511-2517.

184. Ekkebus R, van Kasteren SI, Kulathu Y, Scholten A, Berlin I, Geurink PP, de Jong A, Goerdayal S, Neefjes J, Heck AJ *et al*: **On terminal alkynes that can react with active-site cysteine nucleophiles in proteases**. *J Am Chem Soc* 2013, **135**(8):2867-2870.

185. Mons E, Kim RQ, van Doodewaerd BR, van Veelen PA, Mulder MPC, Ovaa H: **Exploring the Versatility of the Covalent Thiol-Alkyne Reaction with Substituted Propargyl Warheads: A Deciding Role for the Cysteine Protease**. *J Am Chem Soc* 2021, **143**(17):6423-6433.

Record of Contribution

Chapter 1

Cao J, Aichem A, Basler M, Alvarez Salinas GO, Schmidtke G: **Phosphorylated FAT10 is more efficiently conjugated to substrates, does not bind to NUB1L, and does not alter degradation by the proteasome**. *Biomedicines* 2024, 12(12).

Jinjing Cao: formal analysis, investigation, methodology and writing—original draft

Annette Aichem and Gerardo Omar Alvarez: methodology

Michael Basler: methodology and writing—review and editing.

Gunter Schmidtke: supervision, investigation, analysis, methodology and writing—review and editing.

Chapter 2

Cao J, Alvarez Salinas GO, Schmidtke G, Basler M: **The ubiquitin-like modifier FAT10 does not affect IL-12 expression and signaling**. *PLoS One* 2025, 20(5).

Jinjing Cao: formal analysis, investigation, methodology and writing—original draft

Gerardo Omar Alvarez Salinas: methodology

Gunter Schmidtke: supervision, methodology

Michael Basler: supervision, investigation, analysis, methodology and writing—review and editing.

Chapter 3

Cao J, Schmidtke G: **Making FAT10 with a reactive C-terminus for E3 ligase screening.** *Archives of Clinical and Biomedical Research 2025.*

Jinjing Cao: formal analysis, investigation, methodology and writing—original draft

Gunter Schmidtke: supervision, investigation, analysis, methodology and writing—review and editing.

Acknowledgement

First and foremost, I would like to express my heartfelt gratitude to **Prof. Dr. Marcus Groettrup**. It was he who gave me the opportunity to join the FAT10 research project. Without his invitation, I would never have become a part of our research group. During our first discussion, he was incredibly patient and took the time to explain the background of FAT10 to me—how it was discovered in 1996 and its biological significance. Anticipating that I might not fully understand, he even drew diagrams to help illustrate the concepts. I had never met a professor so kind and dedicated before, and I will never forget it.

Secondly, I am deeply grateful to **PD Dr. Gunter Schmidtke**, who took me under his wing and allowed me to continue working on the FAT10 project. Whenever I had questions—no matter how many—he was always ready to help, with unwavering patience. He never grew tired of my inquiries and always supported me. His encouragement gave me the confidence and motivation to keep going. When I encountered obstacles in my project, he always had brilliant ideas to push things forward. His expertise in FAT10 research is beyond question, and his optimistic attitude continues to inspire me every day. I believe that an optimistic attitude is essential in work and life.

I would like to extend my sincere thanks to **Prof. Dr. Alexander Bürkle**. Whether during GBS reports, thesis reviews, or my thesis defense, he was one of my most important supervisors. I am truly grateful for his invaluable advice, which helped me avoid many detours along my scientific journey. His perseverance and passion for research are qualities I deeply admire and will always strive to learn from.

I am deeply grateful to **Prof. Martin Scheffner** for attending my PhD defense and serving as the chair of the examination committee. His prompt and gracious response greatly facilitated the smooth and timely organization of the defense. I sincerely appreciate his support.

I am also sincerely thankful to **Prof. Dr. Michael Basler**, who gave me the chance to explore FAT10 in the context of immunology. He was always there for me, guiding me with great care and precision, correcting my mistakes again and again. His deep knowledge of immunology and his serious, responsible attitude have deeply impressed me—he is someone whose personal and academic qualities I deeply admire. He is a role model for me in every aspect.

I would like to express my heartfelt thanks to **PD Dr. Annette Aichem** for her guidance on my FAT10 project. She is a brilliant and insightful, full of passion for the research on FAT10. I am deeply grateful to her for helping me overcome many challenges throughout my FAT10 study. Her enthusiasm for science is truly inspiring, and I deeply admire her dedication.

Natalie Pach was the first name I remembered among the students in our lab. When I accidentally fell off small car, she stayed with me the whole time and comforted me. She's like an angel, always appearing when you need her the most. Her kindness is something I will never forget.

Gerardo Omar Alvarez Salinas helped me order lab materials and taught me how to adapt to life abroad. He often surprised me with delicious treats. A friend like him is a blessing—one you simply can't say no to.

Christine Wünsch—I am truly thankful that she could understand my broken English! We sat close to each other, which made communication easy. She became someone I could talk to about everything. I'm deeply grateful for her companionship.

I would also like to sincerely thank **Dennis Mink, Ilona Kindinger, Julia Ottlinger, Katharina Inholz, Dennis Horvath**, and **Kritika Saxena, Annette Sommershof**—thank you all for always being there when I needed help.

Our lab is truly like one big family. Each member contributes to its warmth, and because of all of them, our lab became a better and more beautiful place to work.

May 2025

List of Abbreviations

AMBRA1	Activating molecule in Beclin1-regulated autophagy
ATG	Autophagy-related protein
BMDC	Bone marrow-derived DC
CP	Core particle
CuAAC	Copper-catalyzed azide–alkyne cycloaddition
DC	Dendritic cells
DRiPs	Defective ribosomal products
DUBs	Deubiquitinases
FAT10	HLA-F adjacent transcript 10
FAT10 D	Phospho-mimetic FAT10
FAT10 WT	FAT10 wild-type
GSH	Reduced glutathione
H5N1	Influenza A virus subtype H5N1
HCC	Hepatocellular carcinoma
HDAC6	Histone deacetylase 6
HLA	Human leukocyte antigen
HUWE1	UBA and WWE domain containing E3 ubiquitin protein ligase 1
IFN	Interferon
IKKβ	IκB kinase β
IL-12	Interleukin-12
IMDM	Iscove's Modified Dulbecco's Medium
IPTG	Isopropyl β-D-1-thiogalactopyranoside
ISG15	Interferon-stimulated gene 15
Jun	AP-1 transcription factor subunit
LB medium	Luria-Bertani medium
LPS	Lipopolysaccharide
MAD2	Mitotic arrest deficient 2
Mfn2	Mitofusin 2
MHC	Major histocompatibility complex
MNSFβ	Monoclonal nonspecific suppressor factor β
MUB	Membrane-anchored ubiquitin-fold protein
NEDD4	Neural Precursor Cell Expressed Developmentally Down-Regulated Protein 4
NEDD8	Neural precursor cell expressed developmentally down-regulated protein 8
NP	Nucleoprotein
NUB1	NEDD8 ultimate buster 1
NUB1L	NEDD8 ultimate buster-1 long

PC	Pancreatic cancer
PCNA	Proliferating cell nuclear antigen
PEI	Polyethylenimine
PMA	Phorbol 12-myristate 13-acetate
poly I:C	Poly inosinic-poly cytidylic acid
PTMs	Post-translational modifications
RIG-I	Retinoic acid-inducible gene I
RPN10	Regulatory particle non-atpase 10
SIRT1	Silent information regulator 1
SOC	Super optimal broth with catabolite repression medium
STAT	Signal transducer and activator of transcription.
SUMO	Small ubiquitin-like modifier
TBS	Tris-buffered saline
TNF	Tumor necrosis factor
UBA	Ubiquitin-associated
UBE1	Ubiquitin-activating enzyme E1
UBL	Ubiquitin-like
UFM1	Ubiquitin-fold modifier 1
UIMs	Ubiquitin-interacting motifs
URM1	Ubiquitin-related modifier 1
VWA	Von Willebrand A

Appendix 1 to § 6 General Provisions of Doctoral Regulations

Affirmation in Lieu of Oath

1. The doctoral thesis on the topic

This work is structured into three major investigations: the role of phosphorylated FAT10 in protein degradation, the relationship between FAT10 and IL-12, and engineering FAT10 with a reactive C-terminus for E3 ligases screening. These studies collectively aim to advance our understanding of the biochemical and immunological functions of FAT10.

is entirely my own work.

2. ☒ I have used only the sources and aids indicated, and have not received assistance from unauthorized third parties. In particular, texts or ideas that were obtained from other works have been identified as such.

3. ☐ My work does not copy or paraphrase any text passages or other content generated by an AI tool.

   ☒ If I have used text-generating AI tools as **aids**, I understand that I am solely responsible for the accuracy of the content of the AI-generated text passages and other AI-generated content, as well as for referencing other people's wording and ideas in accordance with the principles of good scientific practice. I have used AI tools as described below.

ChatGPT- Helped me with some translations or checked my English grammar

(If necessary, please use additional insertion sheets!)

4. ☒ The work or parts of the work ~~have already been~~/have never been [1] submitted to an institute of higher education in Germany or abroad as part of an examination or qualification procedure.

Title of the work:

Institution of higher education; year:

Type of examination or qualifications procedure:

5. ☒ I hereby affirm that the above statements are true and correct.
6. ☒ I am aware of the significance of the affirmation in lieu of oath and the consequences under the penal code of giving an incorrect or incomplete affirmation in lieu of oath.

I hereby affirm that I have stated the truth to the best of my knowledge and have concealed nothing.

konstanz, 13.05.2025 — Jinjing Cao

place and date **(signature)**

[1] **Delete as appropriate. If the work has already been submitted, complete the fields indicating the title of the submitted work, the institute of higher education, the year in which it was submitted, and the type of examination or qualification procedure**